Function of Gata-2 in thymic epithelial cells – A transcription factor identified from gene expression analysis of endodermal cells committed to thymic epithelial cell fate

Inauguraldissertation

zur

Erlangung der Würde eines Doktors der Philosophie

vorgelegt der

Philosophisch-Naturwissenschaftlichen Fakultät

der Universität Basel

von

Kyung-Jae Na

aus

Jindo-Kun, Süd-Korea

Bern, August 2010

Function of Gata-2 in thymic epithelial cells – A transcription factor identified from gene expression analysis of endodermal cells committed to thymic epithelial cell fate

Inauguraldissertation

zur

Erlangung der Würde eines Doktors der Philosophie

vorgelegt der

Philosophisch-Naturwissenschaftlichen Fakultät

der Universität Basel

von

Kyung-Jae Na

aus

Jindo-Kun, Süd-Korea

Bern, August 2010

Genehmigt von der Philosophisch-Naturwissenschaftlichen Fakultät

auf Antrag von

Prof. Dr. med. G.A. Holländer

Prof. Dr. phil. E. Palmer

Basel, den 13.Oktober 2009

Prof. Dr. Parlow

Dekan der Philosophisch-Naturwissenschaftlichen Fakultät

“The tragedy of life is not that it ends so soon, but that we wait so long to begin it.” - Anonymous

Hiermit bestätige ich, dass ich die Dissertation visiert habe.

Datum: _____

Unterschrift: _____

Prof. Dr. med. G. A. Holländer

Acknowledgements

The present work was done in the laboratory of Pediatric Immunology at the Department of Biomedicine of University of Basel under the supervision of Prof. Dr. med. G.A. Holländer.

First I would like to thank Prof. Dr. med. G.A. Holländer for giving me the opportunity to do this Ph.D. thesis work in his laboratory. I am not only grateful for his constant support, helpful discussions and the freedom to improvise in his laboratory but especially for his patience during my Ph.D. thesis work. In his laboratory, I have not only learned to handle and improve all the abilities required for the presented work, but also lessons which have influenced my life.

I would like to express my thanks for the great time and support to all who worked in the laboratory: Marcel Keller, Jason Gill, Simona Rossi, Mathias Hauri, Lukas Jeker, Luca Piali, Saulius Zuklys, Katrin Hafen, Noriko Shikama-Dorn, Thomas Boulay, Annick Peter, Werner Krenger, Elli Christen, Gretel Nusspaumer, Sebastian Löffler, Gabor Szinnai, Tatjana Zalac, Emanuela Burchielli, Caroline Berkemeier, Radhi Praba Velayutham, Thomas Barthlott, Saule Zhanybekova, Yves Mathieu.

I thank Marcel for the gene chip data analysis. A special thanks goes to Katrin Hafen who taught me basically everything that I needed to know for the cellular analysis (FACS, cell staining, TEC isolation) and also for the whip she used to motivate me throughout the Ph.D. time and to keep myself fit for the work in the lab. Without her the Ph.D. time would have been much harder. I am glad that Werner and Thomas were there when I needed help in TEC sorting. I thank Lukas and Mathias for their support and suggestions and also Noriko for the scientific and non-scientific discussions. I enjoyed it so much.

I would like to thank Prof. E. Palmer for his time for being the co-referent of this thesis.

There are not enough words to express my gratitude to Madeleine and my son Maximilian for their endless patience and for their support during rough times and Elisabeth for her time she spent with Maximilian, when I could not. They always gave me a reason to smile and to look forward

Table of Content

Abbreviation

ATP	adenosine triphosphate
B-cell	bone marrow-dependent lymphocyte
BM	bone marrow
bp	base pairs
BSA	bovine serum albumin
cDNA	complementary DNA
°C	degree Celsius
CD	cluster of differentiation
c-kit	tyrosine kinase receptor for stem cell factor
cTEC	cortical thymic epithelial cell
CTP	cytosine triphosphate
DC	dendritic cells
DMEM	Dulbecco`s modified Eagle`s medium
DMSO	dimethylsulfoxide
DNA	deoxyribonucleic acid
DN	double negative T-cell
dNTP	2`-Deoxyribonucleoside-5`-Triphosphate
DP	double positive T-cells
dscDNA	double stranded DNA
DTT	dithiothreitol
E	embryonic day of gestation
EB	elution buffer
ECM	extracellular matrix
EDTA	ethylenediaminetetraacetic acid
i.e.	as for example
EtOH	ethanol
FACS	fluorescent-activated cell sorter
FCS	fetal calf serum
FITC	fluorescein isothiocyanate
FTOC	fetal thymic organ culture
g	gram
G	gravity
GAPDH	glyceraldehydes-3-phospahte dehydrogenase
GTP	guanosine triphosphate
h	human
hr	hour
HEPES	N-2-Hydroethylpiperazine-N`-2-ethansulfonic acid
H&E	Hematoxylin and eosin
HSC	hematopoietic stem cell
Ig	immunoglobulin
ISH	in situ hybridization
K	cytokeratine
Kb	kilo base
KDa	kilo Dalton
L	liter
LB	lurea broth
LCM	laser capture micro dissection
LN	lymph node
M	molar
2-ME	2-Mercaptoethanol
MHC	major histocompatibility
min	minute
mL	milliliter
µL	micro liter
mM	milli mole
mRNA	messenger RNA
mTEC	medullary thymic epithelial cell

NK	natural killer cell
ng	nano gram
NTP	nucleotide triphosphate
O.D.	optical density
O.N.	over night
ORF	open reading frame
PBS	phosphate-buffered saline
PCR	polymerase chain reaction
PE	phycoerythrin
pg	pico gram
pH	negative logarithm of the hydrogen ion concentration
qRT-PCR	quantitative real time PCR
Rag	recombination activating gene
RNA	ribonucleic acid
rpm	revolutions per minute
RT	room temperature
s	second
SCID	severe combined immuno-defcient
SDS	sodium dodecyl sulfate
SP	single positive T-cell
ssDNA	single stranded DNA
SSC	standard saline citrate
TBS	Tris buffered saline
TCR	T-cell receptor
TE	tris (10mM/EDTA (1mM) buffer
TEC	thymic epithelial cell
Tris	Tris-Hydroxymethyl-Aminomethane
TTP	thymidine triphosphate
U	unit
UTC	uracyl triphosphate
UV	ultraviolet
VDJ	variability, diversity, and joining regions
wt	wild type

Summary

The thymus structure composes of clear morphological regions. The T-cell precursors enter the thymus in the cortico-medullary junction and migrate through the cortex towards the sub capsular region and back through to the cortex into the medulla. During this migration process the thymic epithelial cells provide the microenvironment for the maturation and selection of the majority of the peripheral T-cells. The thymic epithelial cells have their origin in the endodermal cells of the ventral aspect of the 3rd pharyngeal pouch while endodermal cells of the dorsal aspect of the 3rd pharyngeal pouch give rise to the parathyroid glands. For a better understanding of genes which might be involved in determination of endodermal cells to the thymic epithelial cell fate, the gene expression profile of the ventral aspect of 3rd pharyngeal pouch was compared to the dorsal aspect of 3rd pharyngeal pouch using microarrays. The analysis revealed 69 genes which were up regulated in the ventral aspect of 3rd pharyngeal pouch. Eleven genes with the largest differential expression values were further assessed (Gata-2, dll-1, C1qdc2, Samd5, Msx2, Msx1, Ehox, Tgfbi, Unc5c, FoxG1, 1110006E14Rik) using RT-PCR and whole mount in situ hybridization. The genes dll-1, Tgfbi, Msx1 and Msx2 are involved in the Notch, Tgfβ and Bmp pathways, respectively. All these pathways are associated with thymus development. The role of the genes Ehox, Gata-2, C1qdc2, Samd5 and Unc5c in thymus development is so far undefined.

Gata-2, a transcription factor, known to be involved in hematopoiesis, was the only gene of which its expression was detected by gene chip data, RT-PCR and whole mount in situ hybridization. These results identified Gata-2 as a novel candidate that might be involved in the thymic epithelial cell development. To characterize the function of Gata-2 in thymus development, Gata-2 was specifically deleted in thymic epithelial cells using Foxn1-Cre. The thymi of 3, 6, 13, and 25 weeks old mice were removed and detailed studies were performed. FACS analysis of these thymi revealed an increased thymus cellularity in DN1-DN4, CD4, and CD8 in 6 weeks old thymi and onwards. The thymus architecture which was analyzed by H&E and immunohistochemistry (UEA-1, CK8, CK18, ERTR7) was unaffected when Gata-2 was deleted in TECs. The assessment of TEC population of Gata-2 KO mice did not show any difference. But the gene expression analysis of Gata-2 deficient TECs for the genes c-Jun, CXCL-12, CCL-25, IL-7, c-Fos, c-kit ligand, Edn-1, Edn-Ra, und Edn-Rb showed that CXCL-12 and c-kit ligand were higher expressed. CXCL-12 is involved in homing of T-cell precursors while c-kit L is involved in survival and proliferation of T-cell precursors.

In conclusion, Gata-2 might negatively regulate the transcription of CXCL-12 and c-kit ligand. A lack of Gata-2 expression in thymic epithelial cells, therefore, might lead to an increased T-cell precursor attraction and survival/proliferation, thus, explaining the higher cellularity observed in thymus of Gata-2 deficient mice.

I. Introduction

In the past years several breakthrough experiments provided important results for a better understanding of the molecular mechanisms of the thymus development. But the advances which are made so far remain small when compared to the progress in research addressing the cellular pathway and the molecular mechanisms of developing T-cells. The unique function of the thymus in establishing and maintaining the T-cell pool makes the thymus crucial organ in the immune system. The aim of this project was therefore to characterize the genetic program that determines thymic epithelial cell fate and differentiation and, in particular, new genes critically involved in this process. Among 11 genes which were selected upon Affymetrix Gene Chip data analysis, Gata-2, a transcription factor, was chosen for an extended *in vivo* model study.

1.1. Thymus function and structure

The thymus structure composes of clear morphological regions. The cortico-medullary junction (CMJ) in which the T-cell precursors enter the thymus and migrate through the cortex (C) towards the sub capsular area (SCA) and back through cortex to the medulla (M) (Fig. 1.1a). Petrie et al. suggested a more detailed division of the thymus into several zones depending on where the developing T-cells migrate to after their entrance into the thymus (Fig.1.1b,c). The thymus stroma, which is responsible for the thymus structure and provides the matrix on which thymocytes develop, can be divided into two groups depending on their expression of CD45. The further identification of the thymic stroma lacking the pan hematopoietic marker CD45 is based on keratin expression. The keratin$^+$ cells represent the thymus epithelium and the keratin$^-$ cells represent a mixture of mesenchymal cells. Keratin$^+$ cells are composed of two major subsets: cortical thymic epithelial cells (cTEC) and medullary thymic epithelial cells (mTEC) (Gray et al., 2007) while the keratin$^-$ cells include fibroblasts, non-fibroblastic mesenchymal cells (Muller et al., 1993), capsule- and septae forming connective tissue cells and endothelial cells forming the thymus vasculature (Muller et al., 1993; Raviola et al., 1972; Anderson et al., 2000). The majority of the mTEC and cTEC can be further distinguished upon their expression of keratin (K) expression pattern. While the mTEC are $K5^+K8^-$, cTEC are $K5^-K8^+$ (Klug et al., 1998; Klug et al., 2002).

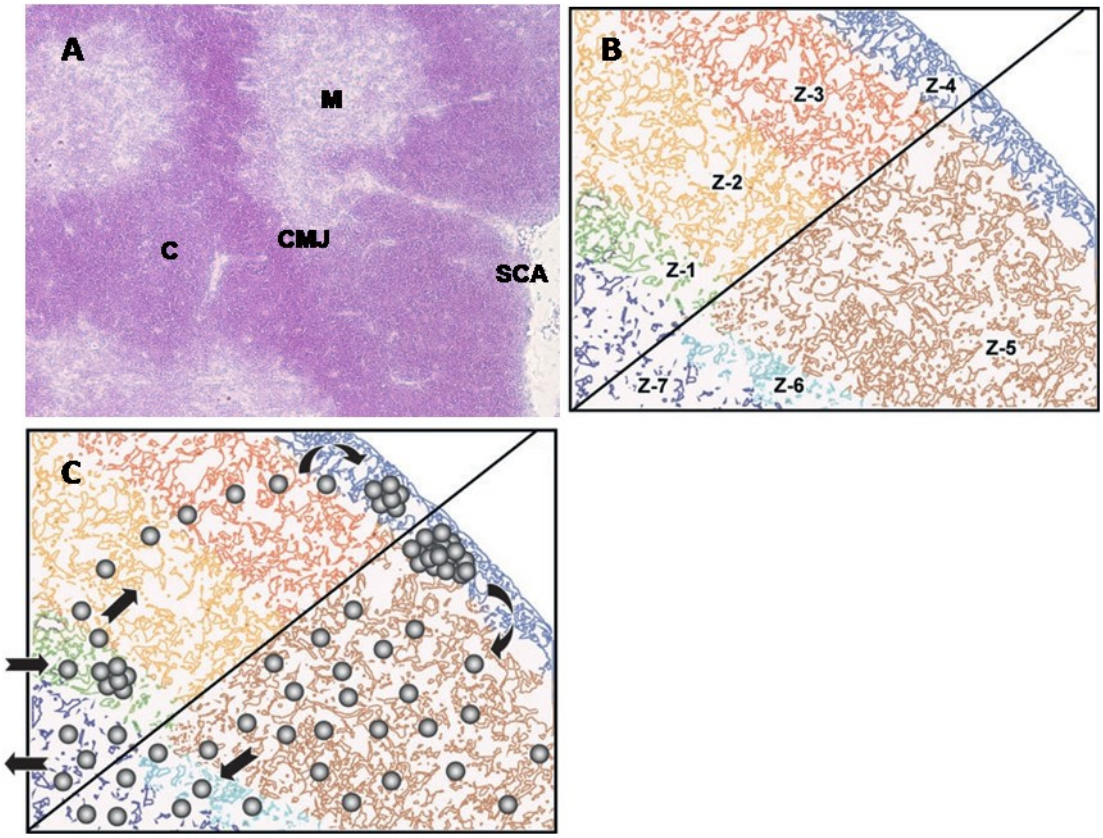

Fig 1.1: A) Thymus section from a healthy mouse stained with hematoxylin and erythrosine. M: medulla, C: cortex, CMJ: cortico-medullary junction, SCA: sub capsular area **B)** Zones 1 to 7. The diagonal line separates the zones for outward movement of DN cells (upper left) from those defined by movement of DP and SP cells inward (lower right). **C)** The pattern of progenitor migration within the thymus is depicted by an overlay of lymphoid cells. (This figure has been partially adapted from Petrie *et al.*, 2007)

The cortical thymic stroma consists of epithelial cells that are closely associated with the early maturation stages of developing T-cells. The medullary thymic stroma consists of epithelial cells together with the hematopoietic macrophages and dendritic cells which interact with mature thymocytes (Anderson et al., 2001; Petrie et al., 2007). Finally, dendritic cells and macrophages, that are $CD45^+$ hematopoietic cells, are also important elements of thymus stroma.

The successful completion of the thymus development has his importance in providing the required primary lymphoid an unique microenvironment for the differentiation of the hematopoietic precursor cells into functional T-cells. The maturation and selection during thymocyte development are affected by the thymic stroma. The outcome is the production of self-restricted but self-tolerant T-cells. The establishment of a functional T-cell repertoire is achieved by positive and negative thymic selection. Positive selection occurs upon low affinity binding of the T-cell receptor (TCR) with a peptide self-MHC (major

histocompatibility complex) complex expressed by the cTEC that results in the transduction of survival and differentiation signals in the developing thymocytes. Thymocytes that fail to receive these signals do not undergo positive selection and die by neglect. Negative selection occurs when the TCR of thymocytes engages a peptide-MHC ligand in the mTEC with high affinity that leads to the apoptotic death of the cell. Thus the thymus generates a repertoire of peripheral T-cells that are largely self-tolerant (Anderson et al., 2002; von Boehmer 2004; Kyewski et al 2006; Martinic et al., 2006). For these reasons fewer than 5% of the developing thymocytes survive and leave the thymus as mature T-cells. For auto-reactive T-cells that escape regular negative selection additional mechanisms regulates their function in periphery e.g. by regulatory T-cells (FoxP3$^+$, CD4$^+$, CD25$^+$).

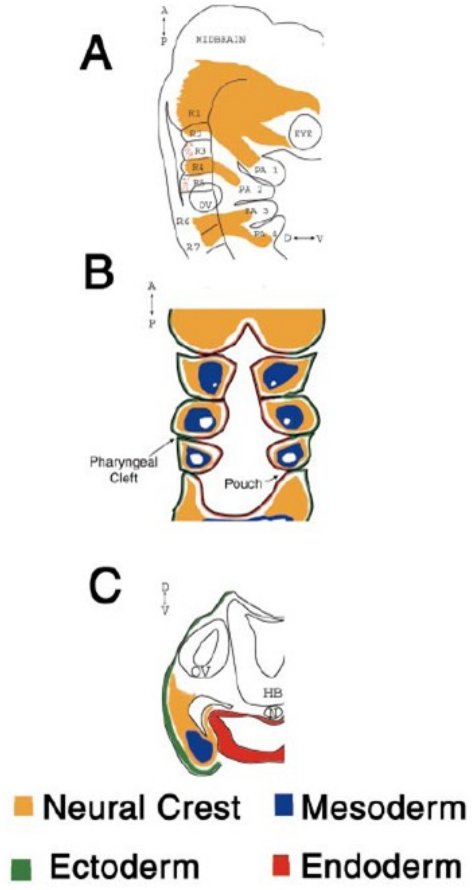

Figure 1.2 The pharyngeal arches. A) Side view. The segments of the hindbrain, the rhombomeres, are labeled R1 through R7. The 3 crest streams destined for the pharyngeal arches are shown in orange. **B)** A longitudinal section through the pharyngeal arches showing the different embryonic populations that contribute to the arches. The ectoderm which surrounds the outer face of the arches is green, while the endoderm which forms the inner surface of the pharynx is labeled in red. The neural crest is shown in orange and the mesodermal core of the arches is blue. **C)** A transverse section through the third pharyngeal arch showing the arch components and the surrounding structure. Otic vesicle (OV), hind brain (HB), notochord (N). (The figure has been adapted from Graham *et al.*, 2001)

1.2 Thymus organogenesis

1.2.1. The pharynx

The pharyngeal apparatus develops from a series of bulges found on the lateral surface of the head, the pharyngeal arches, which consist of a number of different embryonic cell types (Fig. 1.2). Each arch has an external covering of the ectoderm and inner covering of endoderm and between these a mesenchymal filling of neural crest with a central core of mesoderm. The ectoderm forms the epidermis and the sensory neurons of the epibranchial ganglia (Verwoerd et al., 1979; D'Amico-Martel et al., 1983; Couly et al., 1990), while the endoderm gives rise

to the epithelial lining of the pharynx, and forms the taste buds as well as the thyroid, parathyroid and thymus (Le Douarin et al., 1975, Cordier et al., 1980). The neural crest forms the skeletal and connective tissues of the arches (Noden, 1983a; Couly et al., 1993; Trainor et al., 1994).

1.2.2. Pharyngeal pouches

In mammals the walls of the developing pharyngeal regions consist of a series of individual pairs of branchial (a.k.a. pharyngeal) arches, designated ba1-ba4 and ba6. The boundaries of each arch are demarcated on the embryo`s surface by intervening grooves. The anterior region of the foregut, which forms the primitive pharynx, expands toward the surface within this framework and is directed along the intervals between the branchial arches. Consequently, bind ending sacs extend from the foregut laterally in the direction of the embryo`s body surface, producing a bilateral series of different pharyngeal pouches (pp) that are lined by endodermal epithelium. These pouches designated 1^{st}, 2^{nd}, 3^{rd} and 4^{th} are located between ba1, ba2, ba3 and ba4 and ba6, respectively. Since the thymus emerges in mice from the 3^{rd} pp, its formation is juxtaposed to the 3^{rd} and 4^{th} branchial arches (ba3 and ba4). The developing endodermal lining is at specific locations directly juxtaposed to the surface ectoderm. Consequently thin, narrow diaphrahms, known as pharyngeal membranes, are formed that connect the separate arches.

At E10.5 the neural crest cells are adjacent to endodermal lining (Fig. 1.3) (Gordon et al., 2004; Le Douarin and Jotereau, 1975). These mesenchyme surround the emerging thymus primordium and provide molecular signals that are necessary for the expansion of the TEC (Jenkinson et al., 2003; Revest et al., 2001b; Suniara et al., 2000). Interfering with the mesenchymal derivatives from neural crest cells during the functional development of the epithelial primordium inhibits thymic development in a manner similar to that observed in congenital conditions such as the DiGeorge syndrome or the fetal alcohol syndrome (Ammann et al., 1982; Bockman, 1997; Suniara et al., 2000). In the fetal thymus, neural crest derived mesenchymal cells contribute to the thymic capsule and septae, and can also be located within the thymic cortex where they interact with immature thymocytes as shown by immunohistochemistry analysis (Anderson et al., 1997; Owen et al., 2000; Suniara et al., 2000). As thymus development proceeds, the mesenchyme of neural crest origin surrounding the pharyngeal organs is replaced by mesodermal mesenchyme (Yamazaki et al., 2005).

The first morphological signs of thymus organogenesis are apparent approximately at day 10.5 of gestation (E10.5). Around E11.5 the mouse thymus primordium emerges as an epithelial anlage budding from the ventral endodermal lining of the 3rd pharyngeal pouch while dorsal aspect of this invagination develop into the parathyroid glands (Rowen et al., 2002). Each organ is surrounded by a mesenchymal capsule that still contacts both the surface ectoderm and the pharyngeal endoderm. Seeding of lymphoid precursors cells into the epithelial primordium occurs at about E12.5 and is paralleled by rapid epithelial cell proliferation and differentiation giving eventually rise to the typical thymus structure which consists of medulla that is surrounded by the cortex.

By E13.5, the parathyroid and the thymus are separated from the pharynx and these two organs start to migrate into their final destination. The thymus descends to the mediastinum where it sits on the top of the heart with the two lobes touching each other at the midline while the parathyroid glands are positioned at the lateral margins of the thyroid gland.

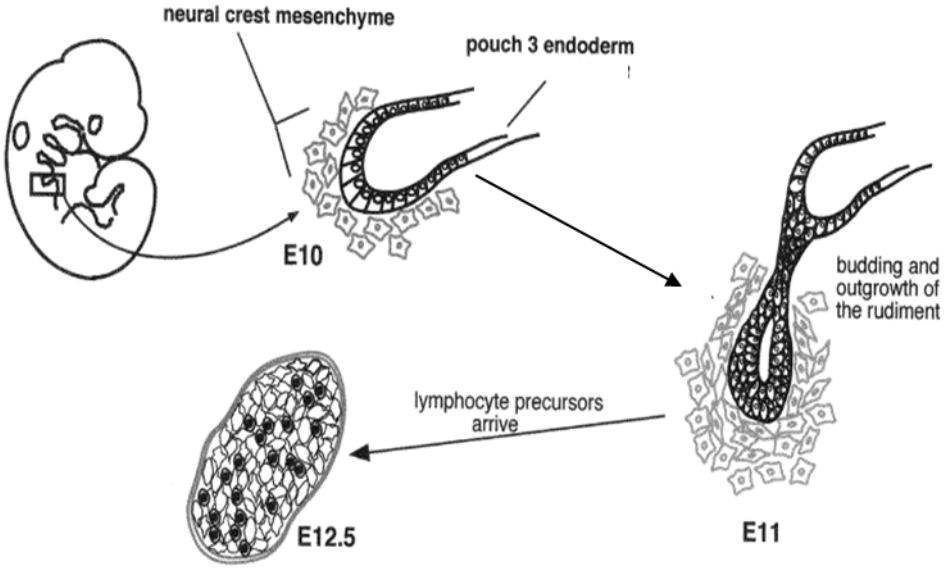

Fig.1.3 Formation of the early thymic rudiment in mouse. Neural crest derived mesenchymal cells surround the endoderm of the 3rd pp. At E11.5, a thymic rudiment buds from the endoderm, consisting of epithelial cells surrounded by a neural crest-derived capsule. Around this time point hematopoietic cells migrate into the epithelial anlage. At E12.5 patterning and differentiation begin via epithelial-thymocyte interactions. (The figure has been adapted from Manley *et al*., 2000)

1.2.3 Neural crest cells as a source of mesenchyme

The majority of the mesenchymal cells that fill the pharyngeal arches are the progeny of neural crest cells and are crucial for thymus organogenesis and thymus functions (Anderson et al.. 2001; Manley et al., 2000; Rodewald 2004; Owen et al., 2000; Petrie 2002). Neural crest cells are of ectodermal origin and originate at the most dorsal aspect of the neural tube. Their importance lies in the ability to migrate extensively and generate various differentiated cell types such as neural cells, smooth muscle cells and chondrocytes. Neural crest cell from the 2^{nd} and 4^{th} rhombomeres migrate to the 3^{rd} and 4^{th} pharyngeal arch whereas neural crest cells from the 3^{rd} and 5^{th} rhombomeres enter the migrating as separate streams of an adjacent rhombomere. Once in their respective pharyngeal regions, they transform to ectomesenchymal cells and interact with epithelial cells of the pharyngeal endoderm. This interaction is important for the proliferation, migration, and differentiation of the epithelial cells (Bockman, 1997). A possible molecular link between neural crest derived mesenchyme and thymus epithelium is provided via fibroblast growth factors (Fgf) and their receptors (FgfR). Fgf7 and Fgf10 are expressed by the mesenchyme surrounding the embryonic thymus epithelium, and the latter expresses FgfR2-IIIb. Defects in this signaling pathway perturb thymus development (Revest et al., 2001), demonstrating a growth-promoting role for mesenchyme toward thymic epithelium. Signals via Fgfs also induce TEC proliferation (Erickson et al., 2002; Rossi et al., 2007), and protect thymus epithelium from injury by irradiation (Min et al., 2002) or by conditions of graft versus host disease (Rossi et al., 2002).

1.2.4. Interference with epithelial-mesenchymal interaction

The cellular interactions between endodermal epithelium and mesoderm and ectodermal mesenchyme are responsible for the formation of a regular thymus was experimentally verified in mice and chicken (Auerbach, 1960). Removal of E12.5 thymus and culturing it as fetal thymic organ culture (FTOC) produces robust epithelial proliferation. This does, however, not occur if the thymus has been stripped of its mesenchyme (Suniara et al., 2000).

The fibroblast growth factors (Fgf) are involved in the epithelial-mesenchymal interactions (Xu et al., 1999), which are assumed to regulate directly the differentiation and/or proliferation of the thymic epithelial cells. Such interactions show the importance in the organogenesis of many organs, such as in the limb development, where the mesenchymal production of fibroblast growth factors stimulates the growth and differentiation of Fgf-receptor-bearing epithelial cells (Xu et al., 1999).

Mice lacking either Fgf10 (Ohuchi et al., 2000) or its receptor FgfR2-IIIb (Revest et al., 2001a) display a thymus that is reduced in size (Revest et al., 2001b). These results suggest a role for specific Fgfs for epithelial-mesenchymal interactions during thymus development. However, signals of Fgf10 via its receptors, FgfR2-IIIb, seem not to be essential for the commitment to a thymic epithelial cell fate and the ability to support thymocyte development, as mice deficient for Fgf10 or its receptor display a phenotypically regular maturation of the few thymocytes that are present in their thymus. However, any conclusion as to the competence of the thymus in these mutant mice to generate a regular repertoire of functional T-cells is unknown, since FgfR2-IIIb deficient mice die at birth because those mutant mice fail to develop lungs. A time constrained role of the mesenchyme for thymic epithelial cell development was claimed by Jenkinson and colleagues who provide evidence that the differentiation of immature thymic epithelia into cortical and medullary phenotypes is after E12 independent of a sustained interaction with mesenchyme (Jenkinson et al., 2003). However, the continued presence of Fgf7 and Fgf10 is necessary to support the proliferation of thymic epithelial cells leading to thymus growth.

A role for mesenchyme in thymic development has also been shown in experiments using reaggregate thymus organ cultures (RTOC) (Anderson et al., 1993; Anderson et al., 1997) which proved that mesenchymal fibroblasts are necessary for the maturation of thymocytes precursors beyond the most immature, intrathymic developmental stage i.e. DN1 (c-kit^{+}, CD44^{+}, CD25^{-}) thymocytes (Anderson et al., 1993). However, it remains uncertain just how mesenchymal cells influence thymocytes development. Possible mechanisms include the generation of specific components of the extracellular matrix (ECM) and/or soluble growth factors such as cytokines (Banwell et al., 2000).

1.2.5 Epithelial patterning, differentiation and crosstalk between thymocytes and epithelium

Around E12 hematopoietic cells colonize the thymus which undergoes further patterning and differentiation (Gill et al., 2003; Rodewald 2004). Around that time, first signs of cortex and medulla separation occur which are accompanied with a change in keratin expression pattern in the epithelium and adult thymic epithelial cells can be distinguished according to their expression of the keratin (K) expression. Majority of the adult mTEC are K5^{+}K8^{-} while cTEC are K5^{-}K8^{+} (Klug et al., 2002; Ritter et al., 1993). Several reports suggests that the 3rd pouch epithelium at E11.5 express K5 but not K8 (Ritter et al., 1993; Gill et al., 2002) whereas others found co-expression of K5 and K8 (Benett et al., 2002). At the embryonic stage of E12

and E13 majority of the TECs express K5 and K8 (Bennett et al., 2002; Gill et al., 2002). These double positive TEC are thought to be the progenitors of mature single positive $K5^{+}K8^{-}$ and $K5^{-}K8^{+}$ TECs. A blockade in T-cell development such as in the common γ chain (γc^{-}) or $RAG2^{-/-}$ γc^{-} mice, the majority of the thymic epithelial cells fail to differentiate and remain in the stage of $K5^{+}K8^{+}$ stage (Rodewald et al., 1998) which indicates that an interaction of T-cell progenitors with the developing thymic epithelial cells are necessary for the TEC differentiation but the initial patterning of the embryonic thymus is T-cell independent and only dependent on the expression of Foxn1 in the epithelium. The necessity of the crosstalk between the T-cell progenitors ($CD45^{+}CD25^{-}$) and TEC have been further supported by mice experiments by Rodewald and their colleagues who used a $Kit^{W/W}$ γc- mice, a mutant in which thymocytes development was completely abrogated (Rodewald et al., 1997). These mice had a severely dysmorphic thymus structure but their architecture could be restored when the thymus was grafted postnatally into a recipient mice that provide wild type hematopoietic stem cells (Rodewald et al., 1997). However, according to the studies of Klug et al. and Jenkinson et al. signals for thymocyte signals are not required for the initial differentiation of TEC progenitor in to cTEC and mTEC lineage but influence later stages of TEC differentiation (Klug et al., 2002; Jenkinson et al., 2005).

1.2.6 Origin of thymic epithelial cells: Dual origin versus single-origin model

Until 2006 there has been a controversial discussion about the origin of the two different TEC types. The dual origin model is mainly supported by very early experiments performed by Cordier, Haumont and Hereman. This model suggests that both the third pharyngeal cleft ectoderm and the third pharyngeal pouch endoderm contribute physically to the thymus during organogenesis. The facts are drawn from histological sectioning and reconstruction approach to compare thymus organogenesis in nude and wild-type embryos (Cordier and Haumont, 1975; 1980). Cordier and Heremanns reported that the endodermal and ectodermal germ layers made physical contact at E9.5, followed by a strong proliferation of the ectoderm positioned at the 3rd pharyngeal cleft. These changes result in a situation where the ectodermal cells cover the 3rd pouch endoderm for a period from E10.5 to E11.5. At E12.5 this compound structure detaches from both the ectoderm and endoderm and gives rise to the thymus primordium. Markedly diminished proliferation of the ectoderm was reported for nude embryos leading to the conclusion that the primary nude defect affects ectodermal cell (Cordier and Haumont, 1975; 1980).

Independent of these observations and interpretations, strong functional evidence supporting the "single-origin" model had existed since 1975, when Le Douarin and Jotereau generated bird chimaeras by transplanting quail pharyngeal endoderm to the somatopleura of a 3 day old chick (Le Douarin and Jotereau, 1975). The graft had been taken from a donor at the 15-somite stage, a time when neither the development of the 3rd pharyngeal pouch had yet occurred nor pro-thymocytes had homed to the anatomical area from which the tissue for transplantation was taken. Upon engraftment, the donor endoderm developed into a thymus able to support T-cells of chick origin. Importantly, the epithelial cells in both the cortical and medullary compartments of the thymus were exclusively of quail origin. However, these experiments provided evidence that purified pharyngeal endoderm was sufficient to generate the epithelial component of both the cortical and medullary compartments. These data also conveyed that, at least in birds, cells in the developing endoderm have adopted a fate for thymic epithelial cells well before the formation of the 3rd pharyngeal pouch. These experiments did neither test the commitment to a single cell lineage directly but their data provide a stringent assessment of the developmental potential of the pharyngeal endoderm (Le Douarin and Jotereau, 1975).

Two independent experimental approaches finally settled the discussion. Rossi et al. injected single TECs isolated from E12 thymus anlagen of enhanced yellow fluorescent protein (YFP) transgenic mice into wild-type E12 thymus lobes that were then transplanted under the kidney capsule of recipient mice to allow thymus development to occur. Analysis of cells from the transplanted thymus lobes showed that, in all experiments in which fluorescent progeny cells were detected, the cells had contributed to both cTEC and mTEC lineage. Contribution to a single TEC lineage was markedly absent (Rossi et al., 2006). Bleul et al., on the other hand, addressed TEC progenitor activity in thymus organogenesis using genetic in situ labeling. They crossed the well established Rosa26R-eYFP (enhanced yellow fluorescent protein) reporter mice with a cre-expressing mice (hK14::Cre-ERT2) (where ER is human estrogen receptor). The cre-recombinase was driven by the human K14 promoter which is active in epithelial progenitor cells. This way eYFP protein was produced only after cre-mediated chromosomal rearrangement. This way they turned on eYFP expression. Although no labeled cells were found in the thymus at birth, numbers of eYFP^{+} TEC per thymus increase with age after birth. Upon eYFP expression analysis in the thymus they identified three different progenies: 1) mTEC clusters, 2) cTEC clusters or 3) mTEC and cTEC progeny. These patterns suggested that TEC progenitors exhibiting eYFP after cre-mediated recombination at the Rosa26 locus give rise to groups of genetically related progeny (Bleul et al. 2006).

1.2.7 TEC progenitor differentiation into cTEC and mTEC and their function

Although cTEC can be identified using flow cytometry according to their expression of the epithelial-cell adhesion molecule 1 (EpCAM1) and Ly51 (Derbinski et al., 2001), their cTEC development has not been fully understood. However, Wnt pathway seems to be involved in the cTEC development. Osada et al. have shown that an ablation of KREMEN1 (kringle containing transmembrane protein 1) in mice, a negative regulator of WNT signaling, leads to an abnormal cTEC architecture (Osada et al., 2006). Regarding the function of cTEC more details are known. cTECs express on their cellular surface MHC class I and II (Takahma et al., 2006) and are important to mediate positive selection (Anderson et al., 1994). CD83, also expressed on cTECs, seems to be an important candidate for the positive selection of $CD4^+$ T-cells (Fujimoto et al., 2002). CD83 deficient mice have a specific block in $CD4^+$ single positive thymocytes development without increased $CD4^+CD8^+$ double or $CD8^+$ single positive thymocytes which results in a selective 75%-90% reduction in peripheral $CD4^+$ T-cells, predominately within the naïve subset. For positive selection of $CD8^+$ T-cells, proteasome catalytic subunit called β5t which is exclusively expressed by cTEC plays a role. In general proteasomes are responsible for generating peptides presented by the class I MHC molecules. Proteasome subunit β5t deficient mice show a reduction in $CD8^+$ T-cell development. They suggested that β5t is important for generation of MHC class I restricted $CD8^+$ T-cell repertoire during thymus positive selection (Murata et al., 2007).

mTECs can be distinguished from cTEC due to their expression of EpCAM and a lack for the expression of Ly51 (Derbinski et al., 2001), whereas analysis of tissue sections identifies a dominant $K5^+K8^-$ phenotype (Klug et al., 1998). Furthermore, mTECs contained within individual islets were shown to arise clonally and thus providing the first direct evidence for the existence of TEC progenitors (Rodewald et al., 2001). Like cTEC, mTEC express MHC-class I and II molecules on their surface and abnormal mTEC development leads in most of the cases to autoimmunity (Naquet et al., 1999). For a functional T-cell tolerance thymocytes with high affinity for peptide-self-MHC complex must be eliminated and regulatory $FoxP3^+CD4^+CD25^+$ T-cells (T_{reg}) must be positively selected (Fontenot et al., 2005). Studies of Achenbrenner et al. showed that mTEC play a role in Treg-cell development although the nature of the interactions that lead to T_{reg}-cell selection is not fully understood (Aschenbrenner et al., 2007). mTEC population can be further divided into two distinct mTEC subsets the $CD80^-$ mTECs that express a limited array of tissue restricted antigens (TRA) and the AIRE expressing $CD80^+$ mTECs which express a wide array of TRA

(Derbinski et al., 2001, 2005; Anderson et al., 2002). AIRE (auto immune regulator), a transcriptional regulator, plays a central role in tolerance and in human a defect of AIRE expression leads to autoimmune polyendocriopathy-candidiasis-ectodermal dystrophy (APECED) (Bjorses et al., 1998, Bleschschmidt et al., 2002). Mice deficient of AIRE reveal a reduced expression of TRA in mTEC and have organ specific autoimmunity and defective tolerance induction (Anderson et al., 2002, Liston et al., 2003, Gillard et la., 2007). Another interesting candidate which is important for the normal cellularity and architecture of mTEC are lymphotoxin-β receptor (LTβR) on thymocytes and lymphotoxin-β ligand. An interruption of their signaling leads to structural defects which are associated with failure in T-cell selection and autoimmunity (Boehm et al., 2003). RANK (receptor activator of nuclear factor-κB) ligand which is expressed on $CD3^-CD4^+$ inducer cell population is important for the maturation of RANK-expressing $CD80^+Aire^+$ mTEC progenitors into $CD80^+Aire^+$ mTEC (Rossi et al., 2007). Kelly and Scollay described initially the $CD3^-CD4^+$, also known as lymphoid tissue inducer cell (LTi), inducer cell population in neonatal lymph nodes (Kelly et al., 1992) and Mebius characterized them further as fetal-liver derived hematopoietic population that is distinct from and unable to give rise to T and B-cells (Mebius et al., 1996, 1997). These cells are capable to provide RANK-ligand mediated and also lymphotoxin mediated signals which regulate the formation of stromal microenvironment that support lymphocyte recruitment and organization (Cupedo et al., 2002). Regarding thymus development Naquet et al., have shown that NF-κB signaling are important in the formation and organization of the thymic medulla (Naquet et al., 1999). Mice deficient in NF-κB signaling, such as inhibitor of NF-κB signaling (IKKα), have mTEC abnormalities and organ specific autoimmunity (pancreas and liver). Furthermore, the expression of CCL-19 and CCL-21 which are important for attracting developing T-cells into the medulla were also reduced (Lomada et al., 2007). These findings fit with the observation that were made in RANK-deficient mice which resulted in absence of $AIRE^+$ mTECs and deficiency in the stroma with symptoms of autoimmunity (Rossi et al., 2006).

1.2.8 Genes involved in the thymus development

Foxn1, a member of the forkhead box transcriptions factor (Kaestner et al., 2000; Coffer et al., 2004; Jonsson et al., 2005), is the only gene that is known to be necessary specifically for thymus epithelial development (Nehls et al., 1994; Nehls et al., 1996). Foxn1 contains a winged-helix/forkhead DNA-binding domain and a transcriptional activation domain (Boehm et al., 2003; Schuddekopf et al., 1996). Mice deficient of Foxn1 gene are nude and the thymus

anlage fails to differentiate to form a functional organ (Nehls et al., 1994). This phenotype of the thymus becomes evident as early as E12.5 or E13.5 (Cordier et al., 1980; Boehm et al., 2003; Bleul et al., 2001; Tsukamoto et al., 2005). The thymus of the Foxn1 deficient mice has a near absence of hematopoietic cells, which might be related to the loss of expression of chemokines CCL-25, a ligand of CCR-9, and CXCL-12, a ligand of CXCR4, in the embryonic nude thymus (Bleul et al., 2000). Little is known about genes controlling the expression of Foxn1. It has been proposed that Foxn1 expression is regulated through members of the Wnt family (Balciunaite et al., 2002). Using whole mount in situ hybridization in developing thymus, Foxn1 expression can be already detected at E11.5 and is expressed in most of the TEC, if not in all embryonic and adult TECs (Nehls et al. 1996). More recent study that used an anti-Foxn1 antibody suggests that $Foxn1^{+}Keratin^{+}$ and $Foxn1^{-}Keratin^{+}$ TEC exist in the embryonic thymus and that the amount of $Foxn1^{-}Keratin^{+}$ TEC can be 80% of adult TECs (Itoi et al., 2007).

The molecular mechanism of the thymus development is a complex process and not all candidate genes which are involved in its development have been described. But several *in vivo* experiments mainly in mice have been helpful to understand the role of several genes including Hoxa3 (Manley et al., 1998), Eya1 (Xu et al., 2002; Zou et al., 2006), Six1 (Zou et al., 2006; Laclef et al., 2003), Pax1 (Dietrich et al., 1995; Wallin et al., 1996; Su et al., 2000; Su et al., 2001), Pax3 (Conway et al., 1997), Pax9 (Peters et al., 1998; Hetzer-Egger et al., 2002), Edn-1 (Kurihara et al., 1994) and Tbx1 (Jerome et al., 2001). A mutation in these genes leads to thymus aplasia, hypoplasia or failure of the thymus lobes to migrate toward the chest. All the genes are expressed in multiple cell lineages during the embryonic development and hence their loss of function causes pleitotropic defects (Manley et al., 2000; Blackburn et al., 2004; Hollander et al., 2006). Since these genes are involved in the formation of the 3rd pharyngeal pouch and thus upstream of the thymus organogenesis, the genes might nevertheless be involved in the later stages of the thymus development or in the thymus epithelium itself. Hoxa3, Pax1 and Pax9 are such genes which are expressed in the thymus epithelial according to PCR data (Wallin et al., 1996; Gillard et al., 2007; Dooley et al., 2005). In order to understand the functions of these genes in thymic epithelium, a TEC specific deletion would be necessary. An example for such a study was the blocking of the Bmp signaling using Noggin under the control of the Foxn1 promoter. Transgenic expression of the BMP antagonist Noggin in thymic epithelial cells under the control of a Foxn1 promoter in the mouse leads to dysplastic thymic lobes of drastically reduced size that are ectopically located in the neck at the level of the hyoid bone (Bleul et al., 2005).

1.3 T-cell development in the thymus

1.3.1 Commitment of T-cell development in the fetus

The thymus is the main site for the generation of T-cells and requires periodic or continuous input of hematopoietic progenitors to maintain T-cell development (Donskoy et al., 1992; Foss et all., 2001). The earliest T-cell progenitors that are detected in the thymus express $CD4^{lo}$c-$kit^{+}CD44^{+}$Thy-1^{-}Sca-1^{+} (Wu et al., 1991). These precursors are also capable to give rise to B-cells, NK and dendritic cells (Matsuzaki et al., 1993; Godfrey et al., 1993). In order to determine the fate of the T-cell precursors Notch signaling seems to be important. In mice a deletion of Notch1 or RBP-J, a signal transducer downstream of Notch in HPC, results in complete defect of T-cell development (Radkte et al., 1999; Han et al., 2002). An enforced expression of the intracellular fragment of Notch (ICN1), an active form of notch, in hematopoietic precursor cells induced the ectopic appearance of $CD4^{+}CD8^{+}$ positive (DP) cells (Pui et al., 1999). In fact, both ligands delta like-1 (dll-1) and delta-like 4 (dll-4) are expressed in the thymus (Hozumi et al., 2003; Schmitt et al., 2004; Heinzel et al., 2007). The TEC specific deletion of dll-4 using Foxn1-Cre Hozumi et al. showed that no DP were present and DNs did not express Thy1, TCRαβ or TCRδγ. Closer analysis of the DN proved that no T-cell commitment occurred (Hazumi et al., 2008).

1.3.2 Thymocyte precursors seeding and migration to the developmental thymus

A major focus of research into the function of the thymus has been dedicated to delineate the precise pathways by which hematopoietic precursor cells develop into mature T-cell of the α/β T-cell lineage. The precursor cells originate from the hematopoietic stem cells (HSCs), which at the time of their seeding to thymus are still located in the aorta-gonad-mesonephros (AGM) region or fetal liver (Gekas et al., 2005; Godin and Cumano, 2002). The HSC pool in the placenta occurs prior to and during the initial expansion of HSC in the fetal liver (Gekas et al., 2005). The hematopoietic progenitors in the bone marrow (BM) are quite heterogeneous and can be divided into subpopulations according to their expression of Flt3 and vascular cell adhesion molecule 1 (VCAM-1) expression (Lai et al, 2006). In the small fraction of $Flt3^{hi}$VCAM-1^{-} multipotent progenitors Lai et al. identified cells which express CCR-9, a receptor for CCL-25. The $Flt3^{hi}$VCAM-1^{-}CCR-9^{+} migrate into the thymus and had the capability to differentiate into B-, T- and dendritic cells. Furthermore, they express Notch1

and Hes1, a direct downstream target of Notch1, in a higher level than their counterpart Flt3hiVCAM-1$^-$CCR-9$^-$ (Lai et al., 2007). Although CCR-9 knockout revealed no deficiency in the thymocytes development, competitive reconstitution of CCR-9 knockout bone marrow revealed that CCR-9 enables superior repopulation by bone marrow progenitors (Uehara et al., 2002, Schwarz et al., 2007). It is possible that CCL-25/CCR-9 mediated cell attraction may have therefore only a synergistic effect on recruitment of thymocyte precursors.
For the homing of the T-cell precursors CXCL-12, a ligand of CXCR-4, has been identified (Bleul et al., 2000). CXCL-12 and its receptor CXCR-4 deficient mice have a similar phenotype which is an impaired expansion of thymocytes subpopulations during embryogenesis resulting in decreased numbers of CD3$^-$CD4$^-$CD8$^-$ (DN1) and CD4$^+$CD8$^+$ (DP) thymocytes. This demonstrates not only the important role of CXCL-12 in the migration progress, but also its critical role for the migration of T-cells from medulla to cortex for normal T-cell development. Furthermore CXCL-12 has been implicated in homing of bone marrow derived precursors (Ara et al., 2003). In postnatal thymus CXCL-12 is expressed in medulla and on scattered cells in the cortex (Misslitz et al., 2004). During embryonic development of the thymus CXCL-12 is expressed at E12.5 onward (Bleul et al., 2000).

Using additional cell surface markers, the population of DN cells can be further subdivided in the mouse into at least four distinct populations. The most immature population of T-cells (known as DN1) is defined by the cell surface expression of CD44 (phagocyte glycoprotein-1/Pgp-1), CD117 (c-kit, tyrosine kinase receptor for stem cell factor), CD127 (IL-7 receptor α-chain), and CD90 (Thy-1) but with the notable absence of CD25 (IL-2 receptor α chain) (Godfrey and Zlotnik, 1993; Wu et al., 1991). The expression of CD25 marks the progression from DN1 to a DN2 (CD44$^+$CD25$^+$) stage in thymocyte development (Godfrey et al., 1993). This developmental stage is characterized by the start of the rearrangement of the β-, γ- and δ-loci of the T-cell receptor (TCR) (von Boehmer and Fehling, 1997). The subsequent loss of CD44 expression defines the DN3 (CD44$^-$CD25$^+$) stage of early T-cell development. DN3 population lack CD117 expression and have completed their rearrangement of the β-, γ- and δ-locus. These cells are now in the position to either express a pre-TCR consisting of a successfully rearranged β-chain plus the surrogate, invariant TCR α-chain (pTα, gp33) or, alternatively, to express a complete γ/δ TCR. Thymocytes that are unsuccessful in expressing any of these two receptors fail to receive survival signal and consequently undergo apoptosis before transiting to the DN4 (CD44$^-$CD25$^-$) cell stage. In contrast, cells that successfully express the pre-TCR on their cell surface begin to proliferate, and reach the developmental

stage of $CD4^+CD8^+$ (double positive, DP) thymocytes. The majority of developing thymocytes have a DP phenotype.

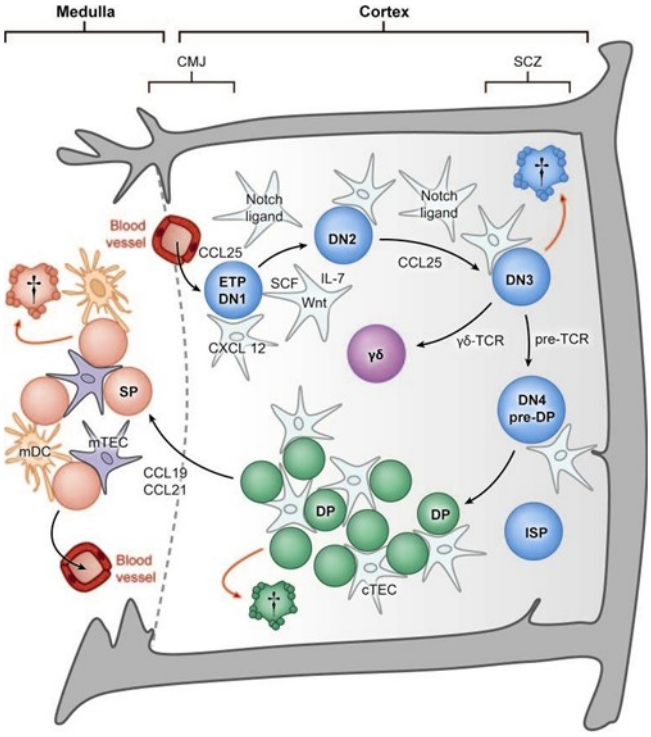

Figure 1.4 Development of T-cell in the thymus. The thymus consists of two distinct regions: medulla and cortex. Each contains specialized thymic epithelial cell subsets. The hematopoietic precursors enter the thymus via the cortico-medullary junction (CMJ). Thymocytes differentiation can be followed phenotypically by the expression of cell-surface markers, CD4, CD8, CD44, CD25 and CD3. (DN1: $CD44^+CD25^-$; DN2: $CD44^+CD25^+$; DN3: $CD44^+CD25^-$; DN4: $CD44^-CD25^-$). During the maturation these cells travel from the CMJ to through the cortex to the sub-capsular zone (SCZ). (The figure has been adopted from Takahama *et al*., 2006)

These cells have successfully rearranged their TCRβ-locus and are rescued from apoptotic cells death and selected for further maturation, before TCRα expression, by signaling through a pre-TCR composed of the TCRβ chain paired with a pre-TCRα (pTα) chain and associated with CD3 (Groettrup et al., 1993; Saint-Ruf et al., 1994; Fehling et al., 1995; von Boehmer et al., 1997). Mice that fail to express a TCRβ-chain exhibit impaired DN-double positive transition while recombination-activating gene (RAG)-1 or RAG-2 deficient mice have complete arrest at the $CD44^{lo}CD25^+$ stage (Moore et al., 1996). The stage of DP thymocytes follows that of DN cells and is attained via a transitional intermediary phenotype referred to as immature single positive (ISP) cells. At the ISP-stage, immature thymocytes express either CD4 or CD8 and are distinguished from mature single positive thymocytes by their lower cell surface expression of their TCR β-chain (Paterson and Williams, 1987; Yu et al., 2004). The ISP to DP transition leads to the generation of a large pool of DP thymocytes (Yu et al.,

2004). At the ISP stage of maturation, the rearrangement of the TCRα-locus is initiated which coincides with cell`s active phase of proliferation. No rearrangement of the α-locus occurs until the proliferation phase has ended. This sequence of events ensures that each successful TCRβ-chain rearrangement gives rise to many DP thymocytes. In consequence, DP cells with identical TCRβ-chain will independently rearrange their α-chain locus so that eventually a single DN4 cell with an unique TCR-β chain will express a diverse repertoire of α-chains. Each of these cells can independently rearrange their α-chain genes once the cells stop dividing, so that a single functional β-chain can be associated in the progeny of these cells with many different α-chains. The expression of α/β TCR allows now for positive thymic selection by peptide/MHC complexes.

1.3.3 Positive and negative selection in the thymus

DP thymocytes are subjected to consequence of selection processes so that only mature T-cells are exported from the thymus which are functional and self-tolerant. In this context, the terms positive and negative selection denote two separate but interconnected steps in selection of a correct TCR repertoire. Positive and negative selection are both dependent on lymphostromal interactions within the thymus (Anderson et al., 1999; Chidgey and Boyd, 2001; Jameson and Bevan, 1998; Klein and Kyewski, 2000; Sebzda et al., 1999). Positive selection occurs if the TCR on DP thymocytes engages with a sufficient high affinity a self-MHC ligand on cortical TECs. Such interaction and their signal(s) will result in the survival and further differentiation of DP thymocytes (Bevan, 1997; Palmer et al., 1993; von Boehmer et al., 1997). Cells either unable to recognize any peptide-MHC-ligand with a lower affinity than required for positive selection will die by a process known as death by neglect. (Boursalian et al., 1999; Raff, 1992; Sprent et al., 2001). Upon positive selection of the DP, they develop further to $CD4^+$ or $CD8^+$ single positive (SP) cells. Transcriptions factors which are involved in the fate determination of $CD4^+$ and $CD8^+$ cells were characterized. RUNX1 and RUNX3 a member RUNX (runt-related transcription factor) family and Th-POK/c-Krox (T-helper-inducing POZ/Kruppel-like factor) have been in the focus of recent studies. Furthermore, GATA-3 binding protein 3 (GATA-3) and thymocyte selection-associated highly mobility group box (TOX), are crucially involved in the CD4/CD8 lineage decision. RUNX1 and RUNX3 sequentially interact with the *Cd4* silencer (Taniuchi et al., 2002). Germline deletion of the *Cd4* silencer resulted in de-repression of CD4 expression in both DN thymocytes and $CD8^+$ T-cells (Leung et al., 2001, Zou et al., 2001), but the conditional

deletion of the *Cd4* silencer in mature $CD8^+$ T-cells did not cause de-repression of CD4 expression (Zou et al., 2001). At the DN stage, *Cd4* silencer may act to actively repress *Cd4* transcription, but it is dispensable for keeping *Cd4* silenced in peripheral $CD8^+$ cells (Taniuchi et al., 2004). RUNX1 was found to bind to *Cd4* silencer in DN cells and RUNX3 to bind to the *Cd4* silencer in $CD8^+$ positive cells (Taniuchi et al., 2002). RUNX3 expression is up regulated during the differentiation of $CD4^+CD8^{low}$ thymocytes into $CD8^+$ T-cells (Dave et al., 1995). There, RUNX3 binds to the *Cd4* silencer element and silences *Cd4* gene transcription (Taniuchi et al., 2002) and RUNX3 binds also to the *Cd8* enhancer element and reinitiate *Cd8* transcription (Sato et al 2005). Additionally, RUNX proteins bind to a sequence in the gene of Th-POK and extinguished Th-POK expression thus promoting $CD8^+$-T-cell differentiation (Setoguchi et al., 2008). Regarding TOX Aliahamd et al. and Hedrick et al. have shown that TOX is important for maintaining or up-regulating CD4 expression in positively selected DP thymocytes (Aliahamd et al., 2008, Hedrick et al., 2008). TOX-deficient thymocytes do not become $CD4^+CD8^{low}$ cells but instead become $CD4^{low}CD8^{low}$ and failed to become $CD4^+$ cells (Aliahamd et al., 2008). GATA-3 is mainly expressed in the $CD4^+$ cells and has been therefore suggested to be important for CD4 lineage commitment (Hendriks et al., 1999). The deletion of GATA-3 in DP cells markedly reduced the $CD4^+$ population (Pai et al., 2003) but it is not a lineage specific factor since forced expression of GATA-3 does not redirect MHC class-I restricted thymocytes to differentiate into $CD4^+$ T-cells (Hernadez et al., 2003). Positive thymic selection is effected by cTECs. Using reaggregated thymic organ cultures (RTOC), it has been well established that MHC class II positive cTECs are both necessary and sufficient for positive selection of DP of the α/β TCR lineage to $CD4^+$ SP cells (Anderson and Jenkinson, 1997; Anderson et al., 1997). After the positive selection thymocytes migrate from the cortex into the medulla. This migration is mediated by chemokines CCR-7 which is expressed on SP thymocytes that past positive selection (Adachi et al., 2001). CCR-7 ligands CCL-19 and CCL-21 are expressed on medullary epithelial cells (Ueno et al., 2004).

The main function of negative selection which commonly occurs in mTEC is to remove strongly self-reactive T-cells which have a high affinity/avidity for MHC-self-peptide complex (Kappler et al., 1987, Kisielow et al., 1988). This way negative selection prevents the peripheralization of most auto reactive antigen (Mathis et al., 2004). But Huseby et al. have shown in their study that this might not be the only function of negative selection. They studied the effect of a reduction of negative selection on TCR specificity, by examining the

proliferative response of mature immortalized T-cells resulting from various thymic developmental conditions. When negative selection, but not positive selection, was mediated by a single MHC-peptide complex, the resultant TCRs were partially highly cross-reactive for many different peptide-MHC complexes. This study demonstrated that, after TCR rearrangement, most T-cells display a very high affinity for MHC. They concluded that the negative selection is involved in focusing T-cell response on foreign peptides bound to self rather than foreign MHC alleles and that germline-encoded TCR segments are predisposed to react with a feature(s) shared among all MHC proteins (Hersby et al., 2005).

A most basic requirement of negative selection is the thymic expression and presentation of self-antigen to developing thymocytes. The importance of thymic peripheral antigen expression is controlled by the gene AIRE, Anderson et al. demonstrated that AIRE-deficient mice had reduced expression of peripheral antigens in the mTECs (Anderson et al., 2002). Further studies have revealed that although mTECs provide the antigen, thymic dendritic cells were capable of capturing the antigen and presenting it to both MHC class I- and II-restricted thymocyte to induce negative selection (Gallegos et al., 2004). For the negatively selected thymocytes Bcl-2 family members Bim, Bax and Bak are implicated to be involved in the induction of apoptosis. Mice deficient of Bim or combined deficiency of Bax and Bak, can cripple negative selection (Bouillet et al., 2002, Rathmell et al., 2000).

1.3.4 The final step: export from the thymus

After positive and negative selection are completed the correctly selected T-cells exit from the medulla or cortico-medullary junction, but for emigration it is not a prerequisite for the T-cells to be in medulla or cortico-medullary junction. In adult mice CCR-7 up-regulation after positive selection mediates thymocytes migration to the medulla. CCR-7 or CCR-7 ligand deficient mice generate SP thymocytes that do not traffic to the thymic medulla. Nonetheless, CCR-7 deficient thymocytes are able to emigrate directly from the cortex (Ueno et al., 2004). Treatment with FTY20, an inhibitor of thymocyte emigration, let to the accumulation of CCR-7 WT SPs in medullary perivascular spaces (Kurobe et al., 2006). Thus, the perivascular space in the medulla and cortico-medullary junction may not be the vessels used for thymocyte egress. Studies of egress from fetal thymic organ cultures suggested that CCR-7 plays a role in the neonatal period (Ueno et al., 2002). Furthermore, disruption of stromal cell-derived factor (SDF)-1/CXCR-4 interaction by genetic deficiency or pharmacologically with AMD3100 led to a decreased migration in fetal thymic organ culture. *In vivo* treatment with

AMD3100 in newborn mice led to accumulation in the thymus of CD4 SP and fewer CD4 T cells in spleen (Vianello et al., 2005). Emigration of CD8 SP was not affected, so CD4 and CD8 may differ in their thymic emigration requirements, at least in the neonatal period. Another interesting candidate which might play a role in thymocyte emigration is CD69. Feng et al., have shown that constitutively expression of CD69, an early activation marker, inhibit the export of mature SP from the thymus (Feng et al., 2002) similar to FoxJ1, a transcription factor, transgenic mice which also showed an impaired thymic exodus (Srivatsan et al., 2005). More recent studies have discovered that Krüppel-like factor (KLF) 2 as well is involved in thymocyte emigration. The thymus development of the KLF-2 deficient mice is normal but the mature thymocytes are not capable to leave the thymus (Carlson et al., 2006).

1.4 GATA binding protein-2 (Gata-2)

In this study, Gata-2 was identified as a potential candidate to be involved in early thymus development. Therefore, a short overview of the Gata-2 and their family members is given.

1.4.1 Gata proteins

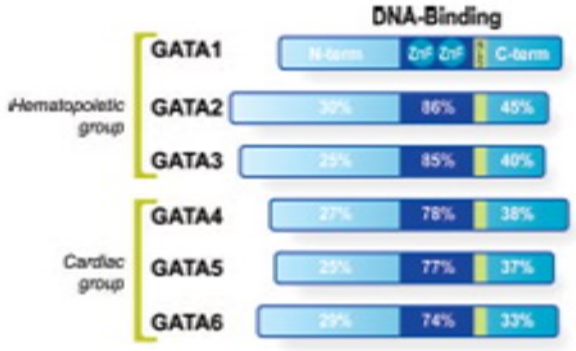

Figure 1.5 Structure and homology of the vertebrate Gata proteins. All Gata factors share a similar zinc finger binding domain. (The figure has been adopted from Viger et al., 2009)

Gata factors are a group of evolutionarily conserved transcriptional factors that play crucial roles in the development and differentiation of all eukaryotic organisms. All Gata members are capable to recognize and bind to a specific DNA sequence WGATAR (W = A or T and R = A or G). In vertebrates, the Gata family comprises six members (from Gata-1 to Gata-6) that can be separated into two subgroups based on spatial and temporal expression patterns. Gata-1,-2,-3 are expressed in hematopoietic cell lineages and are essential for erythroid and megakaryocyte differentiation, the proliferation of hematopoietic stem cells, and the development of T-cells (Weiss et al., 1995). However, their expression is not limited to hematopoietic cells but is also present in brain, spinal cord and inner ear where they play a role in the development of these structures

(George et al., 1997; Nardelli et al., 1999; Lillevali et al., 2004). In contrast, the Gata-4,-5,-6 proteins are mainly found in tissues of mesodermal and endodermal origin such as the heart, gut and gonads (Molketin et al., 2000). Disruption of Gata-4 and Gata-6 genes in mice results in early embryo lethality due to defects in the heart tube formation and extra embryonic endoderm development (Kuo et al., 1997; Morrisey et al., 1998; Koutsourakis et al., 1999). Gata-5 deficiency is not lethal but the female exhibit genitourinary abnormalities (Molketin et al., 2000). The transcription factor Gata-1 is essential for erythroid differentiation as it activates all the known erythroid-specific genes upon binding to specific DNA-motifs (Shimizu et al., 2005; Crispino et al., 2005). Mice deficient of Gata-1 die from severe anemia (Pevny et al., 1991). In contrast to other Gata members, Gata-3 is the only gene that has been associated with the immune-system. Because Gata-3 deficient mice die between E11 and E12 postcoitum due to severe abnormalities in the nervous system and in fetal liver hematopoiesis (Pandoffi et al., 1995) conditionally deficient mice of Gata-3 were generated and studied using the cre-lox system. When Gata-3 was deleted using G3-lckCre, a cre recombinase driven by the proximal lck promoter, Th-cells failed to differentiate into Th2 cells (Pai et al., 2004). These studies showed that Gata-3 is sufficient to direct the differentiation of Th cells into the Th2 pathway. Furthermore, Gata-3 is necessary for optimal β-selection. The DN3 to DN4 transition is dependent on successful β-selection which requires successful rearrangement and expression of TCRβ chain to couple with pTCRα. In Gata-3 deficient DN3 cells the TCRβ chain was significantly diminished (Pai et al., 2003).

1.4.2 Gata-2 and Endothelin-1

Gata-2 was cloned in 1990 (Yamamoto et al., 1990). Gata-2 is expressed at the stem and progenitor stage, including erythroid lineage, in hematopoiesis. In addition, Gata-2 transcripts are also present in the embryonic brain, endothelial cells, urogenital organs, liver, and cardiac muscle. Since the expression of Gata-2 is strongest in stem and progenitor level, Gata-2 deficient embryos failed to survive beyond the stage of primitive hematopoiesis (Tsai et al., 1995). The analysis in of Gata-$2^{+/-}$ showed that Gata-2 haploinsufficiency leads to the reduced number of hematopoietic stem cells and increased percentage of apoptotic cells (Rodrigues et al., 2005). But so far no functional evidence of Gata-2 in thymic epithelial cells has been implicated.

In contrast to Gata-2, the importance of Endothelin-1 (Edn-1) in thymus development, however, has been described. So far three isoform of Edn molecules have been described

Edn-1, -2, -3 and two Endothelin receptors Edn-Ra and Edn-Rb. These receptors have different affinity for endogenous ligands (Inoue et al., 1989; Masaki et al., 2005). Edn-Ra has a high affinity for Edn-1 and Edn-2 while Edn-Rb has equal affinity to all three Edn isoforms (Arai et al., 1990; Sakurai et al., 1990; Ihara et al. 1992). Edn-1 is a 21 amino acid vasoactive peptide initially characterized as a product of endothelial cells of the vascular wall (Yanagisawa et al., 1988). Edn-1 is expressed in the epithelium and mesodermal core of the pharyngeal arches while its receptor Edn-Ra is expressed in neural crest-derived ectomesenchyme. In mice the expression of Edn-1 and Edn-Ra can already be detected at the developmental stage of E9.5. Defects in Edn-1/Edn-Ra pathway result in the malformation of pharyngeal-arch-derived craniofacial structures in mice (Clouthier et al., 1998; Kurihara et al., 1995, 1994; Maemura et al., 1996). Edn-1 deficient mice die shortly before birth due to mechanical obstruction of the upper airways and inability to open the mouth because of poor musculature in the mandibular region. Edn-1 and Edn-Ra deficient mice have abnormalities in all organs developed from the pharyngeal arches whose origin is mainly neural-crest derived like the mandible, thyroid, tongue, middle and outer ear, temporal bones and the thymus which is hypoplastic and displaced (Kurihara et al., 1995; Clouthier et al., 1998; Sato et al., 2008). These finding strongly suggest that Edn-1 and Edn-Ra may participate in the epithelial-mesenchymal interactions to promote pharyngeal pouch development.

The Edn-1 promoter contains at least two essential protein binding motifs. One of these, TTATCT, is located at bp -136 to -131, upstream of the start site and is similar to other eukaryotic sequences known to interact with one or other Gata factors (Lee et al., 1991). The other motif, TGACTAA, is positioned at bp -108 to -102 and binds Jun and Fos family members (Lee et al., 1991). Co-transfection of endothelial cell line with Gata-2, c-Jun and c-Fos expressing plasmids has then demonstrated to transactivate the Edn-1 promoter of a reporter plasmid (Kawana et al., 1995). These *in vitro* studies indicate that Gata-2 is capable to control the expression of Edn-1.

II. Thesis Objectives

2.1 Analysis of the gene expression of the cells from the ventral aspect of the third pharyngeal pouch at E10.5 using the Affymetrix Gene Chip

The genetic program which drives the thymic epithelial cell fate and the differentiation is still ill defined. Therefore, the aim of this project is to characterize the genetic program that determine thymic epithelial cell fate and differentiation and, in particular, new genes critically involved in this process. For this reason genetic expression profile of the cells from the ventral aspect of the 3rd pp is analyzed using the Affymetrix Gene Chips at the time point of E10.5 of gestation.

2.2 Verification of the Affymetrix Gene Chip data

Although Gene Chips represent a very reliable and standardized technology significant noise which can arise from the unreliable hybridization reaction can falsify the results (Greco et al., 2007). Therefore, the second objective of the thesis is to confirm the gene expression data using RT-PCR and in situ hybridization and to find an appropriate candidate for further detailed analysis.

2.3 *In vivo* study by deleting a candidate gene specifically in the thymic epithelial cells and assess the genes function in thymic epithelial functionality and development

Once a candidate gene is identified, it is important to study its function in the thymic epithelial cells. The most effective way is to abrogate the expression of the candidate gene specifically in the thymic epithelial cells using the cre-lox system. The third objective is to interrupt the expression of the candidate gene using the Foxn1 promoter driven cre which is specifically expressed in the TEC and to study the consequence of the aborted gene expression in the TEC development and function.

III. Material and Methods

3.1 Materials

3.1.1 Mice

The C57BL6, B6;D2-Tg(Foxn1-Cre)8Ghr,designated Foxn1-Cre, and B6.Gata-2$^{loxP/loxP}$ were housed in our animal facility in the accordance with Institutional and Cantonal Review Boards. B6.Gata-2$^{loxP/loxP}$ mice were kindly provided by Dr. S.H. Orkin (Bosten, MA, USA). For developmental staging, the day of the virginal plug was designated as E0.5.

3.1.2 Tissues

Tissues were obtained from adult mice and embryos at distinct developmental stages. Mouse embryos at E10.5 and thymi of 3, 6, 13 and 25 weeks old mice were embedded in optimum cutting temperature (O.C.T.) (Tissue-Tec, Miles, Elkhart, IN) and dissected into 10µm for laser dissection and 6µm for hematoxylin and eosins staining (H&E) and immunohistochemistry analysis.

3.1.3 Cell lines

The following cell lines were used as part of this thesis work:

Cell line	Origin	Reference
cTEC 1.2	Mouse thymic cortical epithelium	(Kasai *et al.*, 1996)
cTEC 1.4	Mouse thymic cortical epithelium	(Kasai *et al.*, 1996)
cTEC C9	Mouse thymic cortical epithelium	(Kasai *et al.*, 1996)
mTEC 2.3	Mouse thymic medullary epithelium	(Kasai *et al.*, 1996)
mTEC 3.10	Mouse thymic medullary epithelium	(Kasai *et al.*, 1996)
mTEC C6	Mouse thymic medullary epithelium	(Kasai *et al.*, 1996)
HEK293	Human kidney	(Graham *et al.*, 1977)

Cells were grown at 37°C and in 5% CO_2 in Iscove`s Mod. Dulbecco`s Medium (IMDM) containing 2% fetal calf serum (FCS). To detach cell from vessels, cells were incubated for 2-3 minutes in undiluted Trypsin solution (Invitrogen Cooperation, Basel, CH).

3.1.4 Cell cultures, plastic ware and chemicals

IMDM was supplemented with 2.2g $NaHCO_3$ (Invitrogen Cooperation, Basel, CH) and 15mL of 200mM L-Glutamine (Invitrogen Cooperation, Basel, CH). Additional supplements were employed according to the specific requirements (see 3.1.4.1 and 3.1.4.2). Sterile disposable plastic ware for tissue culture was purchased from Falcon Labware (Oxnard, CA, USA). Chemicals were purchased from Fluka (Buchs, Switzerland), Sigma (St. Louise, MO, USA) and other commercial venders as indicated.

Supplements for thymic epithelial cells

For 1000mL of IMDM for TECs, 10mL of 1M Hepes, 1mL of Gentamycin (50mg/mL) and 100 mL of FCS were added.

Supplements for HEK 293 cells

For 1000mL of media for HEK 293 cells, 20mL of FCS and 100µL of β-Mercaptoethanol (1M) were added.

3.1.5 Statistical evaluation of data

For the analysis of the obtained data from qRT-PCR and fluorescence activated cell sorting student`s t-test was applied whenever possible.

3.1.5 Antibodies

Used in FACS:

Antibody	Clone	Source
Anti-CD44 PE	IM7	eBioScience
Anti-CD25 FITC	PC61.5	eBioScience
Anti-c-kit APC	2B8	eBioScience
Anti-CD19 Biotin	ID3	Generated in the lab
Anti-CD4 Biotin	GK1.5	eBioScience
Anti-Gr1 Biotin	RB6.8C5	eBioScience
Anti-NK1.1 Biotin	PK136	eBioScience
Anti-CD3ε Biotin	145-2C11	eBioScience
Anti-CD8 Biotin	53-67.2	eBioScience
Anti-CD11c Biotin	N418	eBioScience
Anti-CD11b Biotin	H1/70	eBioScience
Anti-CD4 PE	GK1.5 RM4-5	eBioScience
Anti-CD24 FITC	M1/69	eBioScience
Anti-CD3	1452 CLM	Generated in the lab
Anti-CD3 Cy5	KT3	Generated in the lab
Anti-CD8 PeCy7	53-67	BioLegend
Anti-CD69 FITC	H1.2F3	eBioScience
Anti-CD62L FITC	HEL-14	eBioScience
Anti-MHCII FITC	AF6-120.1	eBioScience
Anti-G8.8 Bio	G8.8	Generated in the lab
Anti-CD45 APC	30-F11	eBioScience
Anti-SA PE	According to company not given	eBioScience
Anti-SA PeCy7	According to company not given	eBioScience

Used in immunohistology:

Antibody	**Clone**	**Source**
Anti-CK5, rabbit		
Anti-CK8, goat		
Anti-ERTR7,		

Used in whole mount in-situ hybridization:

Antibody	**Source**
Anti-Digoxigenin Fab	Roche Biochemicals

3.1.6 Standard buffers

The buffers were prepared according to manufacturer's manuals or have been purchased directly from the supplier.

Name	**Composition**
FACS Buffer	2% BSA, 0.1% NaN_3 in PBS
Saline sodium citrate (SSC) (Eurobio)	150 mM NaCl, 15mM Na-Citrate
Tris-acetate-EDTA (TAE)	40mM Tris/Acetate, pH 8.0, 1mM EDTA
Tris-EDTA (TE)	10mM Tris/Cl, pH 8.0, 1mM EDTA
Phosphate buffered saline 1x (PBS)	0.14M NaCl, 2.7mM KCl, 6.5mM Na_2HPO_4, 1.5mM KH_2PO_4, pH 7.3, autoclaved
20% Paraformaldehyd (PFA)	2g electron microscopy-grade para-formaldehyd in 10mL PBS and 10µL 10M NaOH.
Maleic acid buffered tween (MABT)	100mM maleic acid, 150mM NaCl, 0.1% Tween 20, pH 7.5
Phosphate buffered salin with tween (PBT)	0.1% Tween in PBS

3.2 Methods

3.2.1 Laser capture micro dissection

The preparation of the tissue for LCM was carried out as follows:

- Embryos were immediately removed from the euthanized pregnant mice of E10.5 days of gestation and rapidly frozen in O.C.T. (Tissue-Tec, Miles, Elhart, IN) using a plastic support submerged in a mixture of dry ice (stored at -80°C until use) and a few mL of isopentyl (Fluka, Buchs, CH).
- For sectioning by the cryotome (Roche, Basel, CH) the embedded tissue was placed onto the support block at -20°C with some O.C.T.. Once O.C.T. was solidified, each edge of the block was cut with a razor blade to form a small rectangular shape.
- The 10µm thick sections were mounted on glass slides covered with a 1mm thin polyethylene foil (PALM Microlaser Technologies, Germany) which were treated first with RNaseZap (Ambion, CA, USA) and then UV radiated in a cell culture sterile hood for 30-60 min.
- The sections were dried in air for 2 minutes and ethanol (Fluka, Buchs, CH) fixed for 45s.
- The sections were fixed and stained for 1 min in a solution in which cresylviolette was dissolved in 100% ethanol and washed for few seconds in 70% ethanol and dehydrate in 100% EtOH for 1 min.
- After a short drying on air (couple seconds) the sections were kept in -80°C until they were needed.

Only DEPC-treated water was used to prepare the different ethanol containing solutions and all working space was cleaned with RNaseZap to avoid contamination with RNases.

- The tissue of interest was micro dissected using the laser of the microscope according to the manufacturer's recommendations
- The micro dissected tissue was catapulted by slight increasing the energy (Δ5-10 U) of the laser.
- All micro dissected tissues were catapulted in to the PALM AdhesiveCaps (PALM Microlaser Technologies, Germany).

- At the end of each LCM session which last at maximum one hour the cap was closed and resuspended immediately in cell lysis buffer or Trizol.

3.2.2 Total RNA extraction for micro dissected tissue

For the RNA isolation the RNAeasy Micro Kit (Qiagen AG, Hombrechtikon, Switzerland) was used. In short:

- 350µL of cell lysis buffer were added to the laser captured cells and vortexed for 20 sec.
- 350µL of 80% ethanol were added and applied to the columns provided
- The columns were spun at 14000g for 20 sec. This step was repeated one more time using the flow through
- DNase was added according to the manufacturer's recommendation
- The columns were washed by adding 750µL of RLT buffer and spun at 14000g for 20 sec.
- 500µL of RPE buffer were added and spun at 14000g for 20 sec.
- 750µL 80% ethanol were added and spun at 14000g for 2 min.
- The columns were dried by spinning it at 14000g for 5 min.
- 14µL of RNase free water were added and spun at 14000g for 1 min. This step was repeated using the flow through

3.2.3 Two round Amplification of RNA and synthesis of cRNA

- Day1: Total RNA was resuspended in 1µL RNase free water and 1µL T7-oligo (5µM) were thoroughly mixed in 0.5mL tube and incubated at 70°C for 6 min and cooled for 2 min on ice and spun down at 12.000g for 20 sec.
- 3µL of RT-Premix 1 were added to the RNA and mixed thoroughly and spun full speed at 4°C for 10 sec.
- The samples were than incubated at 42°C for 1 h and after that incubated at 72°C for 10 min.
- SS Premix 1 was prepared and 32.5µL (final volume 37.5µL) of the SS Premix 1 were added to each sample tube and mixed thoroughly and spun for 10 sec at 4°C.

- The samples were then incubated at 16°C for 2 h. After that, 1µL of DNA polymerase (5U/µL) was added to each sample tube, mixed and incubated for 10 min at 16°C.
- The samples were then transferred into a fresh 1.5mL tube and 104µL of RNase free water were added.
- In order to precipitate the cDNA 2µL of glycogen (5mg/mL) than 48µL of 7.5 M Ammonium-acetate and finally 480µL of pre-cooled (-20°C) absolute ethanol were added and mixed thoroughly.
- The cDNA was spun at 12.000g at 4°C for 20 min and the supernatant was removed.
- The cDNA was washed with 800µL pre-cooled (-20°C) 70% ethanol and centrifuged at 12.000g for 5 min.
- Supernatant was removed and the pellet was dried for 5-10 min and the pellet was dissolved in 2µL RNase-free water.
- Day2: 7µL of IVT Premix 1 were added to each sample (final volume 9µL), mixed, and incubated at 40°C for 5 min. 1µL of enzyme mix was added and the samples were placed into a pre-warmed 37°C box and left at 37°C for 6 h. Every hour the sample tubes were mixed and spun down at 12.000g for few seconds and then placed back into 37°C.
- 90µL RNase-free water were added to the cRNA product, mixed and spun.
- To purify the cRNA 350µL of RLT buffer (Qiagen, AG, Hombrechtikon, Switzerland) were added and mixed with 250µL 100% ethanol.
- The samples were loaded onto RNeasy mini column (Qiagen, AG, Hombrechtikon, Switzerland) and spun for 20 sec at 12.000g at 4°C. In order to increase the yield the flow through was reloaded and this step was repeated.
- The columns were washed with 500µL of RPE buffer (Qiagen, AG, Hombrechtikon, Switzerland) and spun for 20 sec at 12.000g at 4°C. The flow through was discarded. This step was repeated one more time.
- The columns were dried by spinning them for 1 min 12.000g at 4°C and after that column were transferred to a new 1.5mL tube.
- 30µL of RNase free water were added onto the center of the column, incubated for 3 min at room temperature and spun 1 min 12.000g at 20°C. The column was reloaded with 30µL of RNase free water and re-eluted.

- The concentration of RNA was calculated from the OD measurement at 260nm wave length.
  260/280 ratio was used to determine the quality of the cRNA.
- The purified cRNA was transferred into a new 0.5mL tube and the total volume was reduced using speed-vacuum to a final volume of 4µL.
- Day 3: 1µL of random primers (0.2µg/µL) was added to the cRNA and mixed and incubated at 70°C for 10 min and incubated on ice for 2 min and spun for 20 sec at 12.000g at 4°C.
- 5µL of RT Premix 2 were added (final volume 10µL) and mixed gently and incubated first at 25°C for 10 min and then at 42°C for 1 hour.
- In order to remove the RNA template, 1µL of RNase H (2U/µL) was added and incubated at 37°C for 20 min and finally incubated at 95°C for 5 min to inactivate the RNaseH. The samples were cooled down immediately on ice for 2 min and spun for 20 sec at 12.000g at 4°C.
- 2µL of T7-Oligo (5µM) primer were added to the samples and incubated at 70°C for 6 min. The samples were cooled on ice for 2 min and spun for 20 sec at 12.000g at 4°C.
- After that, 62µL of SS Premix 2 were added to each sample (final volume 75µL), mixed and incubated at 16°C for 2 h.
- 2µL of T4 DNA polymerase 5U/µL (Invitrogen, USA) were added to each tube and incubated for 10 min at 16°C.
- The reaction was transferred to 1.5mL tube and 15.7µL of RNase-free were added.
- To precipitate the cDNA 2µL of glycogen (5mg/mL) then 48µL of 7.5 M Ammonium-acetate and finally 480µL of pre-cooled (-20°C) absolute ethanol were mixed together.
- The cDNA was spun at 12.000g at 4°C for 20 min and the supernatant was removed.
- The cDNA was washed with 800µL pre-cooled (-20°C) 70% ethanol and centrifuged at 12.000g for 5 min.
- Supernatant was removed and the pellet was dried for 5-10 min and the pellet was dissolved in 20µL RNase-free water by shaking for 5 min at 40°C. The cDNA was spun at 12.000 g at 4°C.
- 20µL of IVT Premix 2 (see below) were added to a final volume 40µL, mixed and incubated for 16 hours at 37°C.

- Day 4: 60µL of RNase-free water were added to the samples and mixed.
- The samples were loaded onto RNeasy mini column (Qiagen, AG, Hombrechtikon, Switzerland) and spun for 20 sec at 12.000g at 4°C. In order to increase the yield the flow through was reloaded and this step was repeated.
- The columns were washed by applying 500µL of RPE buffer (Qiagen, AG, Hombrechtikon, Switzerland) and spun for 20 sec at 12.000g at 4°C. The flow through was discarded. This step was repeated one more time.
- The columns were dried by spinning it for 1 min 12.000g at 4°C and after that columns were transferred to a new 1.5mL tube.
- 50µL of RNase free water were added into the center of the column, incubated for 3 min at room temperature and spun for 1 min 12.000g at 20°C. The columns were reloaded with 50µL and re-eluted.
- The OD at 260nm wave length was measured for the calculation of concentration and the samples were stored at -80°C until needed.

3.2.3 Quantitative PCR (real time PCR)

The primers for qRT-PCR were designed so that the amplicon were relatively short in size (< 250bp) to ensure a maximum amplification. Primers pairs were ordered from Sigma-Aldrich, USA and Microsynth, Switzerland. The primers were designed using FastPCR 4.0. The amplified products were loaded on a 1% agarose/ethidium bromide gel for verification of the amplicon size.

- Depending on the concentration of the cDNA 1-4 µL of cDNA were added, 1µL (10µM) of the forward primer, 1 µL (10µM) of reverse primer and 6µL of 2x SybrGreen master mix (Qiagen AG, Hombrechtikon, Switzerland) and water were mixed to the final volume of 12µL. The sequence of the respective used primers can be found in Appendix 1.

The real-time PCR was performed using Rotor-Gen (Corbett Research, Australia) and the RT-PCR data analysis was performed using Rotor-Gen 6 (Corbett Research, Australia).

<u>Two round amplification of the total RNA:</u>

PCR conditions: The reactions were incubated for 10 min at 95°C and subsequently for 15 sec at 95°C and 1 min at 60°C, for the denaturation, the annealing and the elongation of amplificons, respectively. These subsequent steps were repeated 40 times.

Analysis:

The baseline of the amplification plot was selected from cycle 6 to cycle 15 (default settings). In case the measured fluorescence was detected earlier than cycle 15, the baseline was adjusted appropriately according the manufacturer's instructions as well as the threshold for the C_t values. The specificity of the amplicons was verified by loading the samples on a 1% agarose/ethidium bromide gel. Only samples with the proper amplicon size were considered for the calculation of the C_t values.

The $\Delta\Delta C_t$-value was calculated as following:

$\Delta\Delta C_t = \Delta C_t^1$ (RT-data from condition 1) - ΔC_t^2 (RT-data from condition 2) where ΔC_t = Ct gene of interest – Ct housekeeping gene e.g. GAPDH

The fold change in RNA expression levels was calculated as following:

Fold change = $2^{\Delta\Delta Ct}$

3.2.4 Total RNA extraction and RT-PCR for non-micro dissected tissues

Isolation of total RNA:

- The extracted tissue was homogenized in 1mL Trizol reagent per approx. 100 mg tissue using a Polytron homogenizer for 20-30 sec. If the total RNA was isolated from cell cultures or from purified thymocytes or from TECs, 1mL of Trizol reagent was resuspended with 10^4-10^6 cells. In case of less than 10^4 cells, the RNAeasy Micro Kit was used. 100µL of BCP were added to the mixture and mixed for 30 sec.
- Next, the mixture was incubated at room temperature for 5 min, centrifuged at 12,000g for 15 min at 4°C in a micro-centrifuge. The aqueous phase was transferred into a new 1.5mL tube and 500µL of isopropanol (Sigma, Buchs, Switzerland) was added. The mixture was then left for 15 min at the room temperature for precipitation of the RNA.
- The RNA was then centrifuged at 12,000g for 15 min at 4°C. The supernatant was removed, the RNA pellet was washed afterwards with 75% ethanol (Fluka, Buchs, CH) and centrifuged at 12,000g for 5 min.

- The supernatant was removed and the pellet was allowed to dry for 5 min under in a RNase free environment. The RNA pellet was then resuspended in 20-50µL of RNase free water.
- The RNA quality was confirmed by gel electrophoresis. For RNA amount smaller than 50ng Agilent Bio Chip (Agilent Technology, USA) was used for the quality assurance. All samples considered were found to have intact RNA. The samples were then stored at -80°C until they were further processed.

cDNA synthesis:

As a negative control, a test reaction was included whereby the reverse transcriptase was omitted on purpose.

- For the preparation of the reverse transcription, 9µL of total RNA were added to a 0.5mL micro-tube containing the following master mix solution (per 9µL: 5µL of 5x First strand buffer (Invitrogen, Basel, CH), 1µL DTT 0.1M (Invitrogen, Basel, CH), 1µL dNTP 10mM, 1µL DNAseI 10U/µL (Roche, Basel, CH), SuperaseIn 20U/µL (Ambion, Huntingdon, UK) and RNase free water. The final volume after adding all the reagents for cDNA synthesis was 25µL. The total RNA never exceeded 5µg of RNA to ensure a maximum efficiency of synthesis. The mixture was then gently mixed and incubated in a thermal cycler for 30 min at 37°C for digesting the genomic DNA contaminants and was incubated for 10 min at 65°C in order to inactivate the DNase.
- 1µL of a mixture of oligo dT (500ng/µL) and random hexamers N6 (500ng/ µL) was added.
- Next, the samples were incubated in a thermal cycler for 5 min at 70°C to allow the secondary structure of the RNA to denature. The samples were then chilled on ice for 2 min to avoid the reformation of the secondary structure of the RNA.
- 1µL of Superscript III (200U/µL) (Invitrogen, Basel, Switzerland) was added to each sample. After having gently mixed the sample and briefly spun down the mixture, the samples were incubated in a thermal cycler for 1 h at 50°C.The cDNA was stored at -20°C until the samples were further processed.

Conventional PCR amplification:

As a positive control, a test reaction was included whereby the used cDNA originated from a tissue known to express the examined gene.

- Each lyophilized oligonucleotide (Sigma, USA and Microsynth, Switzerland) was stored in TE-buffer with a final concentration of 100µM and aliquoted in samples of 10µM in TE-buffer.
- Up to 10ng of cDNA were added to a master mix consisting of 1µL forward and 1µL reverse primer, 1µL dNTP 10mM, 0.1µL Taq polymerase 2.5U/µL (Sigma, Switzerland), 4µL 10x PCR buffer (Invitrogen, USA) and filled up with water to a final volume of 40µL in a 96 well-plate.
- The plate was then transferred to a thermocycler using the following PCR conditions: 2 min at 95°C and subsequently for 30 sec at 94°C and then 40 sec at 55°C - 65°C (depending on the optimal annealing temperature of the primers) finally for elongation 30 sec – 60 sec at 68°C (depending on the amplicon size). These subsequent steps were repeated 34 times.

Analysis:

For the analysis of the amplicon, 15µL of each PCR reaction were examined by gel electrophoresis using a 1% agarose/ethidium bromide gel (0.25µg/mL). The GelDoc2000 system (Biorad, Switzerland) was used to verify the specificity of amplicon.

3.2.5 Whole mount in-situ hybridization

Preparation of RNA probe:

- Specific primers were used to amplify the area from a gene of interest using standard PCR-protocol and cloned into a pCR-Topo 2.1 vector (Invitrogen, USA).
- The products of the PCR reaction were run on a 1% agarose/ethidium bromide gel (0.25µg/mL). The proper PCR products were cut out from agarose gel and purified using the Gel Extraction Kit (Qiagen, Germany) according to manufacturer`s instructions.
- SP6 and T7 RNA polymerase, 20U/µL (Invitrogen, USA) were used to generate sense and antisense probes. For this purpose 1µg of DNA template was added to 4µL of 5x transcription buffer (Invitrogen, USA) and 2µL Dig-labeled NTP

mixture (Roche, Switzerland), 1µL RNaseIn (Ambion, USA), 2µL RNA polymerase (Invitrogen, USA) were mixed and RNase free water was added to a final volume of 20µL.

- The mixture was incubated at 37°C for 2 hours.
- After that RNA was precipitated by adding 100µL of isopropanol and 1µL glycogen (Ambion, USA) and spun at 12.000 g for 15 min, washed once with 70% ethanol. The pellet was dried and dissolved in 50µL of RNase free water.
- In order to estimate the amount of RNA and confirm the size of the product 2µL of the samples were run on a 1% agarose/ethidium bromide gel.

As negative control sense probe was used. DEPC water was used to prepare all the solutions.

- E10.5 mouse embryos were taken out from pregnant mice and kept on ice-cold PBS.
- A 1mL pipette tip, with the end cut off, was used to transfer the embryos in small volume of PBS to a 15mL conical tube of ice-cold 4% para-formaldehyd in PBS made fresh from a 20% PBS stock solution. The embryos were gently inverted several times, then replaced with fresh 4% para-formaldehyd solution and incubated for 2 h at 4°C.
- The embryos were washed three times 5 min in ice cold PBT and then washed three times in 100% methanol and stored in methanol until further processed.
- Day1: the embryos were bleached in a solution containing 30% H_2O_2:methanol (Sigma-Aldrich, USA) 1:5 for 2 h and then rinsed with methanol three times.
- The embryos were rehydrated through 75, 50, 25% methanol/PBT, spending 20 min in each methanol concentration. After that the embryos were washed three times 5 min in PBT for 20 min each.
- The embryos were transferred to 2mL tubes using a cut pipette tip. In order to allow efficient washing, the maximum number of 2 embryos processed in a single 2mL tube during procedure.
- The embryos were treated then with 10µg/mL proteinase K (Merck, Germany) in PBT and rinsed briefly with PBT. Since the embryos were very fragile the solution were added very gently. Then they were post fixed for 20 min in 4% para-formaldehyd, 0.1% glutaraldehyde (St. Louise, MO, USA) in PBT.
- The embryos were rinsed and washed four times 5 min with PBT and than rinsed with 2mL hybridization buffer (see below) made fresh from the stock.

- After the embryos were settled in the tube the hybridization buffer was replaced with fresh 2mL hybridization buffer and then replaced again with 2mL hybridization buffer and incubated at 65°C, three times, for 1 h each.
- Finally 2mL pre-warmed hybridization buffer with approximately 1µg/mL of digoxigenin-labeled RNA probe was added and incubated at 65°C over night.
- Day2: The solutions were removed and stored at -20°C for reuse. The embryos were rinsed twice and then washed 30 min with pre-warmed hybridization buffer at 65°C.
- After that the embryos were rinsed twice and washed 30 min and 1 h with pre-warmed washing solution at 65°C and washed for 30 min with 1:1 washing solution/MABT at room temperature.
- The embryos were washed for four time 30 min with MABT at room temperature and then replaced with MABT + 2% Boehringer Blocking Reagent (Boehringer Ingelheim, Germany) for 1 h.
- After that blocking solution was added to the embryos for 1-2 h and incubated at room temperature.
- The blocking solution were than replaced by 1mL of 1/5000 diluted anti-Dig Fab (Roche, Switzerland) in Blocking solution and incubated at 4°C over night.
- Day 3: The embryos were first rinsed, than four times washed for 15 min, than 30 min and finally twice for 1 h each.
- The embryos were incubated in 1mL BM Purple AP Substrate (Roche, Switzerland) until clear signal was observed.

Hybridization Buffer		
Stock concentration	**Final concentration**	**Volume**
Formamide, 100%	50%	25mL
20xSCC, pH 5, with citric acid	1.3x	3.25mL
EDTA, 0.5 M, pH 8	5 mM	0.5mL
Yeast ribonucleic acid core particle, 20mg/mL	50µg/mL	125µL
Tween 20, 10%	0.2%	1mL

CHAPS, 10% Heparin, 50mg/mL H_2O	0.5% 100µg/mL	2.5mL 100µL 17.5mL
Total		50mL

3.2.6 Enrichment of TEC population using Percol

- The thymus dissected from the mice and placed in ice cold 2% FCS containing IMDM.
- The fat residues were removed and small holes were pinched into the lobes
- The lobes were placed into 1mL HBSS containing Collagenase D (final concentration of 1mg/mL) and DNase (final concentration 20µg/mL) in a 5mL tube and incubated for 5 min at 37°C water bath.
- The lobes were pipetted up and down about 20-30 times with a 1mL tip. After 5 min incubation in 37°C water bath the supernatant were transferred into 5mL PBS containing 2% FCS.
- Fresh HBSS containing Collagenase D (final concentration of 1mg/mL) and DNase (final concentration 20µg/mL) were added and the steps were repeated 3-5 times.
- For the last digestion 5µg/mL of DNase were added.
- Cells were washed with PBS 2% FCS, resuspended in 5mL PBS 2% FCS. EDTA was added to a final concentration of 10mM and the cells were incubated for 5 min at 37°C. After that cells were washed with PBS 2% FCS and resuspended in 2mL PBS 2% FCS, filtered through a nylon mesh (40µm).
- Cells were counted.
- 3mL of Percoll (Amersham, USA) with a density of 1.115 kg/m^3 were added to the cells and mixed well in a tube which was coated with PBS 2% FCS. After that, 3ml of Percoll (Amersham, USA) with a density of 1.063 kg/m^3 were carefully pipetted and overlaid with 2mL PBS.
- Cells were than centrifuged for 30 min at 4°C at 1220g without using the brakes of the centrifuge.

- Cells were harvested from the upper layer with a Pasteur-pipette (TEC-fraction) into a fresh tube with PBS 2% FCS.
- The cells were than washed again with PBS 2% FCS twice and finally resuspended in 1mL to 2mL PBS 2% FCS, cells were count and 2-3x10^6 cells were used for staining.

3.2.7 Staining protocol for flow cytometry

The antibodies for the staining were diluted to manufacturer`s recommendations.

- To obtain thymocytes the dissected thymus were placed in 1mL of 2% FCS containing IMDM medium and mashed through a nylon mesh (40µm). Thus obtained cell suspension was harvested and resuspended and washed once in PBS 2% FCS buffer and finally resuspended in 1 – 2mL PBS 2%FCS buffer.
- The cells were filtered through a nylon mesh (40µm) and cells were counted.
- For the staining of single positive and double positive cells population 1x10^6 cells and for the double negative population 2x10^6 cells were used and distributed into a 96 well round bottom plates.
- Cells were spun down and resuspended well in 100µL of antibody solution/1x10^6 cells and incubated for 30-45 min on ice in the dark.
- After that cells were washed twice and harvested for flow cytometry.

3.2.8 Cell proliferation assays

The cells used for the cell proliferation assays were obtained from the lymph nodes.

For all assays un-stimulated cells with anti-CD3 were used.

<u>H_3-Thymidine assay:</u>

- For the thymidine labeling of the cells 0.1x10^6 cells / well were seeded into a 96 well plate.
- The cells were than stimulated with anti-CD3 with the following concentrations: 0.1µg/mL, 2.5µg/mL, 5µg/mL and 10µg/mL.
- The supernatant of the cells were discarded after 48 hours and exchanged with 100µL containing 1µCurie of H_3-Thymidine.

- The cells were than harvested and counted using the cell harvester

CFSE assay:

- For the CFSE labeling of the cells 10-20 x 10^6 cells were resuspended with 1mL PBS and 1mL PBS containing 10µM of CFSE.
- The cells were quenched using equal volume of FCS.
- $1x10^6$ cells were than distributed / well into a 24 well plate.
- The cells were stimulated with 4µg/mL of anti-CD3 antibody for 48 hours.
- After that the cells were harvested and cells were stained for CD4 and CD8 as described previously.

IV. Results

4.1 Introduction

The thymus and the parathyroid glands develop in mice from the ventral and the dorsal aspect of the 3rd pp. To identify the molecular events that determine the early thymus development and thymus fate commitment, the gene expression profile was compared between the ventral and the dorsal circumference of 3rd pp lining in mouse E 10.5 embryos. Laser capture micro dissection (LCM) was used to isolate endodermal cells of these two distinct regions. Total RNA was extracted, the quality of each sample was verified using the Agilent Chip analysis, the nucleic acids were amplified using the standard unbiased approach and the cRNA was finally analyzed using gene chips.

Because only minute amounts of RNA could be isolated from the cell of the ventral-anterior aspect of 3rd pp (100-1000 pg) several technical issues needed to be addressed:

1. total amount of 10ng total RNA needs to be collected
2. the isolated RNA needs to be of a sufficiently high quality for a two round amplification

Therefore, a new methodological protocol for RNA isolation from small amount of cells (1000-2000 cells), captured from LCM, had to be established. This included the development of methods for staining of tissue sections for RNA isolation to be used for LCM and to find a ideal method for the RNA isolation that ensures a high RNA quality in pico to nano gram range. The Agilent Bioanalyzer was used for the quality confirmation of the isolated RNA. After hybridization of cRNA to the gene chip in the core facility of Biocenter, Basel, the data were normalized and thus obtained candidate genes from the data analysis were selected according to the following criteria:

1. Genes that were significantly higher expressed in the ventral aspect of the 3rd pp compared to the dorsal aspect of 3rd pp was considered for further analysis because these genes might be up regulated for the early thymus development and/or TEC fate commitment. 2. Only genes that were at least 2-fold higher expressed in the ventral aspect of the 3rd pp compared to the dorsal aspect of the 3rd pp were considered to be significant and studied in more details. Candidate genes fulfilling these criteria were verified first by quantitative PCR (qPCR) using cDNA synthesized from independent RNA samples of the ventral and dorsal 3rd pp, respectively. In addition, the expression patterns of selected candidate genes were further

analyzed by whole mount in situ hybridization. The genes to be analyzed displayed an increased expression of at least 2 fold difference when analyzed by gene arrays and qRT-PCR. Among 69 genes that were obtained after the evaluation of the gene chip data, Gata binding protein 2 (Gata-2) was chosen for further analysis.

Using an *in vivo* model, the Gata-2 gene was conditionally deleted by using Foxn1-Cre mice, a cre that is expressed in the thymic epithelial cells. In this study, thymus cellular architecture, thymus cellularity and thymus function of 3, 6, 13 and 25 weeks were analyzed. Furthermore, qRT-PCR was performed on cDNA synthesized from sorted thymic epithelial cells at the time points of 3, 6 and 13 weeks and the expression of AP-1 complex, CXCL-12, CCL-25, IL-7, c-kit L, Edn-1, ET_A and ET_B were quantified. The following sections of this thesis will describe these results in detail.

4.2 Optimization of RNA purification from endodermal epithelial cells isolated by LCM

4.2.1 Isolation of RNA from LCM captured endodermal epithelial cells

Since 10µg of RNA are required and since not sufficient amount of RNA is to be recovered from cells by LCM, two RNA amplification steps had to be introduced. To assure that the RNA quality meets the necessary conditions the staining dye was changed to cresylviolette because this dye can be dissolved in 100% EtOH, thus reducing the RNAse activity and offering the possibility to fix the section at the same time as the sections were stained. Furthermore, the time for drying the sections was also reduced to two minutes, before they were stored in -80°C until they were needed. Before the new protocol was established in our laboratory, the cells were stained with toluidin blue, dried for 1-2 hours and then the cells were dissected with LCM for several hours and RNA was isolated using the Trizol reagents. This method led to a significant degradation of the RNA. Therefore, several methods were tested for the RNA isolation (RNA isolation using Trizol, RNA isolation Kit from Palm, total RNA isolation Kit from Agilent, RNA-Micro Kit from Ambion and RNeasy Micro Kit and Mini Kit from Qiagen). The optimal quality of RNA was obtained from the Qiagen RNeasy Micro Kit which also reduced the preparation time to only 30 minutes. These changes improved the quality of the RNA significantly in comparison to the protocols that were used previous in our laboratory (Fig 4.1). Taken together these results reveal that the new established protocol is better suited to obtain high quality of RNA from LCM dissected cells.

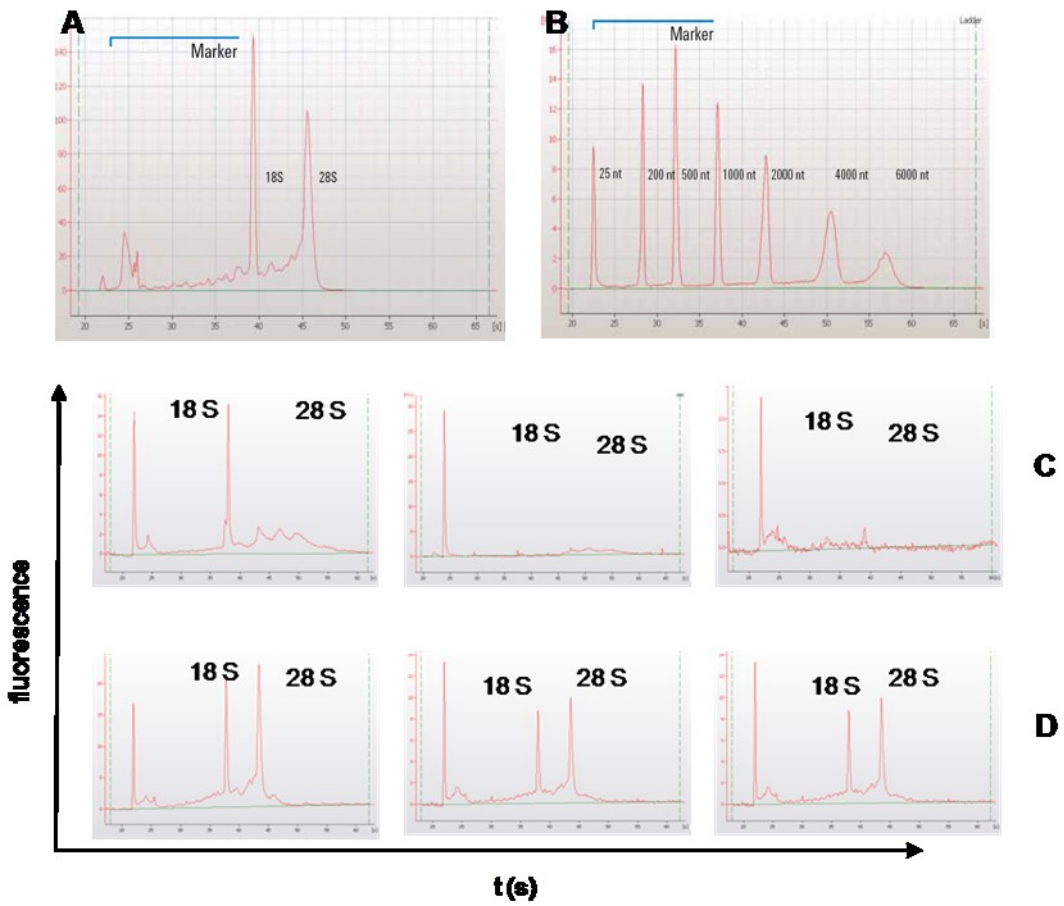

Fig. 4.1: Agilent Biochip Data analysis. Ribosomal 18S and 28S are outlined **A)** Profile of a RNA sample with very high quality. **B)** Nucleotide marker, which runs with every biochip to confirm the size of the rRNA. **C)** Isolation of RNA from LCM dissected cells (1000-2000) of the ventral aspect of 3rd pp using the previously established protocol using toluidin blue staining and Trizol **D)** Isolation of cells using the new protocol and cresylviolette staining.

4.2.2 Expression of Foxn1 in the 3rd pp

To verify the feasibility of LCM on the 3rd pp endothelium and to test the correctness of dorsal and ventral distinction, we analyzed the expression of the genes Gcm2 and Foxn1 using qRT-PCR. Using whole mount in situ hybridization Foxn1 mRNA can be detected as early as E11.25 in the anterior part of the ventral circumference of the 3rd pp (Gordon et al., 2001; Manley et al., 2004). Gcm2, on the other hand, is expressed at E10.5 and E11.5 throughout the dorsal aspect of the 3rd pp. Cells from the posterior and anterior part of the ventral aspect of the 3rd pp of E10.5 embryos were therefore dissected, and cDNA was synthesized from the RNA and qRT-PCR was performed. Foxn1 mRNA was already detectable by qRT-PCR at E10.5 in the anterior part of the ventral aspect of the 3rd pp whereas Gcm2 was expressed at the same time point only in the dorsal aspect of the 3rd pp (Fig.4.2). These results were in agreement with the results of Balciunaite et al. (Balciunaite et al., 2002)

who have shown that Gcm2 expression is limited in the dorsal aspect of the 3rd pp and Foxn1 expression in the ventral aspect of 3rd pp. These results indicate that the commitment to a thymic epithelial cell fate is already set at E10.5 and that the earliest signs for a commitment start in the anterior part of the ventral circumference of the 3rd pp. In consequence of these findings, cells only of the anterior part of the ventral aspect and of the dorsal circumference of the 3rd pp were used for comparative analysis of gene expression.

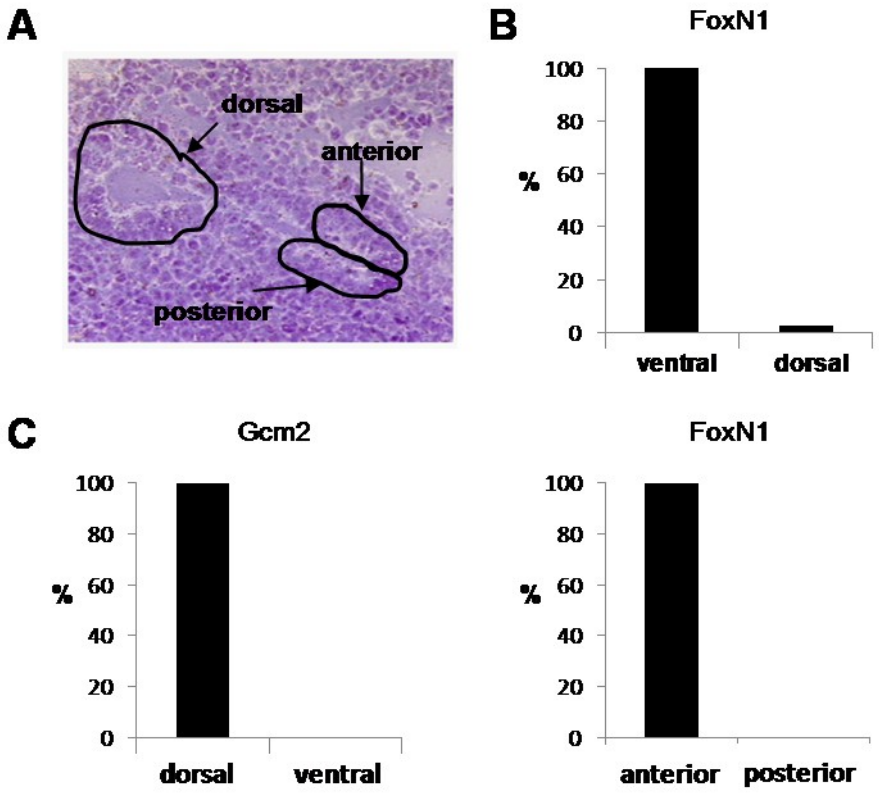

Fig. 4.2: Isolation of RNA from 3rd pp at E10.5 developmental. A) The ventral aspect of 3rd pp is divided into anterior and posterior part. **B)** qRT-PCR of Foxn1 gene from the cells of anterior and posterior part of the ventral aspect of 3rd pp. Foxn1 was not detectable in the anterior aspect of 3rd pp (n=3). **C)** qRT-PCR for the genes Gcm2 and Foxn1 from the cells of the dorsal and ventral aspect of 3rd pp (n=3).

4.2.3 RNA amplification for microarray analysis

Substantial amounts of cRNA (10µg cRNA per Chip) are required for gene expression studies using gene chips. Since the numbers of endodermal epithelial involved in the early thymic development is limited, a reliable amplification method for small amount of RNA had to be established. A linear amplification protocol was therefore employed that consists of two cycles of cDNA synthesis each followed by *in vitro* transcription (Eberwine et al. 1992). These methods were further optimized by the Biocenter Core facility and adopted for the

synthesis and amplification of cRNA. After two rounds amplification steps of the RNA the average size of the RNA length was reduced to 500 nucleotides after the first round of amplification, and to 200 nucleotides after the second amplification step (Fig. 4.3).

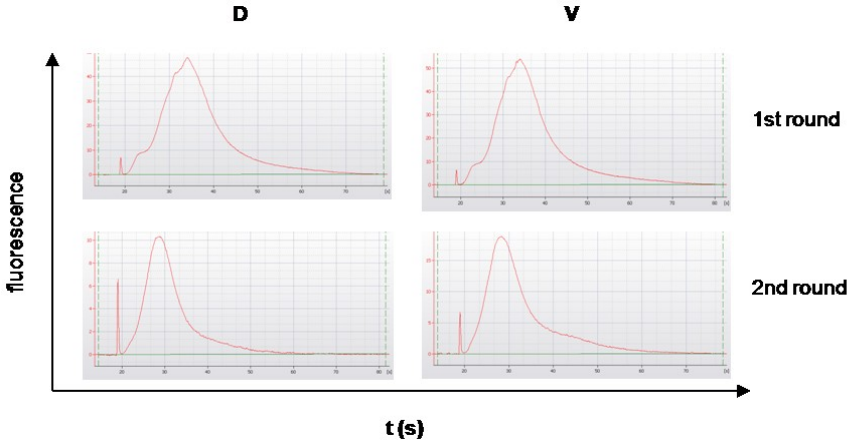

Fig. 4.3: **RNA amplification.** Only one sample of cell from dorsal aspect of 3rd pp (D) and one sample of the anterior part of the ventral aspect of 3rd pp (V) are shown. These two samples are representative of the six samples, 3 from ventral and 3 from the dorsal aspect of 3rd pp.

4.3.1 Analysis of genes differentially expressed at E10.5 between the dorsal and ventral aspect of the 3rd pp

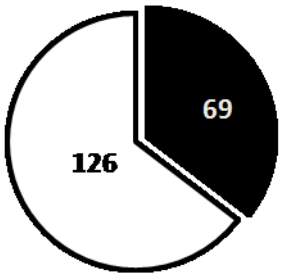

Fig. 4.4: Differential gene expression: Sixty-nine genes were differentially up-regulated in the ventral aspect of 3rd pp and 126 genes were up-regulated in the dorsal aspect of the 3rd pp.

The gene expression profile was compared at E10.5 between cells isolated from the dorsal aspect of the 3rd pp and the anterior part of the ventral aspect of 3rd pp. To perform statistically relevant data sets, three independent samples of each group were generated and analyzed using Affymetrix Mouse Gene Chip 430 2.0. This array contains over 39000 transcripts. The signal intensity measured on the gene chips was normalized using the D-chip program (Li et al., 2003).

Given these conditions, approximately half of the gene transcripts represented on the Affymetrix gene chip provided a present call meaning that ca. 19500 genes were expressed in the cells which were analyzed.

To verify the differences in the expression of Foxn1 and Gcm2 as observed by qRT-PCR the gene chip data were analyzed. As demonstrated in Fig. 4.5 Gcm2 transcripts were only detected in the dorsal aspect of the 3rd pp whereas Foxn1 specific mRNA

was only detected in the anterior-ventral aspect of the 3rd pp. The intensity values for Foxn1 were lower when compared to those for Gcm2, a finding which is in keeping with previous data (Gordon et al., 2001).

The intensity level of the fluorescence signals of each gene obtained from the gene chips corresponds with the expression level. To narrow the potential candidate genes of interest down the threshold of expressional level in the anterior-ventral aspect of the 3rd pp had to be at least twice as high as in the dorsal aspect of the 3rd pp or the other way around. Sixty-nine genes were revealed to be expressed at least 2-fold higher in the anterior- ventral aspect of the 3rd pp while 126 genes were up-regulated in the dorsal aspect of the 3rd pp. Among the known genes to be expressed more prominently in epithelia commitment to a thymic fate, Gata-2 was most differential.

Eleven genes with the largest differential expression values were further assessed. First, qRT-PCR was used to confirm the differences in expression detected by microarray analysis because genes identified by DNA arrays with more than two-fold difference in expression cannot be eliminated as false nor be accepted as true without validation using qRT-PCR (Rajeevan et al., 2000, 2001). However, this data revealed that only five of eleven (Gata-2, C1qdc, Msx1, delta-like 1, Unc5-homolog) were indeed expressed equal or more than 2 fold when compared to control sequences. Among the genes analyzed, C1qdc was detected most abundantly followed by Unc5-homolog and Gata-2 expression. The outcome of an analysis of a gene chip is highly dependent of bioinformatics and statistical methods used for such a large data set and so far, no unified approach to analyze microarray data has been suggested. The discrepancy in gene expression level observed between gene chip data and RT-PCR were previously reported even if the filtering criteria were highly stringent (Rajeevan et al., 2000; Zhao et al., 2004).

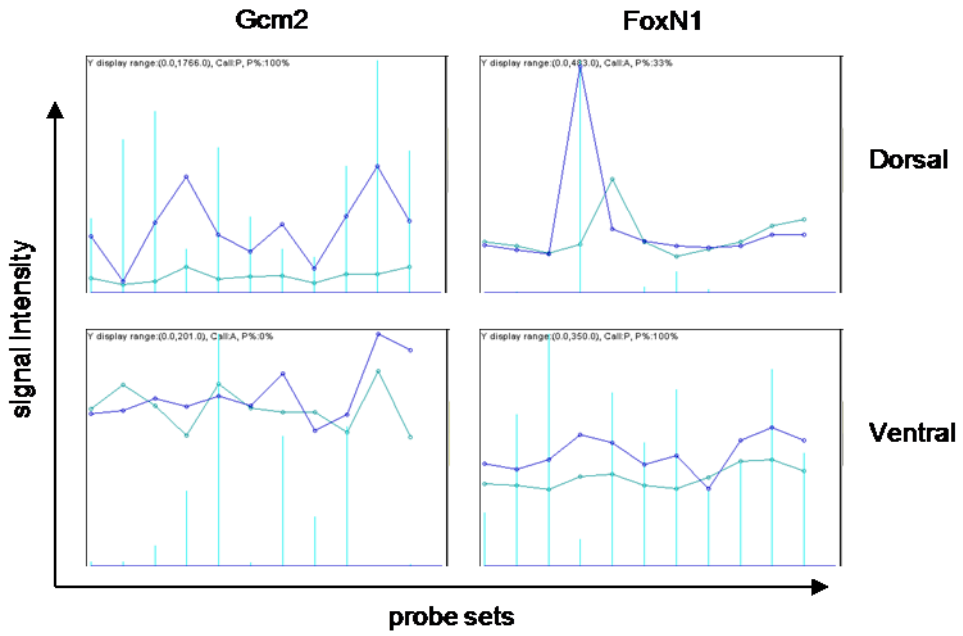

Fig. 4.5: Microarray analysis. At E10.5, Gcm2 was only detected in the dorsal aspect of 3rd pp whereas Foxn1 was detected only in the anterior part of the ventral aspect of 3rd pp. The signal for Foxn1 is weaker when compared to that of Gcm2. The presented data is the average from three independent analysis.

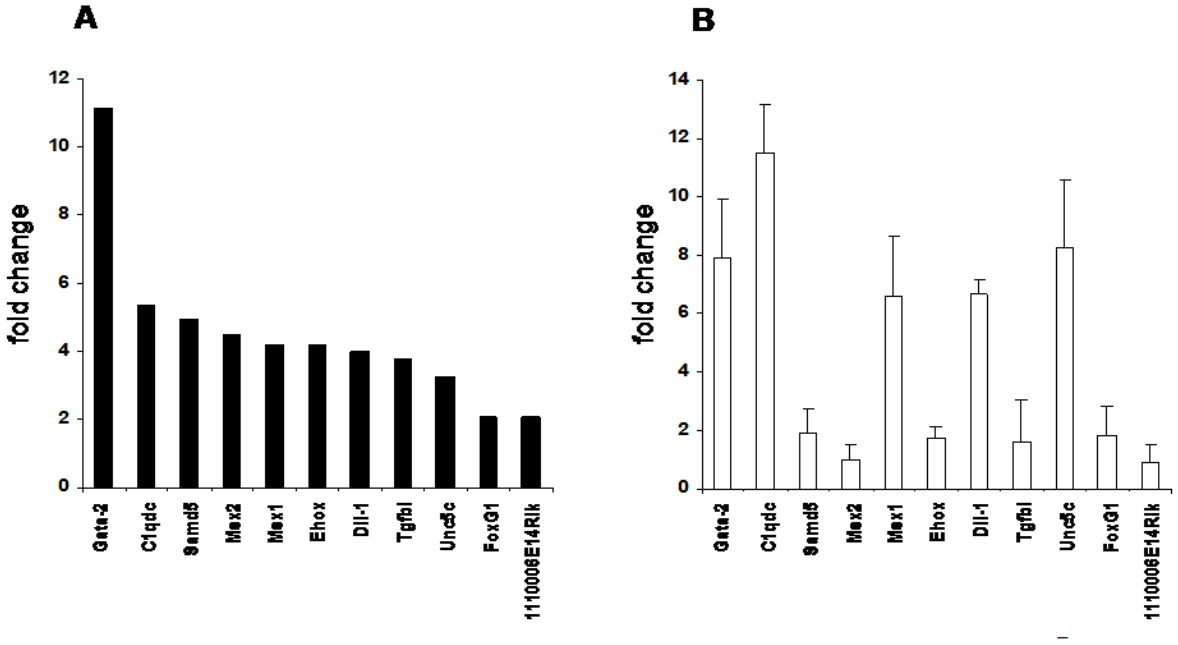

Fig. 4.6: Changes in gene expression as analyzed by microarrays and RT-PCR, respectively. Fold change increase of genes expressed in the ventral aspects as determined by Affymetrix gene chips **A)** and qRT-PCR0 **B)**. The qRT-PCR data were normalized to GAPDH expression. Numbers of independent qRT-PCR analysis (n=3). EST1431094 represents RIKEN cDNA 1110006E14 gene.

Table 1. Table of candidate genes. The probe set ID represents the genes on Affymetrix Gene chip 430 2.0.

Probe Set ID	Gene Title	Gene Symbol	Gene function
1450333_a_at	GATA binding protein 2	Gata-2	- cell differentiation - cell fate determination
1420360_at	delta like-1	dll-1	- ligand of Notch signaling pathway
1417393_a_at	C1q domain containing 2	C1qdc2	unknown
1437403_at	sterile alpha motif domain containing 5	Samd5	unknown
1449559_at	homeobox, msh-like 2	Msx2	- BMP signaling pathway - negative regulation of apoptosis
1448601_s_at	homeobox, msh-like 1	Msx1	- BMP signaling pathway - negative regulation of apoptosis
1419229_at	reproductive homeobox 4 A-G	Ehox	- regulation of transcription
1448123_s_at	transforming growth factor, beta induced	Tgfbi	- cell adhesion
1449522_at	Unc5 homolog C	Unc5c	- apoptosis - regulation of cell migration
1418357_at	Forkhead box G1	FoxG1	- regulation of mitotic cell cycle - dorsal/ventral pattern formation
1431094_at	RIKEN cDNA 1110006E14 gene	1110006E14Rik	unknown

4.3.2 Whole mount in situ hybridization for candidate genes

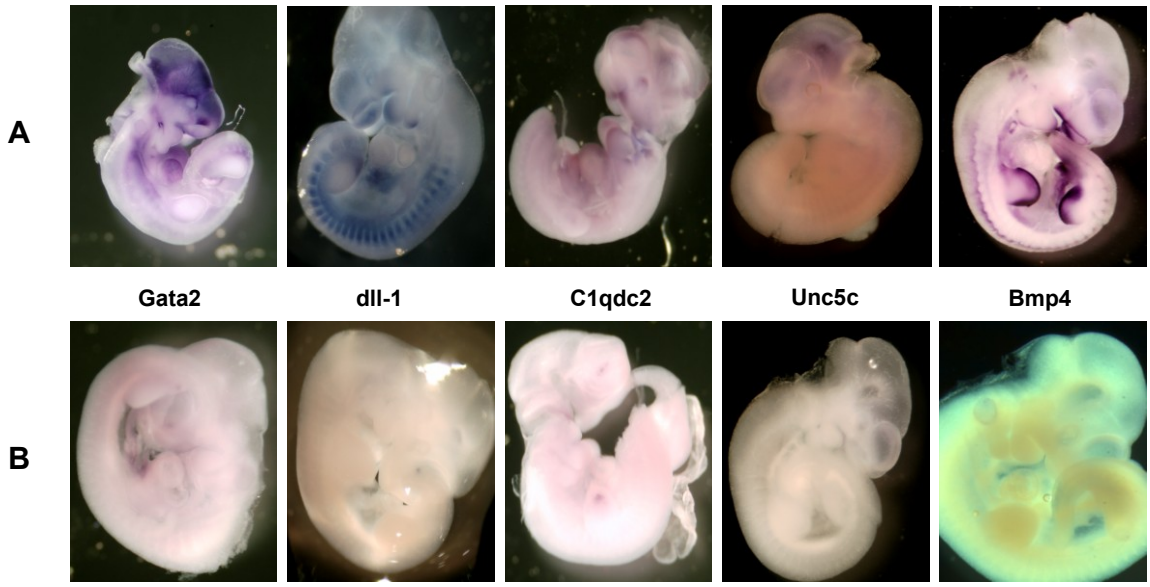

Fig. 4.7: **Whole mount in situ hybridization of candidate genes in E10.5 embryo. A)** Anti-sense probe. **B)** Sense probe as negative control. Bmp4 antisense probes were used as positive control. For negative control sense probes were generated for each gene of interest negative control. (4x magnification, two independent experiments were done for each gene)

To assess the special expression of those genes with a higher than 2-fold change in expression between the ventral and dorsal aspect of the 3rd pp as measured by qRT-PCR whole mount in situ hybridization was carried out on E10.5 wild type embryos (Fig 4.7). The expression of Gata-2, C1qdc2, delta like-1, and Unc5 homolog C was analyzed by this method.

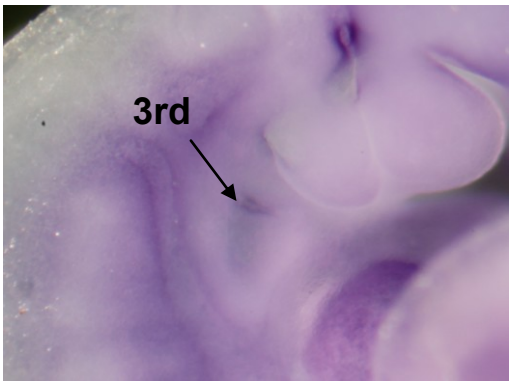

Fig. 4.8: Whole mount in situ hybridization for the Gata-2 mRNA. Detection of Gata-2 gene mRNA form the 3rd pp. (10x magnification)

Msx1 belongs to the homeobox gene family and has its role in controlling cell proliferation and differentiation. Msx1 is important for the teeth, cleft palate and cranial skeleton development (Satokata et al., 1994). Msx1 expression was previously been tested by whole mount in situ hybridization in E10.5 mouse embryos and was localized to an area of mesenchyme that (i) immediately underlying the apical endodermal ridge (AER) and (ii) is situated to craniofacial region especially in the branchial arches of ba1, 2 and olfactory pits (Tribioli et al., 2002). To assess the specificity of the analysis, both a

positive (BMP4 antisense probe) and negative controls (sense probes of the tested sequences) were included in this study. The BMP4 expression displayed a pattern as previously reported with the staining of the limb`s progress zone below the AER. Two different anti-sense RNA probes were designed and tested for each of the four candidate genes. A thorough analysis for C1qdc2 and Unc5 respectively, revealed that for neither probe sets a signal was detected in E10.5 embryos. Of all candidate genes analyzed by whole mount in situ hybridization only Gata-2 sequence provided a positive signal localized in the ventral aspect of the 3rd pp (Fig. 4.8). The results from the whole mount in situ hybridization do not correspond to the expression profile obtained from gene chip and qRT-PCR. According to gene chip data, the gene C1qdc2 was more than 5-fold higher expressed in the anterior-ventral aspect of 3rd pp and according to qRT-PCR, C1qdc2 was even higher expressed than Gata-2 and Unc5 was expressed at the similar level of Gata-2. Among the genes that were analyzed by all three methods, Gata-2 was the only gene of which its expression was detected by all three methods. These results indicate that at the time point E10.5 Gata-2 might play a role in the thymic fate decision and/or development.

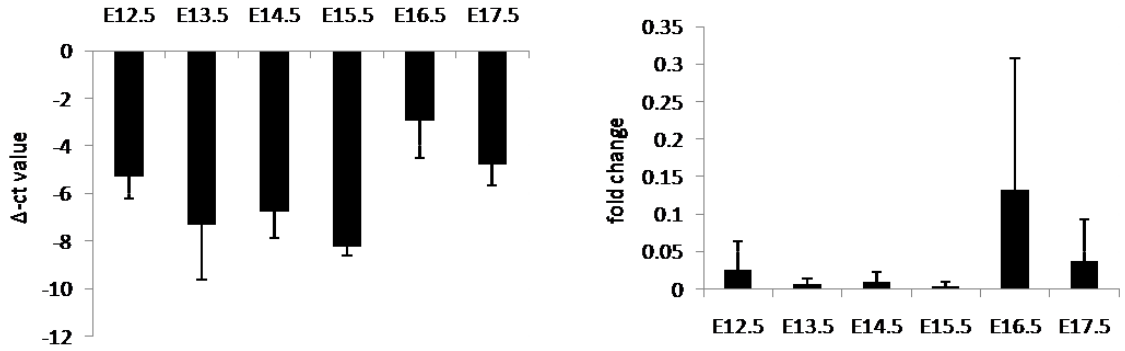

Fig. 4.9: Gata-2 expression kinetics during embryonic thymus development. The expression of the genes was studied by using qRT-PCR. (n=3 for all time points). Δ-ct values were normalized to GAPDH. The expression level of Gata-2 for the time points E12.5 to E17.5 was compared to E10.5. The fold changes were calculated from ΔΔ-ct values and show a decreased Gata-2 expression after E10.5.

First, I determined the kinetics of Gata-2 during early thymic embryonic development. To this end, thymic epithelial cells (TEC) were sorted as $MHCII^+$, $EpCAM^+$ and $CD45^-$ cells from suspensions of thymic tissue. RNA was isolated from samples isolated at E12.5, E13.5, E14.5, E15.5, E16.5 and E17.5, cDNA was synthesized and qRT-PCR was performed (Fig. 4.9). For methodological reasons, endodermal epithelial cells in the anterior-ventral aspect of the 3rd pp were isolated by LCM at the time point of E10.5 (Fig. 4.2a). The expression of Gata-2 decreased very significantly in the cause of embryonic thymus development with a dramatic

drop between E10.5 and E12.5. Subsequently, the decrease continued, albeit to a lesser degree until E16.5 when a transient increase occurred. Thereafter, the Gata-2 gene level was again diminished. It is interesting to observe that the expression of Gata-2 is drastically reduced at the time point E12.5 when compared to E10.5. At E12 thymus anlage has a high proportion of proliferating TECs and this proliferation declines as gestation proceeds (Jenkinson et al., 2007) and Gata-2 has been reported to have a capability to negatively regulate the cell proliferation (Wakil et al., 2006) indicating the role in Gata-2 in TEC proliferation.

4.4 Generation and analysis of mice deficient for Gata-2 expression in thymic epithelial cells

4.4.1. TEC targeted inactivation of Gata-2

Because Gata-2 deficient mice die at E10.5 secondary to anemia and hence before the thymus anlage is formed, the use of conventional knock-out mice did preclude an analysis of the role Gata-2 in thymus organogenesis. A tissue specific deletion of Gata-2 was therefore employed to avoid embryonic lethality. For this purpose, the tissue directed gene deletion was achieved by the use of the cre-lox system. Mice with loxP sequences flanking 5´ exon5 and positioned in exon6 were crossed to mice that express the cre recombinase under the transcriptional control of the Foxn1 locus (Fig. 4.10). Thus, the DNA binding domain which is encoded in the exon5 is deleted disabling Gata-2 protein to bind to the target DNA sequence to induce transcription of Gata-2 target genes. Because Foxn1 is only expressed in the TECs and some cells of the skin, double transgenic mice were expected to develop normally with possible exception of the thymus. (Mice with a TEC-targeted deletion of Gata-2 gene will be referred as Gata-2 KO mice)

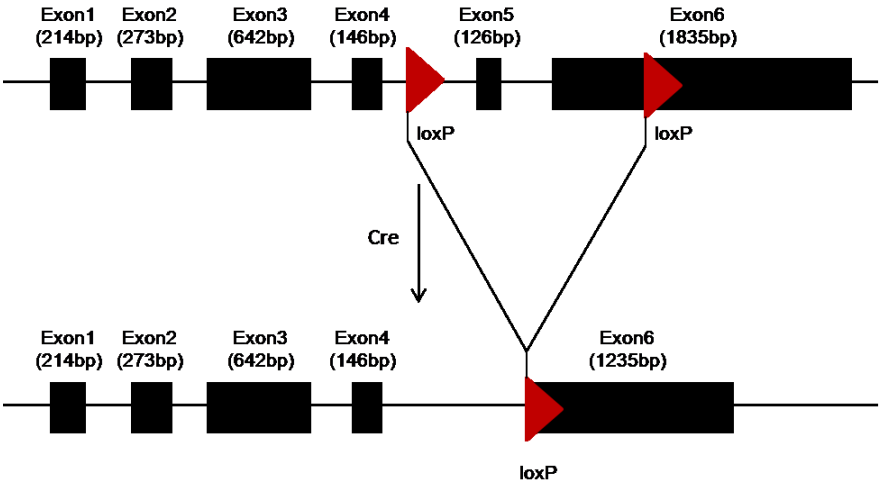

Fig. 4.10: **Deletion of DNA-binding domain of Gata-2 using the Cre/loxP-system.** Cre-protein recognizes the loxP sizes that are located in the intron between the 4th and 5th exon and in the 6th exon. Upon Cre mediated deletion the DNA-binding domain of Gata-2 is deleted.

4.4.2. Thymus architecture of Gata-2 deficient mice

To determine the impact of a Gata-2 deficiency on thymus structure H&E stainings were performed on thymus tissue sections cut from 3, 6, 13 and 25 weeks old thymi. The thymus of Gata-2 KO mice revealed no difference in the morphological organization of cortex and medulla when compared to Gata-2 deficient mice. To detail further the architecture of the thymic microenvironment, fluorescence staining and confocal microscopy were used (Fig. 4.11a, b). cTEC and mTEC were distinguished by their difference in the expression of cellular markers: Anti-CK18 antibody stains cTEC, whereas anti-CK5 and anti-UEA-1 antibodies identify mTEC. The antibody ER-TR7 was used to stain the fibroblasts in the thymus. Neither the composition nor the architecture of the thymic microenvironment were altered as a consequence of Gata-2 deletion. Hence, these results indicate that the Gata-2 deficiency in TECs does not appear to affect the organization and composition of thymic epithelial cells.

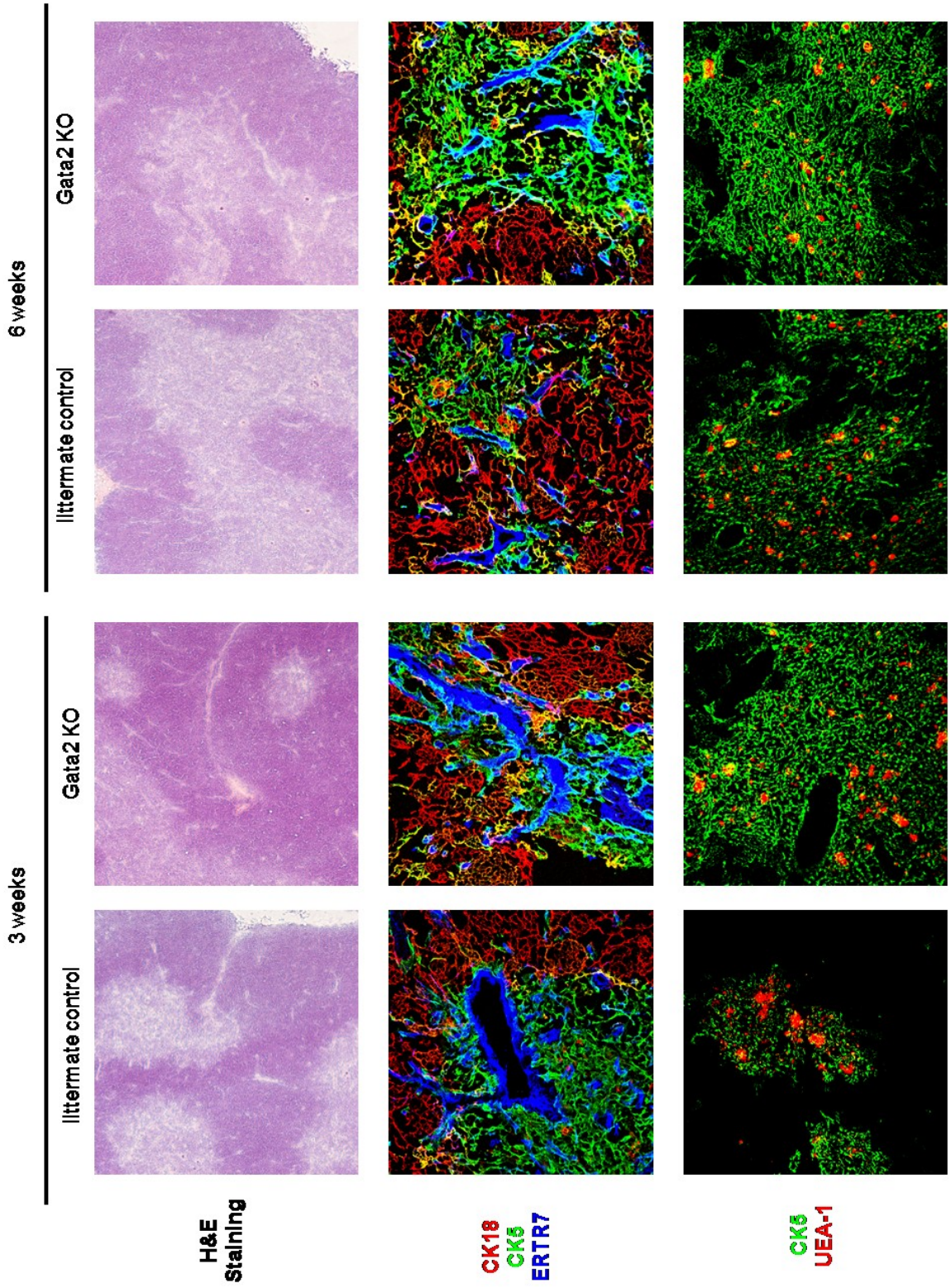

Fig. 4.11a: Analysis of thymus architecture of 3 and 6 weeks of age. H&E staining was used for morphological analysis. TECs were immunohistochemically stained for CK18 (red), CK5 (green) and UEA-1 (red). ERTR7 (blue) stains fibroblasts.

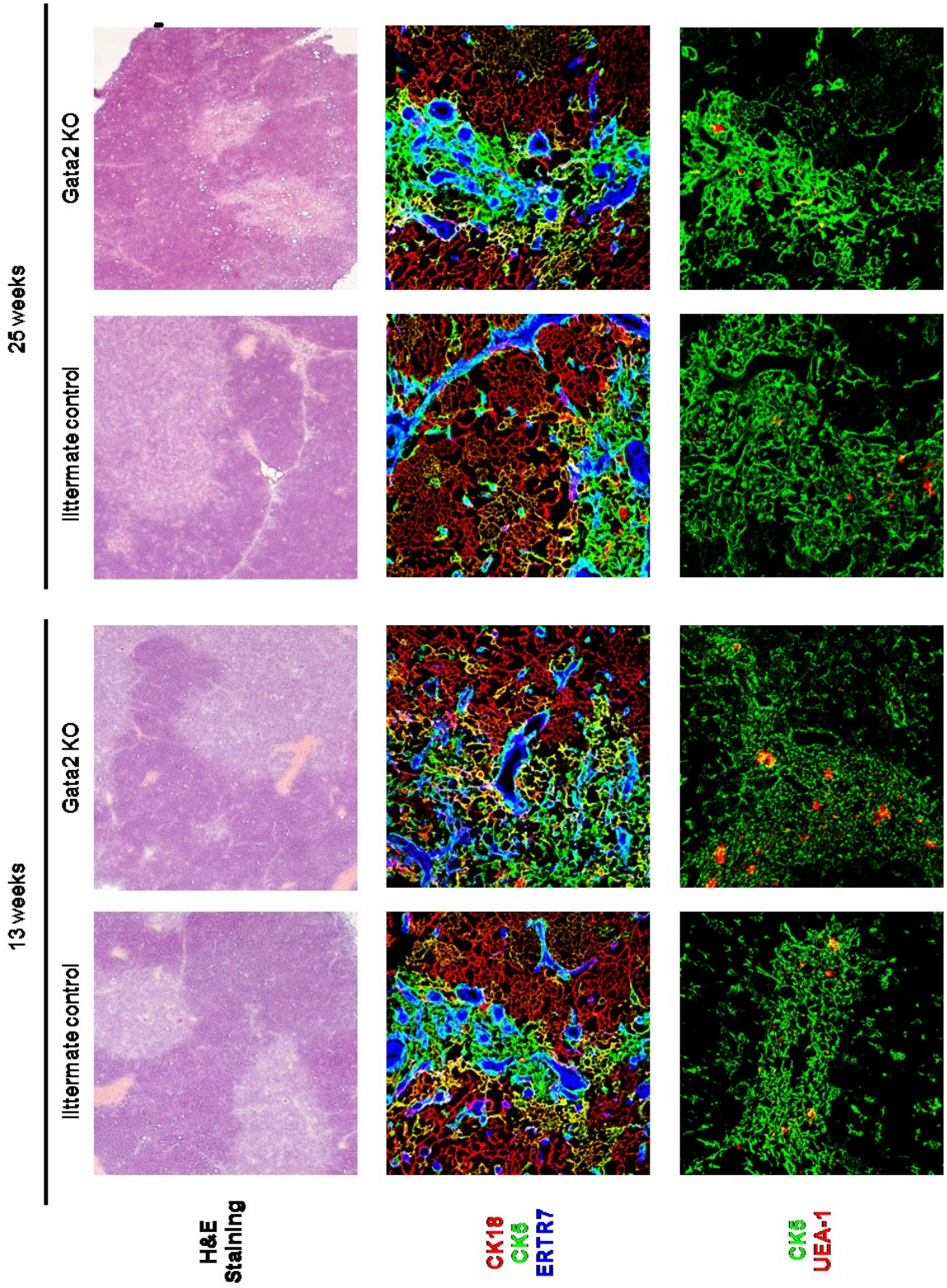

Fig. 4.11b: Analysis of thymus architecture of 13 and 25 weeks of age. H&E staining was used for morphological analysis. TECs were immunohistochemically stained for CK18 (red), CK5 (green) and UEA-1 (red). ERTR7 (blue) stains fibroblasts.

4.4.3 Analysis of the thymus of Gata-2 KO mice

4.4.3.1 Gata-2 expression was significantly reduced after E12.5 in Foxn1-Cre^{+}::Gata-2$^{loxP/loxP}$ mice

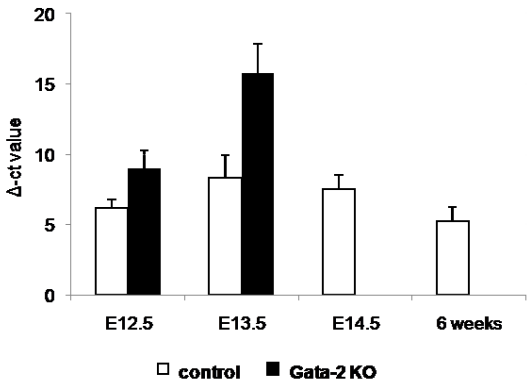

Fig. 4.12: Gata-2 expression in sorted TECs. TECs (MHCII^{hi}, MHCII^{int}, G8.8^{+}, CD45^{-}) form E12.5, E13.5 E14.5 and 6 weeks were screened for Gata-2 expression.

To quantify the efficiency of cre mediated deletion of Gata-2 in Gata-2 KO, qRT-PCR was performed. Foxn1 driven cre is detectable at E12.5 in only few TECs that express Foxn1 (Zuklys et al., 2009). Nevertheless, the Gata-2 expression was ~7 fold decreased in E12.5 old TECs of Gata-2 KO mice and was merely detectable in E13.5 (~170 fold decreased), respectively. Gata-2 transcript could not be detected after E13.5 in TECs of Gata-2 KO mice (Fig 4.12).

4.4.3.2 Higher total thymocyte numbers present in the Gata-2 KO mice

In order to analyze the thymus of Gata-2 KO mice in more detail the thymus from 3, 6, 13 and 25 weeks old mice were removed and thymocytes were stained.

In the three weeks old mice no difference was observed in the total cellularity of the thymus, but in the six weeks old Gata-2 KO mice the total thymocyte numbers were increased by 46% in male and 43% in females when compared to their wild type controls, respectively. The increased cellularity of the thymus was observed at the time points of 13 weeks (25% increase in males, 34% increase in females) and 25 weeks (35% increase in males, 60% increase in females) old mice (Fig. 4.12). These results suggest that Gata-2 KO thymus might be able to support more thymocyte either by stimulating the thymocyte proliferation/survival or/and attracting more thymocyte precursors.

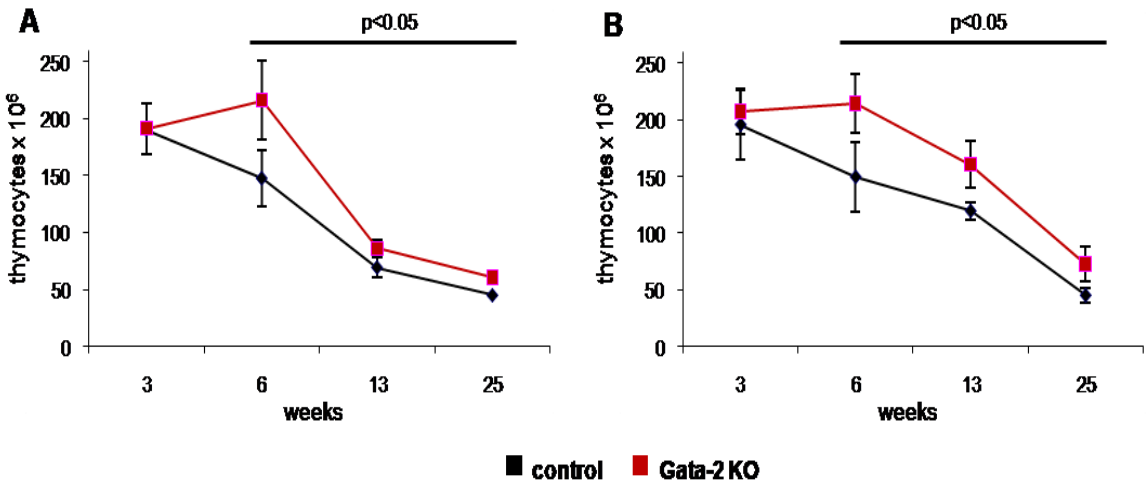

Fig. 4.13: Thymic cellularity. **A)** Males **B)** Females

4.4.3.3 Increased absolute thymocyte at all T-cell developmental stages

FACS analysis was performed to test whether the increased cellularity was associated with an expansion of all thymocyte sub-population or, alternatively, whether a particular development stage was more numerous as a consequence of a lack of Gata-2 expression in TECs. First, Lin^- thymocytes (i.g. with an immature phenotype) were first investigated: DN1 ($CD44^+$,$CD25^-$, Lin^-), DN2 ($CD44^+$, $CD25^+$, Lin^-), DN3 ($CD44^-$, $CD25^+$, Lin^-) and DN4 ($CD44^-$, $CD25^-$, Lin^-). Although the distribution of the different immature (i.g. DN) thymocyte subpopulation in the Gata-2 KO were similar to that of littermate control, the absolute DN cellularity were significantly increased in the Gata-2 KO mice six weeks of age and older (Fig. 4.13). Second the DP, $CD4^+$ and $CD8^+$ thymocytes were analyzed. Gata-2 KO mice with an age of six weeks and older had a significantly increased DP, $CD4^+$ and $CD8^+$ thymocytes. No statistical analysis were possible for the mice of three weeks of age due to low sample number but the preliminary results indicate no difference neither in the DN population nor in the DP, $CD4^+$ or $CD8^+$ (Fig. 4.14 a,b). This experiment showed that Gata-2 deficiency in the TEC did not have any differential effect the size of the different thymocyte subpopulations. However, the increased absolute numbers indicated that either a stronger cell proliferations in the Gata-2 deficient mice occurred in the very early stage of the T-cell development or alternatively that more T-cell precursors were attracted into the thymus. Analysis of the bone marrow derived T-cell precursors ($CD44^+$, $CD117^+$, $CD25^-$, $CD45^-$) revealed that the relative numbers in Gata-2 KO were similar when compared to littermate controls but the absolute numbers were significantly increased at the times investigated, indicating that more precursors were present in the thymus of Gata-2 KO mice (Fig. 4.16).

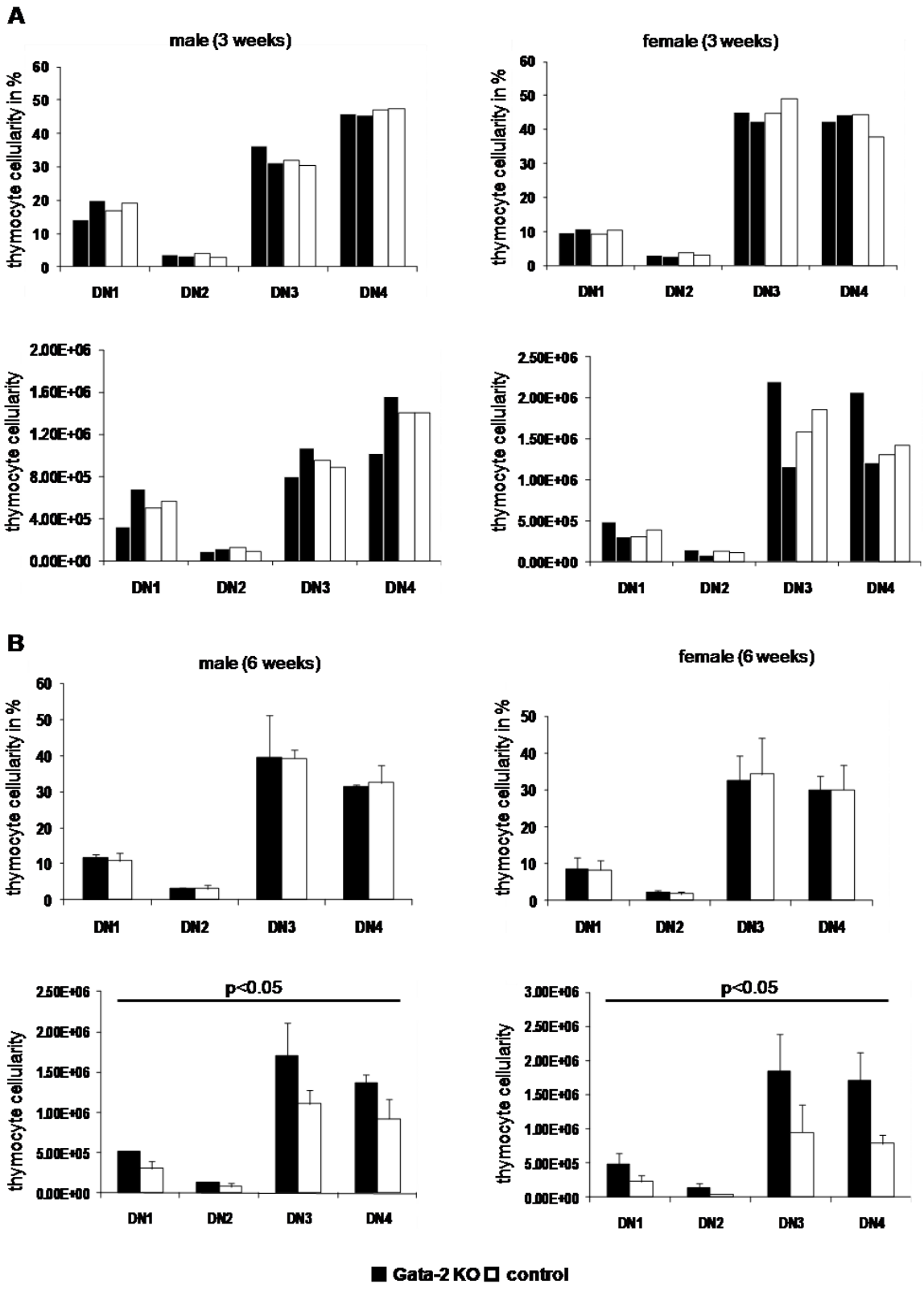

Fig. 4.14a: Analysis of DN1-DN4 population of Gata-2 KO mice. Staining was performed using anti-CD44, anti-CD25 on lineage negative cells ($B220^-$, $CD45^-$, $CD11b^-$, $CD11c^-$, $CD19^-$, $CD4^-$, $CD8^-$, $NK1.1^-$, $Gr\text{-}1^-$). **A)** 3 weeks (male: n=2/group; female: n=2/group), **B)** 6 weeks (male: n=4/group; female: n=4/group).

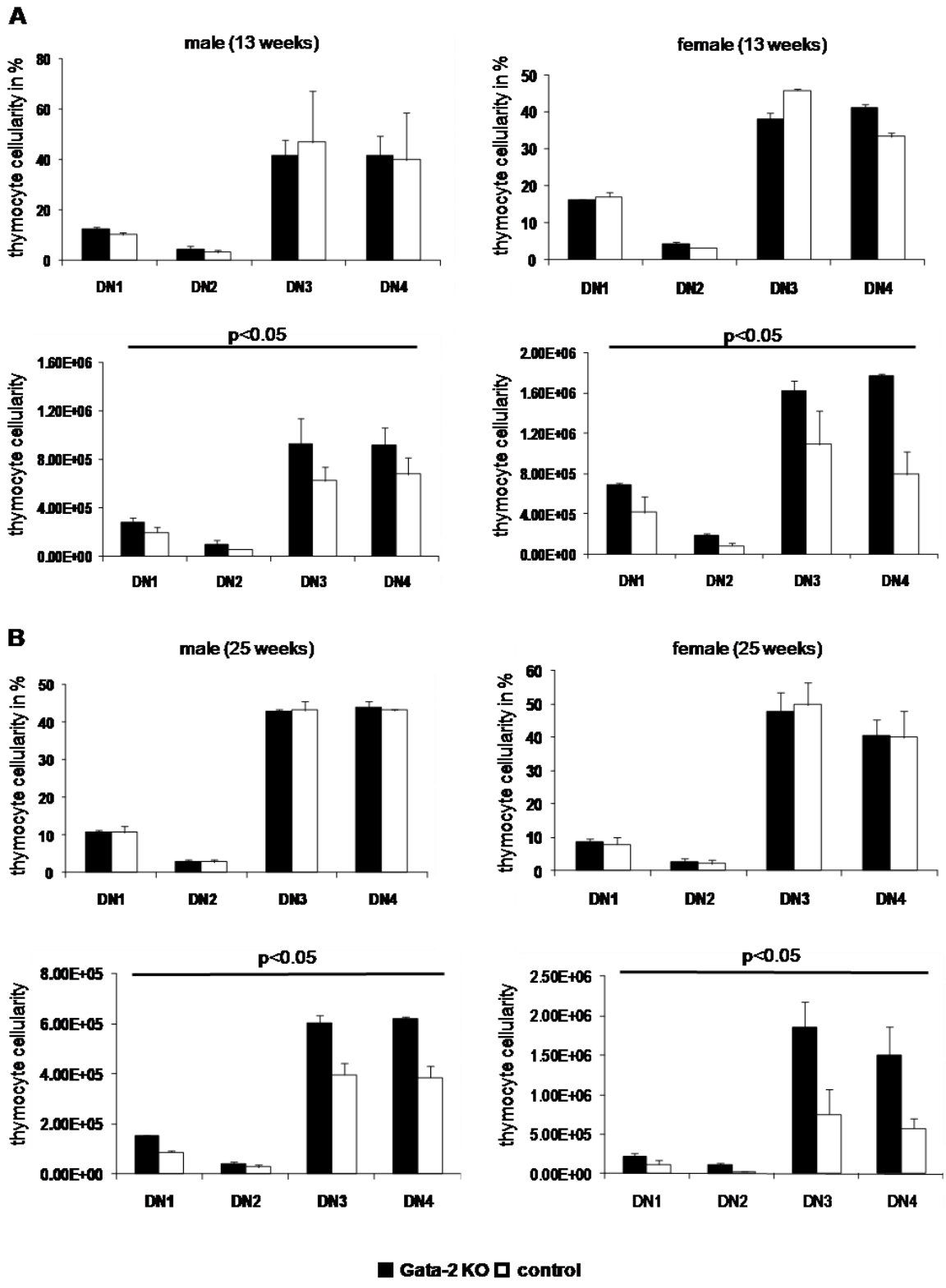

Fig. 4.14b: Analysis of DN1-DN4 population of Gata-2 KO mice. Staining was performed using anti-CD44, anti-CD25 on lineage negative cells ($B220^-$, $CD45^-$, $CD11b^-$, $CD11c^-$, $CD19^-$, $CD4^-$, $CD8^-$, $NK1.1^-$, $Gr\text{-}1^-$). **C)** 13 weeks (male: n=3/group; female: n=3/group) **D)** 25 weeks (male: n=3/group; female: n=6/group).

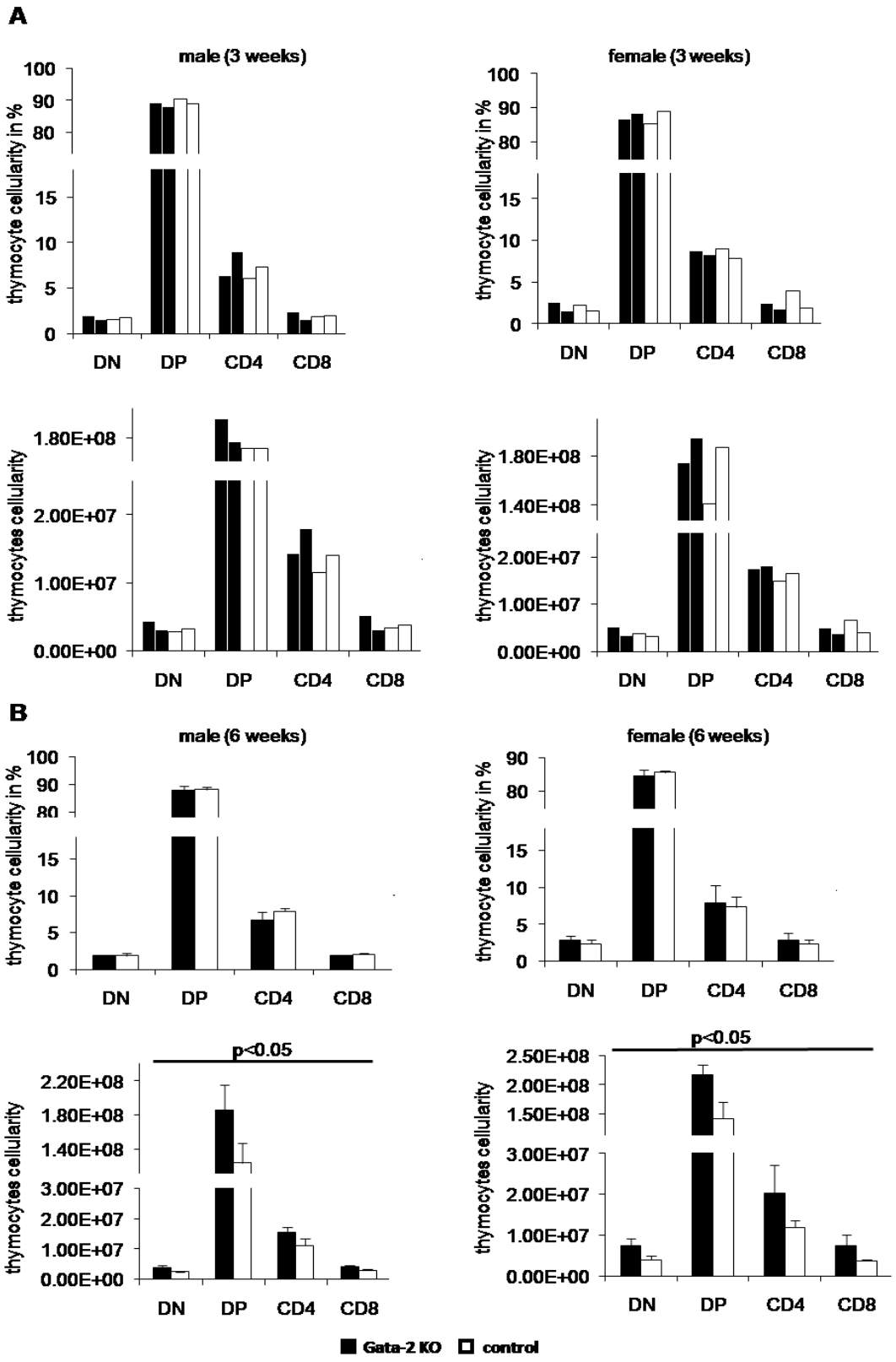

Fig. 4.15a: Analysis of SP and DP thymocytes. Staining was performed using anti-CD4, anti-CD8. **A)** 3 weeks (male: n=2/group; female: n=2/group), **B)** 6 weeks (male: n=4/group; female: n=4/group).

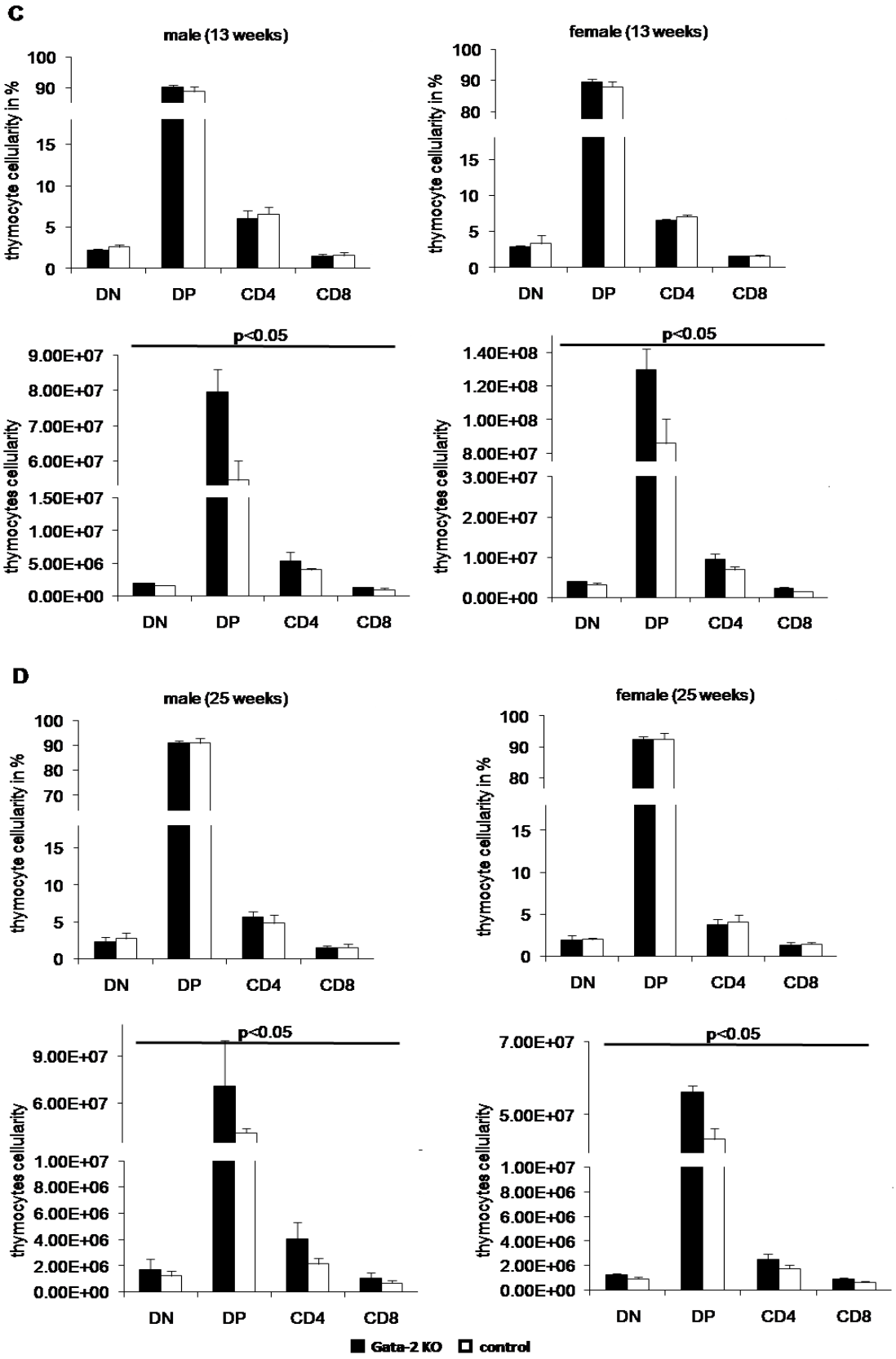

Fig. 4.15b: Analysis of SP ($CD4^+$, $CD8^+$) thymocytes. Staining was performed using anti-CD4, anti-CD8. **C)** 13 weeks (male: n=3/group; female: n=3/group), **D)** 25 weeks (male: n=3/group; female: n=6/group).

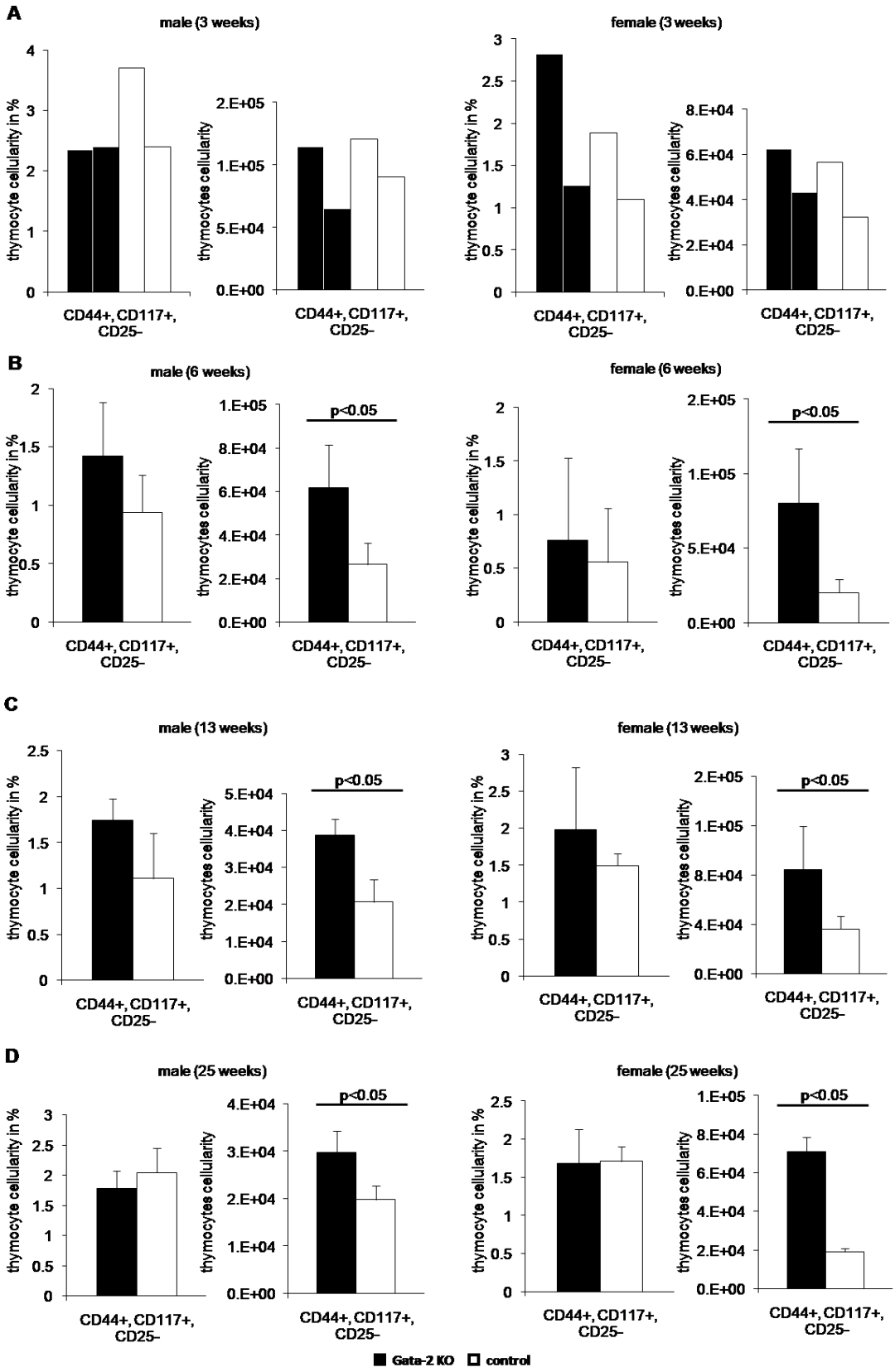

Fig. 4.16 Analysis of T-cell precursors ($CD44^+$, $CD117^+$, $CD25^-$, Lin^-). A) 3 weeks (male: n=2/group; female: n=2/group), **B)** 6 weeks (male: n=4/group; female: n=4/group), **C)** 13 weeks (male: n=3/group; female: n=3/group), **D)** 25 weeks (male: n=3/group; female: n=6/group).

4.4.3.4 Differences in T-cell cellularity are not observed in the periphery

Next, the impact of a lack of Gata-2 expression in TECs on the peripheral T-cell cellularity of mature T-cells was investigated. Lymph nodes and the spleen were isolated from 6 weeks, 13 weeks and 25 weeks of female mice and analyzed for the relative frequency of CD4 and CD8 T-cells, respectively. The total spleen and lymph node cellularities of Gata-2 KO were similar to control mice when analyzed at any of the indicated time points (Fig. 4.17a,b,c). The detailed analysis of naïve CD4 cells ($CD44^{lo}$, $CD62L^{hi}$), effector CD4 cells ($CD44^{hi}$, $CD62L^{lo}$); memory CD4 cells ($CD44^{hi}$, $CD62L^{hi}$), and naïve CD8 cells ($CD44^{lo}$, $CD62L^{hi}$) and effector/memory CD8 ($CD44^{hi}$, $CD62L^{hi}$) showed no difference in relative and absolute cell numbers when Gata-2 KO mice were compared to their littermate controls (Fig. 4.17 a,b,c). Taken together, the peripheral T cell compartment of spleen and lymph nodes were not affected by the Gata-2 deficient thymus.

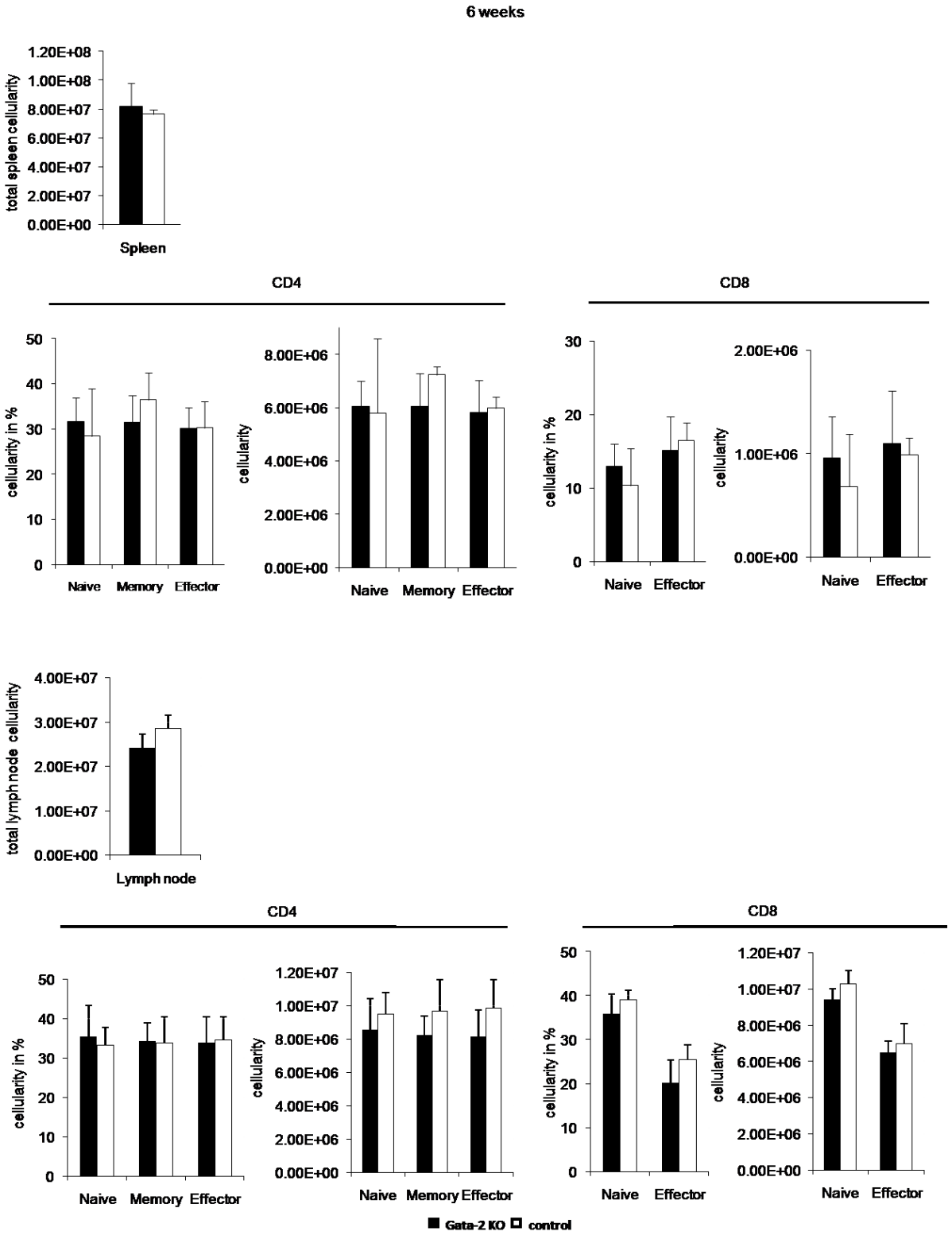

Fig. 4.17a: **Phenotypic analysis of splenic and lymphatic T-cells.** Cells were stained with CD62L, CD44, CD4 and CD8. Naïve CD4 ($CD44^{lo}$, $CD62L^{hi}$), effector CD4 ($CD44^{hi}$, $CD62L^{lo}$), memory CD4 ($CD44^{hi}$, $CD62L^{hi}$); naïve CD8 ($CD44^{hi}$, $CD62L^{hi}$) and memory/effector ($CD44^{hi}$, $CD62L^{hi}$). 6 weeks old females (n=3/group)

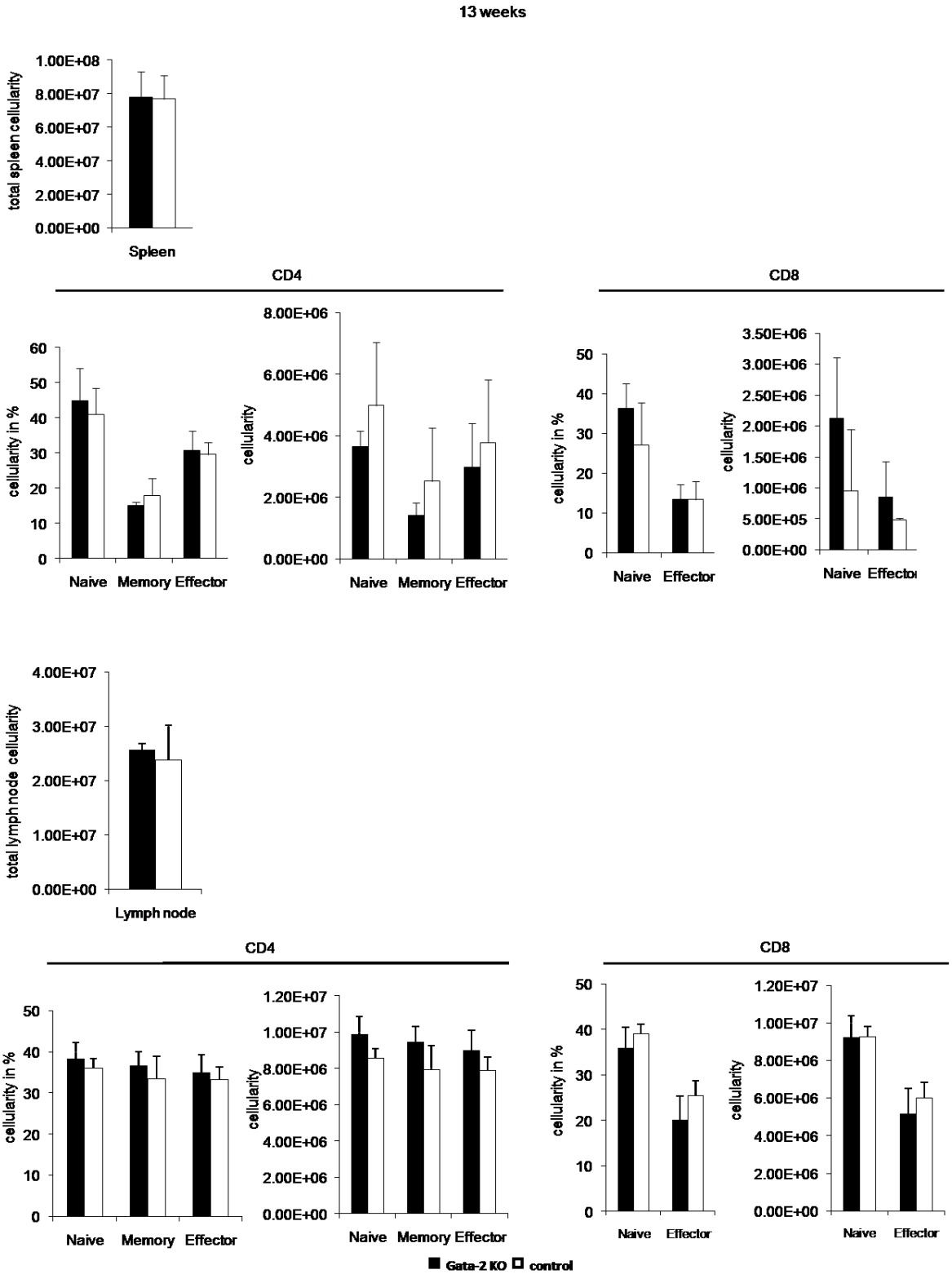

Fig. 4.17b: **Phenotypic analysis of splenic and lymphatic T-cells.** Cells were stained with CD62L, CD44, CD4 and CD8. Naïve CD4 ($CD44^{lo}$, $CD62L^{hi}$), effector CD4 ($CD44^{hi}$, $CD62L^{lo}$), memory CD4 ($CD44^{hi}$, $CD62L^{hi}$); naïve CD8 ($CD44^{hi}$, $CD62L^{hi}$) and memory/effector ($CD44^{hi}$, $CD62L^{hi}$). 13 weeks old females (n=3/group)

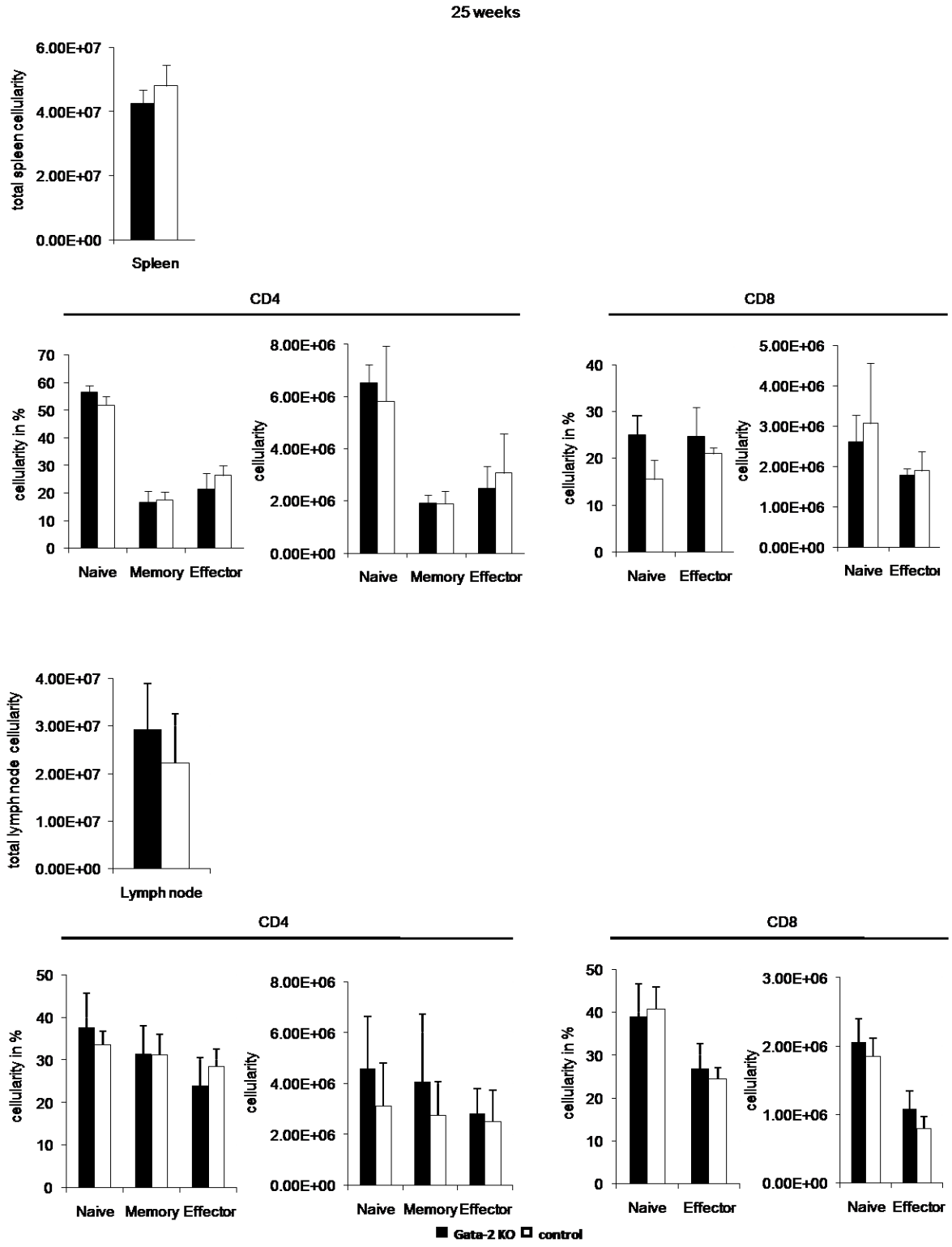

Fig. 4.17c: **Phenotypic analysis of splenic and lymphatic T-cells.** Cells were stained with CD62L, CD44, CD4 and CD8. Naïve CD4 ($CD44^{lo}$, $CD62L^{hi}$), effector CD4 ($CD44^{hi}$, $CD62L^{lo}$), memory CD4 ($CD44^{hi}$, $CD62L^{hi}$); naïve CD8 ($CD44^{hi}$, $CD62L^{hi}$) and memory/effector ($CD44^{hi}$, $CD62L^{hi}$). 25 weeks old females (n=4/group)

4.4.3.5 The proliferative capacity of mature T-cell derived from Gata-2 KO is normal

To study whether Gata-2 deficiency in the TEC has an influence on T-cell proliferation capacity, $CD4^+$ and $CD8^+$ peripheral T-cells were isolated from lymph nodes and stimulated by CD3 cross-linking as a mitogenic stimulus. Cell proliferation was subsequently assayed 48 hours later using thymidine incorporation and CFSE (carboxyflourescein diacetate-succinimidyl ester) labeling. For the experiment, cells from lymph node of 6 weeks old females were isolated and resuspended in 1mL PBS with or without 10µM of CFSE. The cells were stimulated with 4µg/mL of anti-CD3 antibody for 48 hours and then stained with anti-CD4 and anti-CD8 antibody for FACS analysis. For the ^{3}H-thymidine labeling $1x10^5$ cells were seeded into a single well of a 96 well plate. The cells were than stimulated with plate-bound anti-CD3 with the following concentrations: 0, 0.1 µg/mL, 2.5µg/mL, 5µg/mL and 10µg/mL. After 48 hours the supernatant were exchanged with media containing 1µCurie of H_3-Thymidine to quantify DNA via DNA synthesis. The peripheral CD4 and CD8 of Gata-2 deficient mice did not show any differences in their proliferative behavior when compared to their control mice (Fig. 4.18). These results indicated that Gata-2 deficiency restricted in the TECs did not affect the proliferative capacity CD4 and CD8 single positive T-cells. CFSE staining was used as an alternative method to quantify T-cell proliferation and the number of divisions in response to mitogenic anti-CD3 stimulation, because CFSE is equally partitioned among daughter cells with each cell-division. At the end of 48 hours CD4 and CD8 T-cells of both groups had undergone four cell divisions (Fig.4.19). This indicates that the proliferative behavior upon anti-CD3-stimulation was not disturbed in the $CD4^+$ and $CD8^+$ T-cells which developed with the support of Gata-2 deficient TECs.

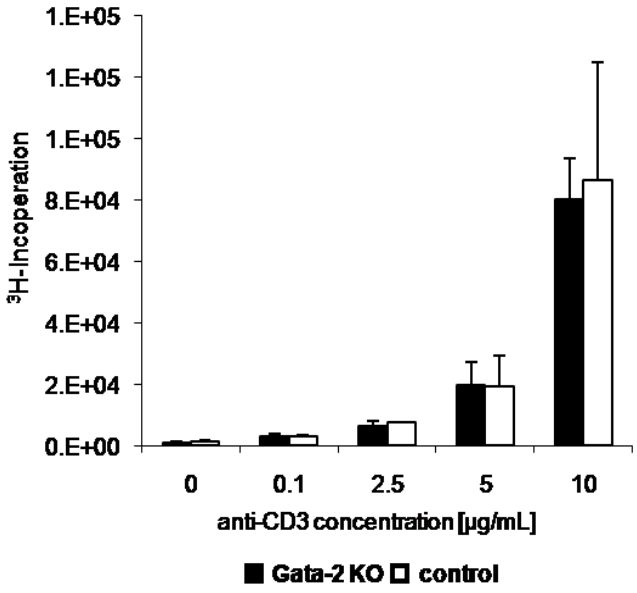

Fig. 4.18: Measurement of ^{3}H-Thymidine uptake in response to anti-CD3 stimulation. Following anti-CD3 concentration was used: 0, 0.1, 2.5, 5, 10 µg/mL. (Gata-2 KO: n=4; Littermate Control: n=3)

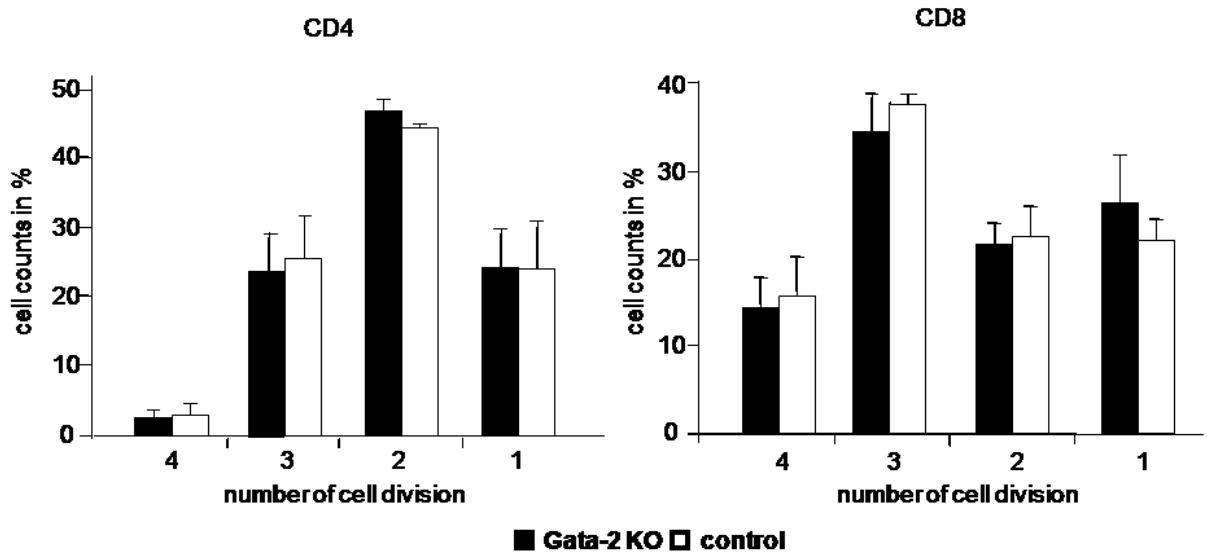

Fig. 4.19: Quantification of T-cell proliferation by CFSE from sorted CD4 and CD8 T-cells isolated from lymph nodes. 10 x 10^6 cells were resuspended in 10µM of CFSE containing PBS. Cells were stimulated for 48 hours with soluble anti-CD3.

4.4.3.6 Increase TEC cellularity in Gata-2 KO mice of six weeks of age

TECs represent in many ways an exceptional epithelial cell type least not because of their architectural organization representing a three-dimensional network of cells largely independent of a basal membrane (van Ewijk et al., 1999). To test whether Gata-2 deficiency led to a change in TECs numbers, thymic epithelial cells from female mice in the age of 3, 6, 13 and 25 weeks were analyzed by FACS. Furthermore, a ratio of total thymocytes and TECs were calculated to see whether TEC deficient of Gata-2 were capable to support more thymocytes than the control group (4.20). At all time points, the TEC numbers from Gata-2 KO remained similar to their controls. Even the thymocytes/TEC ratio between Gata-2 KO mice and the control group remained unchanged in mice of three and six weeks of age. However, 13 and 25 weeks old mice, which lack Gata-2 in their TECs, had a significant increase in thymocyte/TEC ratio. These results indicate that TECs of Gata-2 KO were capable to support more T-cells in their development.

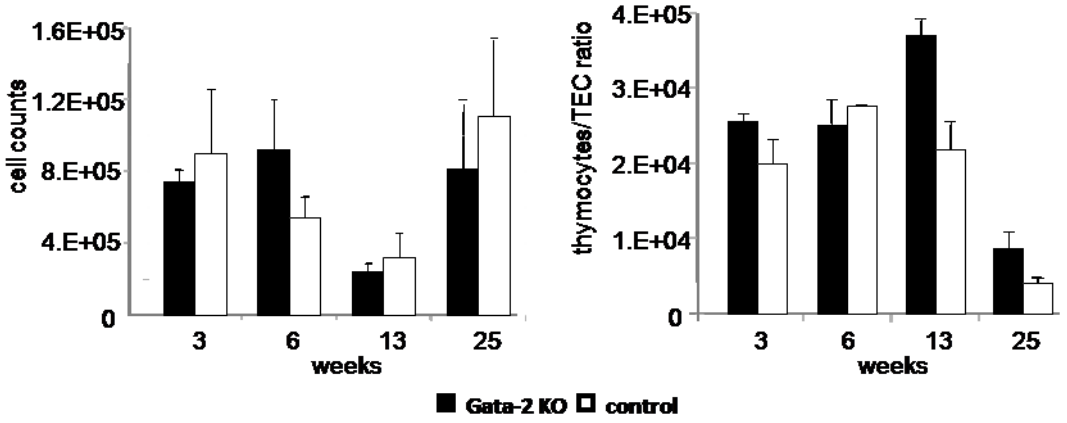

Fig. 4.20: **TEC analysis of Gata-2 KO mice.** Total TEC (CD45$^-$, MHCII^{hi}, MHC^{int}, G8.8$^+$) population of female Gata-2 KO and control mice at the time points 3 (n=3/group), 6 (n=6/group), 13 (n=3/group) and 25 (n=3/group) weeks were compared.

4.4.3.7 RT-PCR revealed an increased expression of c-kit ligand, Edn-1 and CXCL-12 in Gata-2 KO TECs

To find an explanation for the increased numbers of thymocytes in the Gata-2 deficient thymus the gene expression of TECs were analyzed. TECs were sorted from six weeks old mice from Gata-2 KO and the control group, RNA isolated, cDNA synthesized and RT-PCR was performed for genes which were related to cell-cycle progression, cell migration and

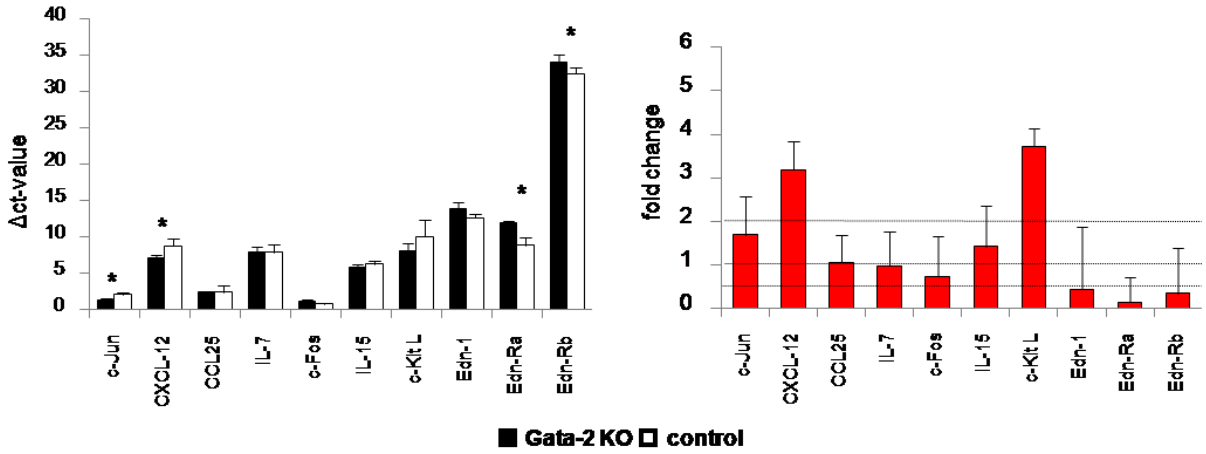

Fig. 4.21 RT-PCR analysis of Gata-2 KO TECs. TECs (CD45$^-$, MHCII^{hi}, MHC^{int}, G8.8$^+$) from Gata-2 KO and littermate controls were sorted, RNA extracted and cDNA synthesized. Δ-Ct values were normalized to GAPDH and the fold changes were calculated from ΔΔ-ct-values. (* = $p<0.05$)

survival, respectively (Fig. 4.21). *In vitro* experiments have shown that Gata-2 is important for expression of c-Fos and c-Jun (AP-1 complex) in endothelial cells. To test whether a lack

of Gata-2 in TECs resulted in an alteration of AP-1 complex quantitative RT-PCR was used for the expression of c-Fos and c-Jun. Endothelin-1 (Edn-1), Endothelin receptor Ra/Rb (Edn-Ra, Edn-Rb), IL-7, IL-15 and c-kit ligand have been shown to be involved in proliferation or/and survival of various cell types (Massa et al.. 2006; Rodewald et al., 1997; Ludwik et al., 1998; El Wakil et al., 2006). c-Jun was slightly increased (1.5 fold) while Edn-1 (0.4 fold), Edn-Ra (0.2 fold) and Edn-Rb (0.3 fold) expression was milder decreased in its expression in TECs (Masatoshi et al., 1995). In the thymus CXCL-12 and CCL-17 are responsible for migration/homing of thymocytes and its precursors. The analysis of the RT-PCR data revealed that the CXCL-12 and c-kit ligand expression was increased 3 to 4 fold in TECs of Gata-2 KO mice. These results indicate that more T-cell precursors might migrate and that they might survive longer in the thymus. The expression of AP-1, CCL-25, IL-7 and IL-15 remained unchanged.

V. Discussion

The thymus is the primary lymphoid organ for the generation and selection of T-cells (Rodewald et al., 1998). The loss of thymic function by malformation of the thymus results in limited individual capacity to maintain a broad T-cell antigen receptor repertoire or in worse cases in a complete lack of the adaptive immune-system (Hong et al., 2001). Therefore, it is important to understand the mechanisms and to characterize the genetic program that determines thymic epithelial cell fate and differentiation. In this context, this thesis intends to identify the molecular players in early thymus development by analyzing the gene expression profile and to understand in an *in vivo* study the function of one particular candidate gene: Gata-2.

The RNA isolation protocol which was specifically established for the purpose of this study made it possible to pool small amounts of RNA in a high quality so that a reliable amplification of RNA was possible for gene expression profiling by Affymetrix Gene Chip. Sufficient RNA quality as determined by Agilent Chip was given since the 18 and 28 ribosomal RNA peaks were clearly present in all samples tested (Fig. 4.1). Once the protocol for isolation of small amount of RNA was successfully established, cells and then RNA of the anterior part of the ventral aspect of the 3rd pp were isolated where Foxn1 is expressed as early as E10.5. Hence, the specific mechanisms that control early thymocyte development are initially located to the anterior aspect of ventral aspect of 3rd pp.

To verify the obtained gene expression data of the anterior part of the ventral aspect of 3rd pp, qRT-PCR and whole mount in situ hybridization was utilized. The fold change difference in gene expression that resulted from Affymetrix gene chip data differed from the gene expression data obtained from qRT-PCR except for the genes Msx1, FoxG1 and 1110006E14Rik. Although the other candidate genes showed a similar expression in the anterior part of the ventral aspect of the 3rd pp, the actual fold change of differential expression in comparison to the dorsal circumference when assessed by RT-PCR differed from that of the Affymetrix data set. The highest expressed gene according to qRT-PCR analysis was C1pdc2 with an 11-fold change over the dorsal aspect of the 3rd pp. The gene C1pdc2 encodes a 308 amino acid long protein with an unknown function. Therefore, it is difficult to assess the role the gene C1qdc2 in thymus development. In regards to Gata-2 expression, a higher level of transcript was identified in Affymetrix gene chip data. This discrepancy in the results between Affymetrix gene chip data and qRT-PCR was previously

reported (Rajeevan et al., 2000, 2001; Zhao et al., 2004). The main reason for the differences observed is due to the methods how the expression of a gene was determined by gene chip and qRT-PCR. Gene chips are limited by its insensitivity to identify transcripts of low abundance like genes expressed at a low levels or in a small fraction of cells studied. Even transcripts of high abundance could be missed by DNA microarray as well due to the poor hybridization between the probes and the labeled cRNA targets (Cao et al., 2004). One factor that could affect the hybridization step is the sequence targeted by the gene chip probes. Since majority of the probes on the gene chip are 3'-biased and limited to match the target generation characteristics of the sample amplification method (in this case two rounds of amplification was performed). The sequences at the 3`end might not have ideal characteristics (G-C and A-T ratio, low repeating sequences to avoid dimerization) for hybridization. Furthermore, the outcome of results from gene chip is also dependent on the program which is utilized to analyze the data set. Independent of the precise fold changes, both methods confirm the differences in the level of expression of the candidate genes when comparing the dorsal and the anterior-ventral part of the 3rd pp. In general DNA microarrays are powerful tools that enable the global analysis of a variety of different cell-systems because expression of thousands of gene can be analyzed simultaneously. However, more sensitive evaluation with qRT-PCR is necessary because genes identified by DNA array with a two-to fourfold difference in expression cannot be eliminated as false nor be accepted as true without validation (Rajeevan et al., 2001, Zhao et al., 2004).

Candidate genes that had by RT-PCR a two- and higher fold increase in expression in the ventral-anterior aspect were further analyzed by in situ hybridization. For positive control Bmp4 was chosen. The expression patterns of the genes Bmp4 and dll-1 (delta-like 1) were previously described (Mathura et al., 2000, Grotewold et al., 2001, Teppner et al., 2007). Bmp4 was detectable in the apical ectodermal ridge (AER) and in the mesechyme of the genital tubercle while dll-1 staining was detected in the somitocoele adjacent to the caudal epithelium (Fig. 4.7) indicating that the technique itself was successful. For the genes Unc5h3 and C1qdc2 no signals were obtained. C1qdc2 transcript consists of 1301 bp and encodes a protein of 308 aa. So far, no studies have been performed to identify the function of this protein. First reports about Unc receptors derived from studies from *Caenorhabditis elegans* (C. elegans): unc5, unc6 and unc40 (Hedgecock et al., 1990). These three receptors are involved in axonal pattering and cell migration. In vertebrates the family of the Unc5 family include: Unc5h1, Unc5h2, Unc5h3 (Unc5c) and Unc5h4. These receptors are capable to bind Netrin-1, a soluble factor that either can induce attraction or repulsion of axon growth

depending on to which receptor Netrin-1 binds (Baker et al., 2006, Round et al., 2007). In neuronal development a binding to Unc5 receptors leads to repulsion, suggesting that Unc5 receptors are involved in cell migration (Guijarro et al., 2006, Barallobre et al., 2005). Expression studies of the different Unc5 receptors in E11.5 embryos have shown that Unc5h1 expression is restricted to the ventral spinal cord, whereas Unc5h2 is present in the developing eye, inner ear, vasculature and limb buds. The detection of the transcript of Unc5h3 is strongest in migrating neural crest cells and in the anterior and posterior part of the proximal limb mesenchyme while Unc5h4 expression is restricted to a thin line at the base of the forelimb and to the limb bud (Engelkamp, 2002). Mice deficient of Unc5h3 are vital but have abnormalities in postnatal cerebella neuronal migration (Ackerman et al., 1997). The mesenchymal cells mediate epithelial cell proliferation and have an inductive effect on epithelial cell morphogenesis and have their origin in neural crest cells. A remove of the neural crest cells leads to a failure in thymus, formation (Bockman et al., 1984). The fact that Unc5h3 is expressed in neural crest cells and are involved in migration processes might indicate its potential role in the very early stage of neural crest cell migration which is needed for the thymus development. In fact, Unc5h3 is expressed in the thymus of six weeks old mice (UniProt Consortium). Since no positive signal was obtained even in the neural crest cells, it is possible that the two probes used for whole in situ hybridization for Unc5h3 did not anneal to mRNA which might explain the results (Fig. 4.7). Since no information for C1qdc2 is available, it is hard to assess whether the results of whole mount in situ hybridization is reflecting the expression pattern of C1qdc2 at the time point of E10.5.

Several of the genes identified by gene expression profiling and RT-PCR (Gata-2, dll-1, Msx1, Msx2, Ehox, Tgfbi, Unc5c, FoxG1) have been linked to play a role in E10.5 thymus anlage except for the genes 1110006E14Rik, C1qdc2 and Samd5 with unknown role in thymus development. Gata-2, Msx1, Msx2, Unc5h3 and FoxG1 are transcription factors. Msx1 and Msx2 are homeobox transcription factors which are important for the development of the structures derived from the cranial and cardiac neural crest cells. During embryonic development Msx1 expression is detected in the mesechyme of the first arch as early as E9.5. At E10.5 Msx1 transcript is restricted to the lateral mesenchyme in the buccal half of the first arch and is present in a medial stripe of the mesenchymal cells in the second arch (MacKenzie et al., 1997), but at E11.5 Msx1 was detectable in the thymus anlage by in situ hybridization (Bleuel et al., 2005). A deficiency of Msx1 exhibits agenesis of the teeth, a cleft palate, and abnormalities of the cranial skeleton (Satokata et al., 1994). Furthermore, Msx1 is crucial for the epithelial-mesenchyme interaction during tooth development (Chen et al., 1996, Bei et al.,

1998). Msx2 deficiency is less severe than Msx1 mutations since Msx2 mice are vital and fertile. Mice homozygous for a targeted mutation in Msx2 have a defect in the development of the frontal bone due to a failure of neural crest-derived calvarial osteogenic cells (Satokata et al., 2000; Ishii et al., 2003). Neither Msx1 nor Msx2 mutation analysis have reported a defect in thymus development, but double mutation analysis of Msx1 and Msx2 deficient mice have a dislocated thymus (Ishii et al., 2005). Whether the thymus structure or function is altered in $Msx1^{-/-}/Msx2^{-/-}$ mice have not been addressed in this study. Several upstream regulators of Msx genes have been identified including Bmp and Fgf pathways. In Fgf8 deficient mice, which have a small or an absent thymus, Msx1 is down regulated in the 1st and 2nd pp at the time point of E10.5 in mice development (Abu-Isha et al., 2002). Bmps are expressed broadly in the pharyngeal ectoderm and endoderm and influence the development of cranial and cardiac neural crest-lineage cells (Waldo et al., 2001; Ohnemus et al., 2002). In E9.5 mice, lacking Msx1 and Msx2 expression, Bmp4 was significantly elevated in the cranial mesenchyme including the migrating neural crest cells, the maxillary prominence, the distal part of the 1st and 2nd pharyngeal arch and the body wall epithelium suggesting the role of Msx genes as a negative regulator of Bmp signals in these structures (Ishii et al., 2005). The role of Bmp4 in thymus development has been shown by Bleul and his colleagues using transgenic mice which express the Bmp antagonist noggin under the control of the Foxn1 promoter. At E10.75, Bmp4 is strongly expressed in Foxn1-positive epithelial cells of the ventral and medial part of the 3rd pp as well as in the neural crest derived mesenchymal cells that surround the anlage (Bleul et al., 2005). In thymus, Msx1 is detectable in the capsular mesenchymal cells as early as E12.5 but not in the TECs suggesting BMP signals might play a role in the epithelial-mesenchymal interaction that shapes the thymic stroma (Bleul et al., 2005; Ohnemus et al., 2002; Bockman et al., 1984). The Affymetrix gene chip data confirms the pathways that are involved in the thymus development: Bmp- and Fgf pathways. Msx1 is involved in both pathways. However, how Fgf and Bmp4 signaling affects Msx1 expression in thymus development need to be addressed. According to gene chip data and RT-PCR data expression of Msx1 is 4.3 fold and 6.2 fold increased, respectively. In regards to Msx2 expression the literature does not provide sufficient information to confirm the results of Fig. 4.6. Taken together, Msx1 and Msx2 might play a role in thymus migration from the pharyngeal region to the mediastinum and act as a mediator for mesenchymal-epithelial interaction during thymus development.

Tgfbi (transforming growth factor-β induced) is a secreted protein induced by transforming growth factor-β (Tgfβ-β). It was identified in human adenocacinoma cell line treated with

Tgf-β (Skonier et al., 1992). Tgfbi is a component of extracellular matrix in lung and mediates cell adhesion and migration though interacting with integrins via integrin receptors: α3β1, αvβ1, and αvβ5 (LeBaron et al., 1995; Billings et al., 2000; Kim et al., 2002, Nam et al., 2003; Jeong et al., 2004). In many tumor cell lines including lung, breast, colon and leukemia, as well as in human lung and breast tumor specimen Tgfbi expression is inactivated. Furthermore, mice lacking Tgfbi develop with a higher frequency tumors than their wild-type littermates because Tgfbi deficient cells have a higher cell proliferation through aberrant activation of cyclin D1 pathway (Zhang et al., 2009). These finding suggest that the expression of Tgfbi at E10.5 in the ventral aspect of 3rd pp might play a role in migration of the thymus anlage and that the induction of Tgfbi expression is caused by other Tgf-β family members like Tgf-β1 which is expressed in the neural crest derived mesenchymal cells in E10.5 mice and in fetal thymus (Schmid et al., 1991).

Delta-like homolog 1 (dll-1) and delta-like homolog 4 (dll-4) are ligands in the Notch signaling pathway which are required for cell differentiation and patterning processes during mammalian embryogenesis. Activation of Notch is depended upon binding to ligands belonging to the Delta or Jagged/Serrate families. Dll-1 and dll-4 are expressed in the fetal thymus anlage and can be detected as early as E12 and is dependent on Foxn1. In Foxn1-deficient mice (nude mice) dll-1 and dll-4 are not detected (Tsukamoto et al., 2005). Although the necessity of dll-1 and dll-4 for the thymocyte development is well established, the role of notch ligands in thymus-thymocytes crosstalk have been unclear (Schmitt et al., 2002, Koch et al., 2008, Hozumi et al., 2008). A recent study has revealed that enforced expression of dll-1 in B-cells is capable to induce mTEC proliferation and maturation indicating that Notch signaling is involved in TEC-thymocyte interaction (Masuda et al., 2009). According to RT-PCR and Affymetrix gene chip data dll-1 transcript is present in the 3rd pp as early as E10.5 (Fig. 4.6), suggesting that the dll-1 is already present on the thymic epithelial cells before the thymocyte precursors enter the thymus around E12 and Notch signaling is not operating at E10.5 in the ventral aspect of the 3rd pp.

Gene Chip (4-fold) and RT-PCR (2-fold) have identified Ehox as another transcript that is up regulated in the ventral-anterior aspect of 3rd pp. ES cell-derived homeobox (Ehox) gene is an X-linked paired like homeobox that is proposed to have a dual role in tropoblast stem cells and compartment of the developing placenta, as well as during development of the pharyngeal pouches, and possibly delineates the area that becomes thymus (Jackson et al., 2003). At the murine developmental stage of E10.5 whole mount in situ hybridization have shown that

Ehox expression in the pharyngeal region was restricted to the ventral aspect of 3rd pp (Jackson et al., 2002; Jackson et al., 2003). A detailed promoter study of Ehox revealed several consensus binding sites for transcription factors which include GATA, DeltaEF, NKX25, USF, AP4, AP1, NF-Y and SP1 (Lee et al., 2006). Interestingly, Gata-2 was also up regulated in the ventral-anterior aspect of 3rd pp suggesting a role of Gata proteins in regulation of Ehox expression. Whether Gata-2 actually binds to the promtor of Ehox needs to be clarified. Since no studies of Ehox deficient mice are available and the characterization of the protein is insufficient, it is difficult to assess the function of Ehox in thymus development.

Another candidate gene which was identified to be up regulated in the 3rd pp is FoxG1. FoxG1 is expressed in the telecephalon, optic and otic vesicles and in the pharyngeal endoderm (Pratt et al., 2002; Arnold et al., 2006). In FoxG1 deficient mice the telecephalon is severely disrupted, but a thymus phenotype was not reported (Pratt et al., 2002).. Furthermore, gene chip data analysis has shown that FoxG1 is down regulated in Tbx1 deficient mice (Ivins et al., 2005). Interestingly, a specific deletion of Tbx1 gene in the pharyngeal pouches using FoxG1-cre in mice showed a phenotype similar to 22q11 DiGeorge syndrome (22q11DS) because pharyngeal arches fail to develop with an exception to the 1st pharyngeal arch. 22q11DS characteristics are craniofacial abnormalities, thymus gland hypoplasia or aplasia, hypocalcaemia and cardiac outflow tract defects (DiGeorge 1965; Shprintzen et al., 1978). Because of the defects observed in Tbx1 deficient mice, it is unlikely that FoxG1 might play role in the thymus development later than E10.5. The development of the pharyngeal area occurs earlier than E10.5. It is possible that FoxG1, as a downstream target of Tbx1, is one of the regulators for the pharyngeal arch development in the very early of embryogenesis.

Sterile alpha motif domain-containing protein 5 (Samd5) and 1110006E14Rik are two other genes which have an up regulated expression in the ventral-anterior aspect of 3rd pp when compared to the dorsal part of the 3rd pp. A thorough search in NCBI, Ensembl and Uniprot for those two genes revealed no functional description or details about the expression pattern in mice. Therefore, it is difficult to make any conclusions from the Affymetrix gene chip and RT-PCR data for the role of Sam5 and 1110006E14Rik in thymus development.

Gata molecules have not yet been linked to the mechanisms operational in thymus development. At E10.5, Gata-2 expression as detailed by whole in situ hybridization is localized to the entire aspect of 3rd pp. RT-PCR shows Gata-2 expression throughout the embryonic development of the thymus starting from E10.5 to E17.5 in the TECs and the

ventral-anterior aspect of the 3rd pp, respectively (Fig. 4.9). Gata-2 expression was highest at E10.5 and drops rapidly at E12.5 and onwards suggesting the role of Gata-2 rather in the very early stage of thymus development when first morphological signs of thymus organogenesis are apparent. Whole mount in situ hybridization of Gata-2 and Ehox showed a similar expression pattern in the ventral circumference of 3rd pp. As previously described, Ehox has a Gata-2 binding site in its promoter region and has been suggested to play a role in the delineating the area that becomes thymus (Jackson et al., 2003; Lee et al., 2006). However, this interaction needs to be proven.

Gata-2 gene was conditionally deleted in TECs. For this purpose, Foxn1-cre was utilized which expresses cre in thymic epithelial cells from E11.5 onwards (Zuklys et al., 2009). The deletion of Gata-2 was confirmed by RT-PCR of sorted TECs from mice embryos of E11.5, E12.5 and 6 weeks old mice, respectively. The deletion was, however, incomplete in E11.5 mice. Gata-2 transcript was detected, although its expression level was decreased in comparison to controls. This could be explained by the delayed Cre expression in Foxn1 positive TECs (Zuklys et al., 2009). A deletion of Gata-2 in earlier developmental stage of thymus was considered because the RT-PCR and Affymetrix gene chip data showed that Gata-2 transcript was most abundant at the time point of E10.5 (Fig. 4.6). Hoxa3-Cre and Fgf15-Cre are two mice strains which express the cre protein earlier than E10.5. Hoxa3 is expressed as early as E8.5 in the surface ectoderm of the pharyngeal region and extends into pharyngeal endoderm and mesoderm (Zhang et al., 2005). Mice deficient of Hoxa3 do not develop thymus, parathyroid, as well as thyroid (Manley et al., 1995). Fgf15 is expressed at E9 onwards and is expressed specifically in the pharyngeal epithelia and in the developing brain. Fgf15 deficient mice present heart defects and die between E13.5 and E18.5 or shortly after birth, respectively (Vincentz et al., 2005). For our purpose Hoxa3-Cre mice could not be used because the genes Gata-2 as well as Hoxa3 are located in the chromosome 6. For a successful deletion of Gata-2 by Hoxa3-Cre a crossing over is needed and therefore, would have been out of the time scale of this thesis because the crossing-over frequency between these two genes is about 12%. The deletion of Gata-2 by Fgf15-Cre however, was feasible. Unfortunately, the expression of Fgf15-Cre was not consistent. Only six mice out of 48 were tested positive for Fgf15-Cre (12.5%). Due to the low frequency of Fgf15-Cre^{+} expressing mice, the use of this mice strain was stopped.

The TEC specific deletion of Gata-2 was confirmed using qRT-PCR in mice E12.5 and E13.5 and in 6 weeks old mice on sorted TECs (CD45^{-}, G8.8^{+}, MHCII^{+}). For morphological studies

and detailed analysis of thymus architecture of Foxn1-Cre^{+}::Gata2$^{loxP/loxP}$ H&E and immunofluorescence (CK18, CK5, UEA-1) were used, respectively. The stainings of thymus from 3, 6, 13, and 25 week old thymus showed no difference in their expression of CK18, CK5, and UEA-1 when compared to their littermate controls. Furthermore, the thymi of Foxn1-Cre^{+}::Gata2$^{loxP/loxP}$ showed a clear distinction of cTEC and mTEC area indicating that Gata-2 deficiency do not disturb the development of thymus structure .

Analysis of the thymus cellularity revealed that Foxn1-Cre^{+}::Gata2$^{loxP/loxP}$ mice have an increased thymocyte numbers. Interestingly, this increased was only observed in mice older than 3 weeks which suggests the thymus of Foxn1-Cre^{+}::Gata2$^{loxP/loxP}$ until the week 3 developed similar to the littermate controls. The largest difference in thymocyte cellularity was observed in the Gata-2 KO mice of 6 week of life. Thymocyte subpopulations and their maturational progression in Foxn1-Cre^{+}::Gata2$^{loxP/loxP}$ thymus was unaltered between mutant and wild-type mice. The increase of T-cell cellularity was not due to a disturbed T-cell development or block at a certain stage of T-cell development. Hence, the increased thymocyte numbers in Foxn1-Cre^{+}::Gata2$^{loxP/loxP}$ mice might be rather due to a higher attraction of T-cell precursors (CD44^{+}, CD117^{+}, CD25^{-}, CD45^{-}) or due to a stronger proliferation of the T-cell precursors. The attraction of T-cell progenitors to the thymus depends on the interaction of chemokines and their receptors. Among 36 chemokines, only 3 (CCL-21, CCL-25, CXCL-12) shows DN1 fetal thymocytes-attracting activity (Alves et al., 2009). Moreover, when antibodies are used to block CCL-21 or CCL-25 pathways fetal thymus attraction is significantly inhibited in contrast to CXCL-12 where no effect in T-precursor attraction is observed indicating that neither CXCL-12 nor its ligand CXCR4 is required for the migration of T-precursors to the fetal thymic primordium (Alves et al., 2009). These results confirm previous data in which CXCL-12 or its receptor CXCR4 deficiency led to normal accumulation of T-precursors to their thymic primordium at E11.5 and E12.5 (Bleul et al., 2000). CXCL-12 is expressed on cTECs but not on mTECs (Plotkin et al., 2003). In hematopoietic chimeras where CXCR4 is conditionally deleted very early after entry into the thymus, mutant thymocytes stop developing at the DN1 stage (Plotkin et al., 2003). A gene expression of thymic epithelial cells from 6 weeks old mice analysis of Foxn1-Cre^{+}::Gata2$^{loxP/loxP}$ showed an increased expression of CXCL-12 (3 fold) compared to their littermate controls while CCL-25 expression remained unaltered (Fig 4.21). The increased expression of CXCR12 might lead to a higher recruitment of T-cell precursors and thus increasing the total thymocyte cellularity. Another candidate that has been implicated with promotion of T-cell proliferation is c-kit ligand. A block of c-kit has been shown to inhibit

proliferation of $CD25^+$ thymocytes which include DN2 population, thus strongly indicating that stromal production of Kit ligand is essential for proliferation and also for differentiation of sub-population of DN1 (Godfrey et al., 1992; Rodewald et al., 1997; Massa et al., 2006, Massa et al., 2006). *In vitro* studies using Gleevec to prevent c-kit signaling have shown that proliferation and development of DN1 ($CD25^-CD44^+$c-kit^{high}) and DN2 ($CD25^+CD44^+$c-kit^{high}) are dependent on c-kit – c-kit ligand interaction when DN1 and DN2 are grown in presence of OP9d1 and IL-7 (Massa et al., 2006). In TECs of Gata-2 deficient mice, c-kit ligand transcript was (~4 fold) up regulated (Fig. 4.21) indicating that a higher expression of c-kit ligand might be another reason for an increased thymus cellularity. If an increased c-kit ligand expression on TECs would lead to an increased cell proliferation of DN1 and DN2 in their development, need to be verified. Interestingly, from more than 80 mice analyzed, about 4 Gata-2 KO did not show any difference to their controls. A possible explanation is that Gata-2 was not deleted in enough TECs due to a lower amount of Foxn1-Cre^+ TECs to cause a phenotype.

To characterize the TECs of Gata-2 KO mice TECs of Foxn1-Cre^+::$Gata2^{loxP/loxP}$ at the stage of 3, 13, and 25 weeks were analyzed. The TEC numbers of Gata2 KO mice did not differ significantly from the control mice. However, the thymocyte/TEC ratio was significantly increased at the week of 13 and 25 while thymocyte/TEC ratio of 3 and 6 weeks old mice did not change (Fig. 4.20) indicating that the thymus of Gata-2 KO mice are capable to support more T-cells. However, the data especially from week 13 and 25, should be considered only as preliminary results, because the numbers of mice used for the experiment might have been too low to assess the TEC population. At least 6-10 thymi per group would provide a better reflection of the actual TEC population in Gata-2 KO and their littermate control.

Because TECs support T-cell development thymidine incorporation assay and CFSE assay to quantify the proliferation of thymocytes after CD3-activation was chosen as a functional readout to test whether Gata-2 deficiency in TECs have an influence on thymocyte function. Therefore, T-cells from lymph nodes were isolated and analyzed. The results showed no difference when cell proliferation of thymocytes that developed in the thymus of Gata-2 KO mice were compared to their controls suggesting Gata-2 deficient TECs are capable to develop functional thymocytes comparable to wild-type mice.

Endothelin-1 is a 21-amino acid vasoactive peptide initially characterized as a product of endothelial cells (Masaki et al., 1993; Masaki et al., 1991). Edn-1 deficient mice have a significant smaller thymus which fails to fuse in the midline (Kurihara et al., 1995). *In vitro*

experiments have shown that Gata2 and AP-1 are capable to control Edn-1 expression. TECs from Gata-2 deficient mice were tested if the Edn-1 expression was altered. As Fig. 4.21 shows, the Edn-1 transcript and Edn-Ra and Edn-Rb are decreased in TECs of Gata-2 KO mice. c-Jun and c-Fos expression remained unaltered, indicating that a lack of Gata-2 for Edn-1 expression is not compensated by AP-1 complex. These findings support the idea that Edn-1 might also be controlled by Gata-2 *in vivo* (Kawana et al., 1995). However, several studies have shown that Edn-1 and Edn-Ra are over expressed in several cancer types including breast, colon stomach and prostate (Kusuhara et al., 1990; Ali et al., 2000, Smollich et al., 2008). Evidence suggests that Edn-1 and the receptors Edn-Ra and Edn-Rb promotes tumor by increasing the survival and proliferation of tumor cell lines (Nelson et al., 1995, 1996). These studies contradict the finding of increased thymocyte in Gata-2 KO mice suggesting that the increased thymocyte phenotype observed in Gata-2 KO mice is not due to the Edn-1 pathway which can mediated cell proliferation/survival. The decreased expression of Edn-Ra and Edn-Rb cannot be explained because there is no published data which correlates Gata-2 or Edn-1 expression with transcription of Edn-Ra and Edn-Rb. However, it is possible that Edn-Ra and Edn-Rb receptor regulation might be dependent on level of Edn-1 expression since the RT-PCR data of the two receptors was reduced in a similar level as Edn-1 itself.

VI. Conclusions & Outlook

This thesis describes an established protocol which enables to recover small amounts of RNA (in pg range) from micro dissected cells. This method combined with gene expression analysis using gene chip allows the identification of gene expression profile from tiny anatomical sites like the ventral-anterior aspect of 3rd pp. After a careful evaluation and verification of the gene chip data the Gata-2 gene was chosen as a candidate for detailed studies. So far, Gata-2 has not been associated with thymus development. Unfortunately, a deletion of Gata-2 in the ventral aspect of 3rd pp at the time point of E10.5 when Gata-2 expression was highest during thymus development was not feasible. The interruption of Gata-2 transcription at the time point of E12.5-13.5 showed that deletion of the Gata-2 gene in TECs has a minor effect on thymus development. The difference observed was an enlarged thymus size due to a higher thymus cellularity which can be explained by an increased expression of CXCL-12 and c-kit ligand.

Several issues still need to be addressed to understand the detailed function of Gata-2 in thymus development and in TECs. An issue that has not been addressed in this thesis is, if the increased/decreased expression of CXCL-12, c-kit ligand and Edn-1 is really translated to the protein level. An ideal experiment would be a western blot or FACS analysis for these two proteins on sorted TECs. Based on the presented data, it is unlikely that Gata-2 have an effect in thymus development at least in Foxn1-Cre^{+}::Gata-2$^{loxP/loxP}$ because an effect is seen only after the 6th week and at later time points.

In this study, only genes which were up regulated in their transcription in the ventral aspect of 3rd pp in the early thymus development were considered. During every phase of embryogenesis genes are not only up regulated but also down regulated like sonic hedgehog (Shh) and Fgf8 expression in limb development where Shh expression is down regulated at a certain time point. The thymus is not an exception. Therefore, attention should also be paid to those genes which were down regulated in the early thymus development.

VII. Appendix

7.1 Gene Chip Data

	Gene	D1	D2	D3	V1	V2	V3	fold change	d. o. m.	paired t-statistic	paired P-value
1450333_a_at	GATA binding protein 2	50.18	44.39	42.05	682.82	364.33	458.63	11.11	456.65	4.914	0.039004
1436041_at	heart and neural crest derivatives expressed transcript 2	91.3	72.19	54.57	470.05	434.39	595.46	6.9	429.27	7.06	0.019477
1434376_at	CD44 antigen	45.4	78.94	48.59	395.66	387.92	400.36	6.84	337.65	21.042	0.002251
1423760_at	CD44 antigen	38.08	81.55	41.49	306.8	376.31	231.93	5.68	251.79	7.477	0.017422
1423753_at	BMP and activin membrane-bound inhibitor, homolog (Xenopus laevis)	113.71	116.58	92.52	704.46	589.54	544.38	5.6	501.83	10.296	0.009301
1417393_a_at	RIKEN cDNA 1110035L05 gene	212.66	119.04	141.46	896.99	713.92	908.36	5.34	682.28	12.991	0.005874
1417466_at	regulator of G-protein signaling 5	81.18	56.55	87.56	481.64	309.47	368.17	5.21	312.33	6.691	0.021612
1420360_at	dickkopf homolog 1 (Xenopus laevis)	66.09	28.87	44.26	187.48	280.28	234.29	5.06	187.05	4.619	0.043813
1439422_a_at	RIKEN cDNA 1110035L05 gene	279.84	140.08	194.46	975.31	909.46	1214.91	5.04	827.77	7.862	0.015794
1448147_at	tumor necrosis factor receptor superfamily, member 19	73.49	116.25	88.49	495.72	573.53	317.41	4.96	367.96	4.968	0.038206
1437403_at	RIKEN cDNA E130306M17 gene	88.74	69	88.55	377.59	397.73	466.33	4.95	330.57	11.794	0.007112
1449559_at	homeo box, msh-like 2	57.29	49.6	49.15	232.51	215.81	247.47	4.5	180.8	13.695	0.005289
1448601_s_at	homeo box, msh-like 1	75.34	54.86	74.79	284.35	218.49	384.58	4.3	227.12	5.143	0.035793
1419229_at	EHOX-like	68.73	53.27	50.85	202.87	228.29	286.61	4.21	182.35	5.665	0.02978
1429896_at	RIKEN cDNA 5830408B19 gene	47.4	45.82	47.13	227.25	169.74	147.76	3.88	134.63	5.582	0.030627
1450923_at	transforming growth factor, beta 2	81.2	50.72	93.02	236.93	334.55	287.34	3.83	212.21	5.229	0.034676
1422912_at	bone morphogenetic protein 4	413.16	283.96	436.16	1411.06	1232.82	1607.91	3.79	1042.65	13.689	0.005294
1453102_at	fibronectin leucine rich transmembrane protein 3	328.39	418.24	348.67	1402.5	1232.19	1388.85	3.69	976.86	11.739	0.007179
1424186_at	RIKEN cDNA 2610001E17 gene	198.62	302.47	141.24	887.31	687.34	677.91	3.52	537.1	6.151	0.025427
1420838_at	neurotrophic tyrosine kinase, receptor, type 2	92.99	64.15	89.39	295.28	287.93	258.6	3.51	199.69	7.618	0.0168
1448123_s_at	transforming growth factor, beta induced	114.5	94.77	69.26	346.98	231.32	381	3.45	227.24	4.469	0.046594
1426255_at	neurofilament, light polypeptide	82.04	353.09	157.81	725.17	638.72	648.16	3.41	474.96	4.561	0.044865
1450729_at	heparan sulfate 2-O-sulfotransferase 1	558.45	646.94	562.43	2391.02	1880.15	1715.05	3.4	1408.2	6.34	0.023987
1451071_a_at	ATPase, Na+/K+ transporting, alpha 1 polypeptide	387.59	208.02	138.48	870.64	930.7	647.15	3.34	571.36	7.043	0.019572
1449522_at	unc-5 homolog C (C. elegans)	125.78	119.6	92.06	321.49	327.9	447.4	3.25	252.86	4.786	0.040996
1448687_at	RIKEN cDNA 1110035L05 gene	115.16	74.46	86.49	279.15	258.65	359.38	3.22	204.39	5.423	0.032365
1418172_at	heme binding protein 1	80.71	69.6	75.03	222.48	232.49	261.32	3.17	163.97	10.125	0.009614
1434129_s_at	lipoma HMGIC fusion partner-like 2	191.02	253.98	183.85	773.4	567.56	558.68	3.04	424.85	5.132	0.035937
1429310_at	fibronectin leucine rich transmembrane protein 3	321.06	497.27	306.9	1162.89	952.06	1272.79	3.01	753.24	4.89	0.039373
1454691_at	neurexin I	38.2	54.39	35.91	111.66	118.4	136.47	2.88	80.12	6.493	0.022906
1424638_at	cyclin-dependent kinase inhibitor 1A (P21)	446.32	360.56	374.89	1299.88	974.54	1058.48	2.81	715.23	9.641	0.010589
1439489_at	G protein-coupled receptor 120	44.31	38.35	55.89	119.7	139.93	131.72	2.8	83.63	7.671	0.016572
1460204_at	cytoplasmic tyrosine kinase, Dscr28C related (Drosophila)	68.85	84.1	64.67	216.31	179.55	202.27	2.75	126.8	7.232	0.01859
1428816_a_at	GATA binding protein 2	39.89	38.51	37.23	105.9	84	119.12	2.66	63.78	4.902	0.039191
1421365_at	follistatin	39.01	41.33	36.35	109.81	83.1	112.26	2.62	62.93	5.606	0.030374
1420941_at	regulator of G-protein signaling 5	33.72	52.81	37.92	108.28	113.42	104.06	2.6	67.02	9.012	0.012089
1433796_at	RIKEN cDNA 2310067E08 gene	320.52	236.45	245.41	708.53	624.5	742.19	2.59	424.25	10.419	0.009086
1428550_at	RIKEN cDNA 1810015A11 gene	89.99	40.03	69.6	148.94	166.04	183.61	2.5	100.1	4.521	0.045612
1416529_at	epithelial membrane protein 1	59.35	98.23	75.55	189.41	223.29	170.87	2.49	116.59	8.158	0.014695
1435631_x_at	SH3-domain GRB2-like B1 (endophilin)	124.44	84.87	85.79	228.18	224.47	277.75	2.47	144.93	5.387	0.032774
1419429_at	ciliary neurotrophic factor receptor	144.06	86.55	61.7	254.8	238.97	231.52	2.46	143.88	6.346	0.023945
1418010_a_at	SH3-domain GRB2-like B1 (endophilin)	1174.7	2144.1	1368.71	4368.54	3862.52	3154.07	2.45	2249.96	4.604	0.044074
1455385_at	SH3-domain GRB2-like B1 (endophilin)	125.38	87.33	93.08	241.49	223.94	272.33	2.42	144.39	7.351	0.018008
1416900_s_at	growth differentiation factor 1	150.68	87.68	76.61	252.52	234.25	267.76	2.41	147.65	5.18	0.035303
1454672_at	neurofilament, light polypeptide	43.94	109.51	66.92	176.27	168.37	188.53	2.41	103.71	4.377	0.048445
1426543_x_at	RIKEN cDNA 2310067E08 gene	85.7	129.85	117.83	268.84	297.99	219.79	2.35	150.31	5.72	0.029226
1425895_a_at	inhibitor of DNA binding 1	384.81	457.7	287.3	984.15	829.26	830.89	2.34	502.89	6.87	0.020539
1415871_at	transforming growth factor, beta induced	26.86	40.79	27.75	74.35	65.86	79.01	2.31	41.22	4.774	0.041182
1419592_at	unc-5 homolog C (C. elegans)	39.15	37.44	40.19	99.52	80.24	84.79	2.28	49.72	7.19	0.018801
1421679_a_at	cyclin-dependent kinase inhibitor 1A (P21)	168.4	136.45	168.13	299.34	413.44	371.83	2.28	202.57	4.342	0.049158

1449877_s_at	kinesin family member C5A	109.42	66.2	69.67	203.55	198.67	154.17	2.28	104.11	6.187	0.025143
1433845_x_at	dual specificity phosphatase 9	750.77	549.98	494.58	1273.19	1280.28	1540.14	2.27	762	4.843	0.040093
1422592_at	catenin delta 2	97.09	140.69	103.75	262.8	225.72	269.33	2.24	140.21	5.07	0.03677
1424797_a_at	paired-like homeodomain transcription factor 2	26.36	22.69	19.59	46.64	54.35	53.34	2.24	28.35	4.654	0.043196
1416630_at	inhibitor of DNA binding 3	856.03	892.85	578.23	1788.97	1566.82	1711.95	2.19	918.52	6.355	0.023878
1435980_x_at	wingless-related MMTV integration site 6	35.43	30.56	28.02	66.25	66.26	69.52	2.16	36.04	6.894	0.020398
1435110_at	DNA segment, Chr 10, Brigham & Women's Genetics 0792 expressed	552.05	710.27	606.44	1466.93	1361.85	1177.48	2.14	712.92	6.723	0.021415
1424842_a_at	Rho GTPase activating protein 24	57.68	89.06	59.52	140.64	175.01	121.71	2.13	77.41	8.064	0.015033
1440204_at	RIKEN cDNA 3110039M20 gene	27.26	24.07	36.42	55.42	68.99	66.59	2.13	33.85	4.694	0.042517
1455436_at	RIKEN cDNA 2900052J15 gene	37.59	35.2	31.33	73.12	70.14	78.71	2.12	38.96	5.904	0.02751
1418357_at	forkhead box G1	202.76	293.05	230.32	517.03	460.11	537.28	2.09	264.36	5.391	0.032723
1449249_at	protocadherin 7	32.08	43.22	33.39	64.89	75.41	84.77	2.06	38.74	4.965	0.038255
1431094_at	RIKEN cDNA 1110006E14 gene	54.75	66.44	81.11	131.8	135.17	149.14	2.06	71.7	10.253	0.009379
1425784_a_at	olfactomedin 1	202.39	255.16	225.09	434.64	404.96	547.12	2.04	235.16	4.589	0.044352
1435321_at	RIKEN cDNA 3732412D22 gene	558.25	493.54	664.39	1059.94	1292.65	1093.78	2.02	578.97	4.732	0.041881
1442865_at	hypothetical protein C130007D14	48.48	49.26	44.86	101.15	85.01	99.73	2.02	48.26	6.394	0.023596
1419708_at	wingless-related MMTV integration site 6	76.97	55.16	91.45	154.94	137.34	150.59	2	73.61	6.602	0.02218
1437250_at	Similar to FLJ10116 protein (LOC381269), mRNA	51.27	69.75	76.36	126.49	145.01	121.1	2	65.73	5.449	0.032065
1418762_at	decay accelerating factor 1	58.71	55.37	64.21	22.97	33.41	32.13	-2.02	-29.88	-4.826	0.040356
1425567_a_at	annexin A5	426.92	456.02	388.2	197.38	192.07	247.64	-2.02	-214.77	-5.409	0.032518
1457349_at	Similar to Tetratricopeptide repeat protein 6 (TPR repeat protein 6) (LOC217602), mRNA	68.5	69.59	87.2	39.15	32.95	40.02	-2.02	-37.64	-5.137	0.035871
1419309_at	glycoprotein 38	701.83	592.95	684.39	262.57	284.14	425.8	-2.04	-336.54	-5.597	0.030475
1418374_at	FXYD domain-containing ion transport regulator 3	70.39	67.36	64.29	31.68	33.78	32.38	-2.05	-34.33	-5.01	0.037607
1418507_s_at	RIKEN cDNA D130043N08 gene	214.72	254.56	213.21	118.58	121.63	93.33	-2.05	-116.37	-8.355	0.014025
1438139_at	hypothetical protein E130310N06	207.1	213.72	236.4	80.39	93.48	148.09	-2.05	-111.65	-6.806	0.020915
1423461_a_at	ubiquitin-like 3	293.34	279.72	244.73	106.33	134.95	153.96	-2.08	-141.39	-4.567	0.044749
1436584_at	sprouty homolog 2 (Drosophila)	185.63	189.04	212.18	80.92	120.92	80.74	-2.08	-102.32	-4.995	0.037819
1420965_a_at	ectodermal-neural cortex 1	335.23	364.21	309.3	168.83	143.49	170.08	-2.09	-175.18	-7.171	0.018898
1424214_at	RIKEN cDNA 9130213B05 gene	271.96	194.13	243.17	108.17	82.14	149.95	-2.09	-123.15	-5.13	0.035963
1451499_at	Ca2+-dependent activator protein for secretion 2	60.13	74.64	79.03	27.41	41.29	31.63	-2.09	-37.1	-5.773	0.02872
1442542_at	RIKEN cDNA B130023L16 gene	167.64	226.95	204.21	95.45	111.93	78.76	-2.1	-104.46	-5.761	0.028834
1455845_at	cDNA sequence BC030477	108.12	112.95	102.74	37.87	51.06	63.11	-2.1	-56.23	-5.078	0.036662
1436142_at	RIKEN cDNA 3526401B18 gene	53.61	78.95	73.74	23.29	38.66	32.44	-2.17	-37.24	-6.061	0.026156
1417625_s_at	chemokine orphan receptor 1	181.99	136.01	172.46	68.56	79.58	75.43	-2.18	-88.35	-4.51	0.045814
1456005_a_at	BCL2-like 11 (apoptosis facilitator)	957.51	1140.97	1239.06	404.29	472.01	651.49	-2.18	-602.52	-16.07	0.00385
1426083_a_at	B-cell translocation gene 1, anti-proliferative	500.84	622.26	591.14	208.98	340.95	228.6	-2.19	-310.37	-9.727	0.010405
1456410_at	expressed sequence AU045128	195.73	175.75	158.51	92.1	69.36	79.76	-2.2	-96.28	-8.427	0.01379
1416983_s_at	forkhead box O1	173.83	172.78	175.21	55.59	93.91	83.78	-2.21	-95.39	-6.133	0.025569
1452624_at	leucine rich repeat transmembrane neuronal 1	68.45	75.83	63.64	31.7	30.31	31.62	-2.22	-38.19	-7.298	0.018265
1442445_at	RIKEN cDNA 2610027H17 gene	44.47	53.42	40.57	14.32	23.95	22.55	-2.22	-25.17	-5.005	0.037674
1456424_s_at	phospholipid transfer protein	400.81	421.97	347.23	145.39	166.26	208.88	-2.24	-215.92	-5.026	0.037381
1433855_at	4-aminobutyrate aminotransferase	102.01	132.61	97.53	49.92	49.96	47.78	-2.25	-61.57	-5.412	0.032487
1449109_at	suppressor of cytokine signaling 2	387.09	407.27	406.31	181.94	177.88	174.5	-2.25	-223.6	-13.368	0.00555
1454889_x_at	RIKEN cDNA C630016B22 gene	120.57	110.42	116.04	41.25	64.71	47.71	-2.25	-64.32	-5.718	0.029254
1435448_at	BCL2-like 11 (apoptosis facilitator)	522.23	617.79	498.86	231.54	213.03	278.83	-2.26	-303.46	-5.234	0.034623
1451466_at	DNA segment, Chr 16, ERATO Doi 472, expressed	285.08	280.73	339.51	91.64	154.29	152.85	-2.26	-168.64	-6.744	0.02129
1419301_at	frizzled homolog 4 (Drosophila)	752.06	884.63	1086.37	316.99	376.44	503.39	-2.28	-510.15	-10.733	0.008569
1460623_at	src family associated phosphoprotein 2	188.66	260.75	303.67	72.99	138.33	116.99	-2.28	-140.9	-5.779	0.028661
1436405_at	dedicator of cytokinesis 4	40.83	65.31	51.36	18.29	29.42	21.42	-2.29	-29.71	-5.998	0.026689
1435349_at	neuropilin 2	204.23	266.12	212.2	94.33	91.53	112.52	-2.3	-128.34	-5.058	0.036938
1434530_at	expressed sequence R75022	251.18	298.86	272.24	112.59	113.38	128.69	-2.32	-156.51	-9.111	0.011833
1416714_at	interferon consensus sequence binding protein 1	115.85	141.96	113.86	51.22	53.07	52.63	-2.36	-70.93	-7.185	0.018825
1439622_at	Ras association (RalGDS/AF-6) domain family 4	70.02	86	65.47	22.84	31.22	38.57	-2.39	-42.92	-4.777	0.041132
1429897_a_at	DNA segment, Chr 16, ERATO Doi 472, expressed	277.09	269.9	358.18	105.71	141.56	132.82	-2.4	-175.97	-5.956	0.027049
1456632_at	RIKEN cDNA D930021L15 gene	57.6	97.07	93.6	21.61	49.73	31.84	-2.4	-48.11	-5.644	0.029983
1417156_at	keratin complex 1, acidic, gene 19	278.36	290.22	273.98	114.85	108.24	128.9	-2.41	-164.5	-12.484	0.006355
1425503_at	glucosaminyl (N-acetyl) transferase 2, I-branching enzyme	67.37	113.08	89.41	27.23	46.41	36.05	-2.41	-52.51	-5.926	0.027317
1419154_at	transmembrane protease, serine 2	118.83	117.65	118.71	42.7	53.21	50.14	-2.42	-69.49	-9.753	0.01035
1459906_at	diacylglycerol kinase, eta	108.99	129.29	132.69	46.57	48.44	56.34	-2.43	-72.8	-9.008	0.012099
1455106_a_at	creatine kinase, brain	1398.64	1360.46	1049.34	525.46	458.43	565.7	-2.46	-749.9	-5.27	0.034167
1455158_at	integrin alpha 3	349.01	367.55	458.61	140.8	167.81	165.3	-2.49	-234.09	-6.423	0.023392

1438231_at	forkhead box P2	162.01	181.31	195.76	68.44	74.46	70.59	-2.51	-107.38	-8.282	0.014269
1448557_at	RIKEN cDNA 1200015N20 gene	66.97	90.11	84.66	31.54	33.53	29.98	-2.53	-48.85	-6.372	0.023757
1438540_at	Transcribed sequences	293.21	299.96	254.89	127.09	94.43	108.46	-2.56	-172.21	-8.681	0.013011
1420911_a_at	milk fat globule-EGF factor 8 protein	1034.3	913.22	977.96	311.67	356.44	452.47	-2.6	-598.32	-7.888	0.015694
1434875_a_at	high mobility group nucleosomal binding domain 3	712.63	616.01	556.26	181.51	227.94	314.85	-2.6	-386.66	-4.461	0.046755
1448823_at	chemokine (C-X-C motif) ligand 12	564.19	757.91	612.46	291.32	235.04	221.49	-2.6	-397.37	-5.479	0.031734
1436761_s_at	RIKEN cDNA 1200015N20 gene	48.76	57.22	73.28	17.69	28.57	23.06	-2.61	-36.84	-4.908	0.039101
1451342_at	spondin 1, (f-spondin) extracellular matrix protein	87.18	79.47	103.7	32.31	39.69	30.99	-2.61	-55.65	-4.933	0.038719
1423952_a_at	keratin complex 2, basic, gene 7	650.23	521.55	622.41	176.81	247.11	263.13	-2.63	-372.24	-5.642	0.030004
1458880_at	Transcribed sequences	165.19	138.89	155.06	59.25	53.35	63.35	-2.63	-95.98	-8.611	0.01322
1422837_at	sciellin	72.87	76.33	90.96	24.96	40.89	25.29	-2.65	-50.09	-4.853	0.039933
1441165_s_at	calsyntenin 2	129.61	138.43	136.72	53.36	53.08	47.56	-2.66	-84.11	-9.768	0.010319
1427508_at	cDNA sequence BC020108	189.96	187.78	125.85	63.56	57.65	65.51	-2.68	-105.05	-4.377	0.048433
1417574_at	chemokine (C-X-C motif) ligand 12	1417.92	1385.55	1463.59	484.67	462.18	644.52	-2.69	-893.94	-18.556	0.002892
1433891_at	G protein-coupled receptor 48	260.36	321.39	267.98	97.59	106.15	110.48	-2.7	-178.5	-9.175	0.011672
1417399_at	growth arrest specific 6	82.62	108.5	112.26	31.86	33.61	42.68	-2.78	-64.52	-5.931	0.027273
1438232_at	forkhead box P2	222.71	279.59	295.37	82.24	105.39	95.78	-2.79	-170.75	-8.426	0.013796
1456283_at	neuropilin (NRP) and tolloid (TLL)-like 1	46.51	40.35	50.77	7.84	20.63	20.37	-2.82	-29.61	-4.427	0.047415
1439827_at	a disintegrin-like and metalloprotease (reprolysin type) with thrombospondin type 1 motif, 12	126.11	161.78	123.94	46.96	54.42	44.19	-2.82	-88.18	-7.797	0.016055
1429185_at	RIKEN cDNA 8430436L14 gene	124.32	171.74	158.5	46.9	61.76	47.46	-2.88	-98.89	-7.605	0.016855
1418157_at	nuclear receptor subfamily 2, group F, member 1	1512.75	1767.51	1449.01	559.65	373.44	694.26	-2.91	-1034.83	-5.461	0.031931
1426301_at	activated leukocyte cell adhesion molecule	154.17	156.92	170.03	67.31	62.13	38.46	-2.91	-105.82	-5.877	0.027757
1450684_at	ets variant gene 1	118.2	124.86	102.42	34.26	39.11	44.93	-2.92	-75.46	-7.019	0.019698
1435832_at	leucine rich repeat containing 4	82.35	72.61	96.87	30.29	30.51	24.5	-2.92	-55.21	-5.503	0.03147
1451991_at	Eph receptor A7	225.28	198.24	236.11	54.47	78.12	90.71	-2.96	-145.22	-7.627	0.016761
1435554_at	RIKEN cDNA C630016B22 gene	177.95	251.81	246.13	41.85	121.89	60.4	-3.02	-150.67	-7.884	0.015709
1422607_at	ets variant gene 1	133.56	172.8	156.75	34.28	58.6	60.7	-3.04	-103.85	-11.143	0.007958
1416097_at	leucine rich repeat containing 4	118.75	109.16	116.77	38.38	36.24	38.56	-3.05	-77.2	-12.343	0.0065
1440990_at	hypothetical protein 4832420M10	221.38	228.27	288.61	61.95	91.33	87.77	-3.05	-165.18	-7.788	0.016089
1459749_s_at	hypothetical protein 6030410K14	120.93	179.47	147.28	47.78	53.98	43.76	-3.07	-100.58	-6.585	0.022291
1449893_a_at	leucine-rich repeats and immunoglobulin-like domains 1	214.08	173.37	216.64	82.57	60.21	61.32	-3.1	-138.96	-6.976	0.019934
1437466_at	activated leukocyte cell adhesion molecule	159.41	149.26	115.6	54.12	43.86	39.17	-3.1	-95.43	-8.718	0.012903
1449368_at	decorin	210.56	243.03	319.9	77.22	99.62	69.66	-3.11	-174.96	-4.559	0.044898
1434917_at	cordon-bleu	235.93	218.42	194.29	55.01	64.61	84.57	-3.13	-145.88	-6.288	0.024372
1438718_at	Transcribed sequences	243.61	297.48	362.97	74.78	125.5	86.25	-3.14	-206.17	-5.457	0.031982
1449533_at	RIKEN cDNA 1810057C19 gene	119.65	129.63	115.69	31.99	37.43	49.98	-3.15	-83.06	-7.944	0.015478
1425506_at	RIKEN cDNA 9530072E15 gene	160.39	260.32	278.42	56.32	103.65	58.33	-3.18	-159.49	-4.658	0.043127
1454984_at	expressed sequence AW061234	124	213.36	214.13	42.47	71.45	57.8	-3.2	-126.61	-5.273	0.034136
1417343_at	FXYD domain-containing ion transport regulator 6	631.26	557.28	540.22	179.58	137.1	219.91	-3.21	-396.09	-9.382	0.01117
1419549_at	arginase 1, liver	161.92	144.82	200.57	44.84	60.23	52.08	-3.21	-116.58	-5.901	0.027539
1427300_at	LIM homeobox protein 8	142.99	188.18	149.14	49.3	41.19	55.9	-3.3	-111.52	-6.128	0.025612
1429418_at	CDC14 cell division cycle 14 homolog B (S. cerevisiae)	469.3	831.94	742.98	189.72	279.45	150.11	-3.31	-475.77	-4.806	0.040677
1438558_x_at	forkhead box Q1	101.72	65.77	74.75	22.78	22.63	28.58	-3.32	-56.25	-4.419	0.047577
1427537_at	epiplakin 1	134.1	195.45	196.9	51.27	73.33	31.6	-3.35	-122.77	-4.888	0.039395
1448944_at	neuropilin	292.9	253.82	328.46	86.77	76.54	93.19	-3.36	-205.04	-11.064	0.00807
1425779_a_at	T-box 1	1093.6	879.5	843.65	236.57	281.05	305.21	-3.42	-664.81	-6.375	0.023731
1418084_at	neuropilin	530.93	548.07	638.35	175.36	140.43	170.53	-3.56	-411.34	-11.487	0.007493
1437983_at	sal-like 1 (Drosophila)	408.13	524.85	512.72	122.75	156.64	122.75	-3.58	-346.86	-10.345	0.009216
1438042_at	short stature homeobox 2	71.38	93.01	116.05	21.94	30.38	25.16	-3.58	-67.35	-5.185	0.035237
1424694_at	RIKEN cDNA 2010011I20 gene	214.17	208.07	198.23	50.01	57.35	62.86	-3.61	-149.15	-13.246	0.005651
1421088_at	glypican 4	663.05	659.02	751.2	206.39	196.61	165.69	-3.68	-502.3	-10.192	0.00949
1439260_a_at	ectonucleotide pyrophosphatase/phosphodiesterase 3	120.17	128.04	164.54	31.08	42.19	37.58	-3.71	-100.56	-7.253	0.018485
1438200_at	sulfatase 1	2218.61	2606.62	2537.01	642.75	741.2	600.56	-3.75	-1805.21	-12.904	0.005952
1434210_s_at	solute carrier family 25 (mitochondrial carrier; phosphate carrier), member 26	232.08	199.94	182.8	53.58	51.85	58.25	-3.76	-150.48	-8.678	0.013019
1437401_at	insulin-like growth factor 1	184.49	210.52	200.08	58.62	46.05	54.03	-3.76	-145.44	-11.238	0.007825
1427436_at	sine oculis-related homeobox 2 homolog (Drosophila)	346.29	326.53	230.55	100.2	65.53	75.56	-3.78	-221.25	-6.353	0.02389
1449254_at	secreted phosphoprotein 1	53.12	59.24	64.96	10.99	18.92	16.54	-3.78	-43.56	-10.891	0.008326
1416953_at	connective tissue growth factor	405.19	444.05	399.29	107.79	110.72	98.97	-3.89	-310.05	-20.599	0.002348
1438531_at	RIKEN cDNA A730054J21 gene	252.2	197.75	285.62	47.39	52.06	84.41	-4.01	-184.09	-8.328	0.014113
1435670_at	RIKEN cDNA E130018K07 gene	233.51	211.49	190.52	58.46	62	39.12	-4.03	-159.64	-13.225	0.005669
1454727_at	expressed sequence AI173486	283.19	348.23	349.56	65.37	89.26	81.94	-4.11	-247.17	-13.869	0.005159

1436319_at	sulfatase 1	747.16	1025.89	907.6	193.68	251.51	196.85	-4.15	-677.66	-9.887	0.010075
1416761_at	hydroxysteroid 11-beta dehydrogenase 2	1464.08	1348.15	1534.18	358.17	320.06	340.69	-4.27	-1108.35	-19.28	0.00268
1455464_x_at	uroplakin 1B	88.94	133.5	117.95	24.84	31.38	18.25	-4.61	-88.82	-6.752	0.021236
1454974_at	netrin 1	155.14	137.57	131.72	26.94	32.77	25.05	-4.92	-112.5	-11.579	0.007377
1433787_at	RIKEN cDNA B230343H07 gene	139.14	123.02	148.67	19.03	35.58	24.92	-5.12	-110.06	-8.648	0.013109
1449244_at	cadherin 2	463.27	411.63	556.89	84.38	86.04	106.67	-5.25	-386.7	-9.665	0.010536
1443832_s_at	serum deprivation response	240.61	259.78	214.92	52.09	39.88	37.02	-5.62	-195.8	-14.56	0.004684
1434413_at	insulin-like growth factor 1	215.74	388.38	263.83	46.09	50.84	57.22	-5.67	-238.43	-4.672	0.042891
1452473_at	RIKEN cDNA E130201N16 gene	348.28	229	323.3	36.69	63.65	55.04	-5.81	-248.24	-5.467	0.031862
1455893_at	RIKEN cDNA 2610028F08 gene	352.45	440.44	503.79	45.31	92.02	61.55	-6.44	-364.52	-8.194	0.014568
1418496_at	forkhead box A1	786.59	1165.03	1057.45	147.83	141.97	153.15	-6.81	-856.48	-7.409	0.017732
1422833_at	forkhead box A2	370.54	242.31	375.24	41.56	30.07	69.36	-7.21	-285.31	-7.033	0.019624
1448201_at	secreted frizzled-related sequence protein 2	612.54	492.82	567.44	57.9	76.83	77.78	-7.9	-487.1	-10.483	0.008977
1416779_at	serum deprivation response	188.85	221.59	220.58	9.57	30.53	30.06	-9.1	-188.7	-20.792	0.002305
1416468_at	aldehyde dehydrogenase family 1, subfamily A7	435.37	781.63	500.59	55.92	58.98	45.77	-10.69	-519.13	-5.013	0.037559
1416967_at	SRY-box containing gene 2	1361.95	1750.51	1838.75	72.97	117.75	216.68	-12.2	-1517.15	-13.167	0.005718
1416778_at	serum deprivation response	900.64	1047.28	840.1	31.04	49.45	62.42	-19.51	-879.06	-13.255	0.005644

7.2 Primers

RT-PCR primers						
Gene	**Forward**	**Reverse**		**Gene**	**Forward**	**Reverse**
Gata binding protein 2	tgctgtggctggctgaatcc	ctctgcagcaactggacacc		CCL-21	gtgtctgttcagttctcttgc	gctgccttagtacagccag
CD44	gttcccgcactgtgactcat	tgtcccattgccaccgttgat		CCL-25	cagcacaggatcaaatggaatg	ggttgcagcttccactcactt
bmp4	acgtagtcccaagcatcaccc	acagtccccatggcagtagaa		CXCL-12	gctgccttagtacagccag	cgttttcaaattatctgggagaaaga
neurofilament, light chain	tgctgccagcctgtgcatgg	attcgtgttgtgtgtggt		c-Kit ligand	aaggagatctgcgggaatcctgtga	actgctactgctgtcattcctaagg
heart&neural crest derivatives expressed transcript 2	aagacactgcgcctggccac	tctccgccttgaaggcctcc		CD-80	gagtctggaacccatctgca	gaagcgaggctttgggaaac
POU domian, class 3, transcription factor 1	aagcgcacgtccatcgaggt	tccttctgccgccggttgca		TSLP	aggctaccctgaaactga	ggagattgcatgaaggaatac
homeo box, msh-like 1	aaaccaggcaggacttgcac	tgctgccaaagcgcttagag		c-Fos	agtctgctggggcttacgcca	gattccggcacttggctgcag
delta like -1	gcttcaccatcctgggcgtg	ccgctgttatactgcaacagg			acccagtctgctggggcttacg	gattccggcacttggctgcag
BAMBI	cagtaaactgctggctggac	agcctccaagggcggctgag		c-Jun	cctgcaccggtattttggggag	ttacagtctcggtggcagcct
Ehox like	tgatgacgcctctgtggggt	aggggtctgcacgtggctcc			gtcacctccgcggcacagccggt	ttggcgtagaccggaggctcac
homeo box, msh-like 2	ctctatgccacgccggttgg	tcaggagcagagttggcacc				
TGF-beta 2	tgacatgagctacctgggtc	ccacatgactcacactgacg		**Primers für in-situ hybridization**		
dickkopf homolog 1	aggtccattctggccaactc	tggaatcacttgcttgggca		**Gene**	**Forward**	**Reverse**
follistatin	tgacaatgccacatacgcca	tcttccgagatggagttgca		bmp4	aacctcagcagcatcccaga	caacatggaaatggcactcag

Gene	Forward	Reverse		Gene	Forward	Reverse
epithelial membrane protein 1	atgactggagtgaaccgtgc	ataacccaccaatgcgatgc		delta like -1	gattcgtcgacaagacctgc	tagcatggcaccagcaacac
FoxG1	ttagttggcaacactgccca	atgcggcatttgcgcaacac		BAMBI	tgtgaaggtctcctgcaagc	aagggcagttctgcatctgc
T-box 3	tttcaagtagagctggctgc	agcccggaagggccattacc		Ehox like	tctcaaggatgctgtggtca	aacatgctggtggaaggcag
Gata2 Genotyping	ccaggatgggtggaacatac	gaaggaccccaagaacacaa		homeo box, msh-like 1	aaacccatgatccagggctg	tgcagtctcttggccttagc
Endothelin-1	cttagggagtgttcgtgtctg	tatgacagtgcagaaaggtgaggt		homeo box, msh-like 2	agttggttgagccgagtctc	gcaaacatccatcctggagtc
	gacatggaggcgtttgctatttgt	tgccgattcttctcttatgcg		TGF-beta induced		
Gcm2	gaggcaagaagcactcaggaca	cttcccagcatgcctttacac		dickkopf homolog 1	atcatcagactgtgccgcag	tttcaaggactaccagccga
IL-7	gggagtgattatgggtggtgag	tgcgggaggtgggtgtag		epithelial membrane protein 1	tgttgctttgacctgggctg	agggaatgcacggttcactc
IL-7	attatgggtggtgagagccg	gttcattattcgggcaattactatca		FoxG1	acccgtcaatgacttcgcag	aggttgttctcaaggcctgc
IL-15	gaatacatccatctcgtgct	ccaggtcatatcttacatctatcc		T-box 3	acagtatccggagcatccac	tggttacacagcccatggtg

VIII. Reference

Abu-Issa, R., Smyth, G., Smoak, I., Yamamura, K., and Meyers, E.N. (2002). Fgf8 is required for pharyngeal arch and cardiovascular development in the mouse. Development *129*, 4613-4625.

Akashi, K., Richie, L.I., Miyamoto, T., Carr, W.H., and Weissman, I.L. (2000). B lymphopoiesis in the thymus. J Immunol *164*, 5221-5226.

Akiyama, T., Maeda, S., Yamane, S., Ogino, K., Kasai, M., Kajiura, F., Matsumoto, M., and Inoue, J. (2005). Dependence of self-tolerance on TRAF6-directed development of thymic stroma. Science (New York, NY *308*, 248-251.

Allman, D., Aster, J.C., and Pear, W.S. (2002). Notch signaling in hematopoiesis and early lymphocyte development. Immunological reviews *187*, 75-86.

Ammann, A.J., Wara, D.W., Cowan, M.J., Barrett, D.J., and Stiehm, E.R. (1982). The DiGeorge syndrome and the fetal alcohol syndrome. American journal of diseases of children (1960) *136*, 906-908.

Anderson M, Anderson SK, Farr AG. (2000). Thymic vasculature: organizer of the medullary epithelial compartment? Int. Immunol. 12:1105–10

Anderson, G., and Jenkinson, E. (1997). Piecing together the thymic puzzle. Immunology today *18*, 363-364.

Anderson, G., and Jenkinson, E.J. (2001). Lymphostromal interactions in thymic development and function. Nature reviews *1*, 31-40.

Anderson, G., Jenkinson, E.J., Moore, N.C., and Owen, J.J. (1993). MHC class II-positive epithelium and mesenchyme cells are both required for T-cell development in the thymus. Nature *362*, 70-73.

Anderson, K.A., Ribar, T.J., Illario, M., and Means, A.R. (1997). Defective survival and activation of thymocytes in transgenic mice expressing a catalytically inactive form of Ca^{2+}/calmodulin-dependent protein kinase IV. Molecular endocrinology (Baltimore, Md *11*, 725-737.

Anderson, M.K., Hernandez-Hoyos, G., Diamond, R.A., and Rothenberg, E.V. (1999). Precise developmental regulation of Ets family transcription factors during specification and commitment to the T cell lineage. Development (Cambridge, England) *126*, 3131-3148.

Anderson, M.K., Weiss, A.H., Hernandez-Hoyos, G., Dionne, C.J., and Rothenberg, E.V. (2002). Constitutive expression of PU.1 in fetal hematopoietic progenitors blocks T cell development at the pro-T cell stage. Immunity *16*, 285-296.

Anderson MS, Venanzi ES, Klein L, Chen Z, Berzins SP, et al. (2002). Projection of an immunological self shadow within the thymus by the aire protein. Science 298:1395–401

Ardavin, C., Wu, L., Li, C.L., and Shortman, K. (1993). Thymic dendritic cells and T cells develop simultaneously in the thymus from a common precursor population. Nature *362*, 761-763.

Auerbach, R. (1960). Morphogenetic interactions in the development of the mouse thymus gland. Developmental biology *2*, 271-284.

Bachiller, D., Klingensmith, J., Shneyder, N., Tran, U., Anderson, R., Rossant, J., and De Robertis, E.M. (2003). The role of chordin/Bmp signals in mammalian pharyngeal development and DiGeorge syndrome. Development (Cambridge, England) *130*, 3567-3578.

Balciunaite, G., Keller, M.P., Balciunaite, E., Piali, L., Zuklys, S., Mathieu, Y.D., Gill, J., Boyd, R., Sussman, D.J., and Hollander, G.A. (2002). Wnt glycoproteins regulate the expression of Foxn1, the gene defective in nude mice. Nature immunology *3*, 1102-1108.

Baldwin, K.K., Reay, P.A., Wu, L., Farr, A., and Davis, M.M. (1999a). A T cell receptor-specific blockade of positive selection. The Journal of experimental medicine *189*, 13-24.

Baldwin, K.K., Trenchak, B.P., Altman, J.D., and Davis, M.M. (1999b). Negative selection of T cells occurs throughout thymic development. J Immunol *163*, 689-698.

Banwell, C.M., Partington, K.M., Jenkinson, E.J., and Anderson, G. (2000). Studies on the role of IL-7 presentation by mesenchymal fibroblasts during early thymocyte development. European journal of immunology *30*, 2125-2129.

Bennett, A.R., Farley, A., Blair, N.F., Gordon, J., Sharp, L., and Blackburn, C.C. (2002). Identification and characterization of thymic epithelial progenitor cells. Immunity *16*, 803-814.

Bevan, M.J. (1997). In thymic selection, peptide diversity gives and takes away. Immunity *7*, 175-178.

Bhalla, D.K., and Karnovsky, M.J. (1978). Surface morphology of mouse and rat thymic lymphocytes: an in situ scanning electron microscopic study. The Anatomical record *191*, 203-220.

Bix, M., and Raulet, D. (1992). Inefficient positive selection of T cells directed by hematopoietic cells. Nature *359*, 330-333.

Blackburn, C.C., and Manley, N.R. (2004). Developing a new paradigm for thymus organogenesis. Nature reviews *4*, 278-289.

Blackburn, M.R., Datta, S.K., and Kellems, R.E. (1998). Adenosine deaminase-deficient mice generated using a two-stage genetic engineering strategy exhibit a combined immunodeficiency. J Biol Chem *273*, 5093-5100.

Blackburn, M.R., Datta, S.K., Wakamiya, M., Vartabedian, B.S., and Kellems, R.E. (1996). Metabolic and immunologic consequences of limited adenosine deaminase expression in mice. J Biol Chem *271*, 15203-15210.

Bleul, C.C., and Boehm, T. (2005). BMP signaling is required for normal thymus development. J Immunol *175*, 5213-5221.

Bleul, C.C., Corbeaux, T., Reuter, A., Fisch, P., Monting, J.S., and Boehm, T. (2006). Formation of a functional thymus initiated by a postnatal epithelial progenitor cell. Nature *441*, 992-996.

Bleul CC, Boehm T. (2000). Chemokines define distinct microenvironments in the developing thymus. Eur. J. Immunol. 30:3371–79

Bockman, D.E. (1997). Development of the thymus. Microscopy research and technique *38*, 209-215.

Boehm, T., Scheu, S., Pfeffer, K., and Bleul, C.C. (2003). Thymic medullary epithelial cell differentiation, thymocyte emigration, and the control of autoimmunity require lympho-epithelial cross talk via LTbetaR. The Journal of experimental medicine *198*, 757-769.

Boursalian, T.E., and Bottomly, K. (1999). Stability of naive and memory phenotypes on resting CD4 T cells in vivo. J Immunol *162*, 9-16.

Brown, S.J., Miller, A.M., Cowan, P.J., Slavin, J., Connell, W.R., Moore, G.T., Bell, S., Elliott, P.R., Desmond, P.V., and d'Apice, A.J. (2004). Altered immune system glycosylation causes colitis in alpha1,2-fucosyltransferase transgenic mice. Inflammatory bowel diseases *10*, 546-556.

Burkly, L., Hession, C., Ogata, L., Reilly, C., Marconi, L.A., Olson, D., Tizard, R., Cate, R., and Lo, D. (1995). Expression of relB is required for the development of thymic medulla and dendritic cells. Nature *373*, 531-536.

Capone, M., Romagnoli, P., Beermann, F., MacDonald, H.R., and van Meerwijk, J.P. (2001). Dissociation of thymic positive and negative selection in transgenic mice expressing major histocompatibility complex class I molecules exclusively on thymic cortical epithelial cells. Blood *97*, 1336-1342.

Carlyle, J.R., Michie, A.M., Furlonger, C., Nakano, T., Lenardo, M.J., Paige, C.J., and Zuniga-Pflucker, J.C. (1997). Identification of a novel developmental stage marking lineage commitment of progenitor thymocytes. The Journal of experimental medicine *186*, 173-182.

Chidgey, A.P., and Boyd, R.L. (2001). Thymic stromal cells and positive selection. Apmis *109*, 481-492.

Chisaka, O., and Capecchi, M.R. (1991). Regionally restricted developmental defects resulting from targeted disruption of the mouse homeobox gene hox-1.5. Nature *350*, 473-479.

Colucci, F., Soudais, C., Rosmaraki, E., Vanes, L., Tybulewicz, V.L., and Di Santo, J.P. (1999). Dissecting NK cell development using a novel alymphoid mouse model: investigating the role of the c-abl proto-oncogene in murine NK cell differentiation. J Immunol *162*, 2761-2765.

Coffer PJ, Burgering BM. (2004). Forkhead-box transcription factors and their role in the immune system. Nat. Rev. Immunol. 4:889–99

Conway, S.J., Henderson, D.J., and Copp, A.J. (1997). Pax3 is required for cardiac neural crest migration in the mouse: evidence from the splotch (Sp2H) mutant. Development (Cambridge, England) *124*, 505-514.

Cordier, A.C., and Haumont, S.M. (1980). Development of thymus, parathyroids, and ultimobranchial bodies in NMRI and nude mice. The American journal of anatomy *157*, 227-263.

Cordier, A.C., and Heremans, J.F. (1975). Nude mouse embryo: ectodermal nature of the primordial thymic defect. Scandinavian journal of immunology *4*, 193-196.

Cosgrove, D., Bodmer, H., Bogue, M., Benoist, C., and Mathis, D. (1992). Evaluation of the functional equivalence of major histocompatibility complex class II A and E complexes. The Journal of experimental medicine *176*, 629-634.

Couly, G., Lagrue, A., and Griscelli, C. (1983). [Di George syndrome, exemplary rhomboencephalic neurocristopathy]. Revue de stomatologie et de chirurgie maxillo-faciale *84*, 103-108.

Derbinski, J., Schulte, A., Kyewski, B., and Klein, L. (2001). Promiscuous gene expression in medullary thymic epithelial cells mirrors the peripheral self. Nature immunology *2*, 1032-1039.

Dietrich S, Gruss P. (1995). Undulated phenotypes suggest a role of Pax-1 for the development of vertebral and extravertebral structures. Dev. Biol. 167:529–48

Dooley J, Erickson M, Farr AG. (2005). An organized medullary epithelial structure in the normal thymus expresses molecules of respiratory epithelium and resembles the epithelial thymic rudiment of nude mice. J. Immunol. 175:4331–37

Douagi, I., Andre, I., Ferraz, J.C., and Cumano, A. (2000). Characterization of T cell precursor activity in the murine fetal thymus: evidence for an input of T cell precursors between days 12 and 14 of gestation. European journal of immunology *30*, 2201-2210.

Epstein, J.A., Li, J., Lang, D., Chen, F., Brown, C.B., Jin, F., Lu, M.M., Thomas, M., Liu, E., Wessels, A.*, et al.* (2000). Migration of cardiac neural crest cells in Splotch embryos. Development (Cambridge, England) *127*, 1869-1878.

Erickson, M., Morkowski, S., Lehar, S., Gillard, G., Beers, C., Dooley, J., Rubin, J.S., Rudensky, A., and Farr, A.G. (2002). Regulation of thymic epithelium by keratinocyte growth factor. Blood *100*, 3269-3278.

Frank, D.U., Fotheringham, L.K., Brewer, J.A., Muglia, L.J., Tristani-Firouzi, M., Capecchi, M.R., and Moon, A.M. (2002). An Fgf8 mouse mutant phenocopies human 22q11 deletion syndrome. Development (Cambridge, England) *129*, 4591-4603.

Franz, T. (1989). Persistent truncus arteriosus in the Splotch mutant mouse. Anatomy and embryology *180*, 457-464.

Gabor, M.J., Scollay, R., and Godfrey, D.I. (1997). Thymic T cell export is not influenced by the peripheral T cell pool. European journal of immunology *27*, 2986-2993.

Garg, V., Yamagishi, C., Hu, T., Kathiriya, I.S., Yamagishi, H., and Srivastava, D. (2001). Tbx1, a DiGeorge syndrome candidate gene, is regulated by sonic hedgehog during pharyngeal arch development. Developmental biology *235*, 62-73.

Gekas, C., Dieterlen-Lievre, F., Orkin, S.H., and Mikkola, H.K. (2005). The placenta is a niche for hematopoietic stem cells. Developmental cell *8*, 365-375.

Georgopoulos, K., Bigby, M., Wang, J.H., Molnar, A., Wu, P., Winandy, S., and Sharpe, A. (1994). The Ikaros gene is required for the development of all lymphoid lineages. Cell *79*, 143-156.

Gill, J., Malin, M., Hollander, G.A., and Boyd, R. (2002). Generation of a complete thymic microenvironment by MTS24(+) thymic epithelial cells. Nature immunology *3*, 635-642.

Gill, J., Malin, M., Sutherland, J., Gray, D., Hollander, G., and Boyd, R. (2003). Thymic generation and regeneration. Immunological reviews *195*, 28-50.

Gillard GO, Dooley J, Erickson M, Peltonen L, Farr AG. (2007). Aire-dependent alterations in medullary thymic epithelium indicate a role for Aire in thymic epithelial differentiation. J. Immunol. 178:3007–15

Godfrey, D.I., Kennedy, J., Suda, T., and Zlotnik, A. (1993). A developmental pathway involving four phenotypically and functionally distinct subsets of CD3-CD4-CD8- triple-negative adult mouse thymocytes defined by CD44 and CD25 expression. J Immunol *150*, 4244-4252.

Godfrey, D.I., and Zlotnik, A. (1993). Control points in early T-cell development. Immunology today *14*, 547-553.

Godin, I., and Cumano, A. (2002). The hare and the tortoise: an embryonic hematopoietic race. Nature reviews *2*, 593-604.

Gordon, J., Bennett, A.R., Blackburn, C.C., and Manley, N.R. (2001). Gcm2 and Foxn1 mark early parathyroid- and thymus-specific domains in the developing third pharyngeal pouch. Mechanisms of development *103*, 141-143.

Gordon, J., Wilson, V.A., Blair, N.F., Sheridan, J., Farley, A., Wilson, L., Manley, N.R., and Blackburn, C.C. (2004). Functional evidence for a single endodermal origin for the thymic epithelium. Nature immunology *5*, 546-553.

Gordon, J., Wilson, V.A., Moore-Scott, B.A., Manley, N.R., and Blackburn, C.C. (2005). In vivo and in vitro assays of thymic organogenesis. Methods in molecular medicine *105*, 303-310.

Gray DH, Tull D, Ueno T, Seach N, Classon BJ, et al. (2007). A unique thymic fibroblast population revealed by the monoclonal antibody MTS-15. J. Immunol. 178:4956–65

Gunther, T., Chen, Z.F., Kim, J., Priemel, M., Rueger, J.M., Amling, M., Moseley, J.M., Martin, T.J., Anderson, D.J., and Karsenty, G. (2000). Genetic ablation of parathyroid glands reveals another source of parathyroid hormone. Nature *406*, 199-203.

Hager-Theodorides, A.L., Outram, S.V., Shah, D.K., Sacedon, R., Shrimpton, R.E., Vicente, A., Varas, A., and Crompton, T. (2002). Bone morphogenetic protein 2/4 signaling regulates early thymocyte differentiation. J Immunol *169*, 5496-5504.

Han, W., Ye, Q., and Moore, M.A. (2000). A soluble form of human Delta-like-1 inhibits differentiation of hematopoietic progenitor cells. Blood *95*, 1616-1625.

Heath, V.L., Moore, N.C., Parnell, S.M., and Mason, D.W. (1998). Intrathymic expression of genes involved in organ specific autoimmune disease. Journal of autoimmunity *11*, 309-318.

Heino, M., Peterson, P., Sillanpaa, N., Guerin, S., Wu, L., Anderson, G., Scott, H.S., Antonarakis, S.E., Kudoh, J., Shimizu, N.*, et al.* (2000). RNA and protein expression of the murine autoimmune regulator gene (Aire) in normal, RelB-deficient and in NOD mouse. European journal of immunology *30*, 1884-1893.

Hetzer-Egger, C., Schorpp, M., Haas-Assenbaum, A., Balling, R., Peters, H., and Boehm, T. (2002). Thymopoiesis requires Pax9 function in thymic epithelial cells. European journal of immunology *32*, 1175-1181.

Hoffmann, M.W., Allison, J., and Miller, J.F. (1992). Tolerance induction by thymic medullary epithelium. Proceedings of the National Academy of Sciences of the United States of America *89*, 2526-2530.

Hoffmann, M.W., Heath, W.R., Ruschmeyer, D., and Miller, J.F. (1995). Deletion of high-avidity T cells by thymic epithelium. Proceedings of the National Academy of Sciences of the United States of America *92*, 9851-9855.

Hogan, B.L., and Yingling, J.M. (1998). Epithelial/mesenchymal interactions and branching morphogenesis of the lung. Current opinion in genetics & development *8*, 481-486.

Hollander, G.A., Simpson, S.J., Mizoguchi, E., Nichogiannopoulou, A., She, J., Gutierrez-Ramos, J.C., Bhan, A.K., Burakoff, S.J., Wang, B., and Terhorst, C. (1995a). Severe colitis in mice with aberrant thymic selection. Immunity *3*, 27-38.

Hollander, G.A., Wang, B., Nichogiannopoulou, A., Platenburg, P.P., van Ewijk, W., Burakoff, S.J., Gutierrez-Ramos, J.C., and Terhorst, C. (1995b). Developmental control point in induction of thymic cortex regulated by a subpopulation of prothymocytes. Nature *373*, 350-353.

Hollander G, Gill J, Zuklys S, Iwanami N, Liu C, Takahama Y. (2006). Cellular and molecular events during early thymus development. Immunol. Rev. 209:28–46

Ishii, M., Han, J., Yen, H.Y., Sucov, H.M., Chai, Y., and Maxson, R.E., Jr. (2005). Combined deficiencies of Msx1 and Msx2 cause impaired patterning and survival of the cranial neural crest. Development (Cambridge, England) *132*, 4937-4950.

Ishikawa, Y., Yokoo, T., and Kitamura, M. (1997). c-Jun/AP-1, but not NF-kappa B, is a mediator for oxidant-initiated apoptosis in glomerular mesangial cells. Biochemical and biophysical research communications *240*, 496-501.

Itoi M,Tsukamoto N, Amagai T. (2007). Expression of Dll4 and CCL25 in Foxn1-negative epithelial cells in the postnatal thymus. Int. Immunol. 19:127–32

Itoi, M., Kawamoto, H., Katsura, Y., and Amagai, T. (2001). Two distinct steps of immigration of hematopoietic progenitors into the early thymus anlage. International immunology *13*, 1203-1211.

Jackson, M., Baird, J.W., Cambray, N., Ansell, J.D., Forrester, L.M., and Graham, G.J. (2002). Cloning and characterization of Ehox, a novel homeobox gene essential for embryonic stem cell differentiation. J Biol Chem *277*, 38683-38692.

Jackson, M., Baird, J.W., Nichols, J., Wilkie, R., Ansell, J.D., Graham, G., and Forrester, L.M. (2003). Expression of a novel homeobox gene Ehox in trophoblast stem cells and pharyngeal pouch endoderm. Dev Dyn *228*, 740-744.

Jaleco, A.C., Neves, H., Hooijberg, E., Gameiro, P., Clode, N., Haury, M., Henrique, D., and Parreira, L. (2001). Differential effects of Notch ligands Delta-1 and Jagged-1 in human lymphoid differentiation. The Journal of experimental medicine *194*, 991-1002.

Jameson, S.C., and Bevan, M.J. (1998). T-cell selection. Current opinion in immunology *10*, 214-219.

Jenkinson, W.E., Jenkinson, E.J., and Anderson, G. (2003). Differential requirement for mesenchyme in the proliferation and maturation of thymic epithelial progenitors. The Journal of experimental medicine *198*, 325-332.

Jerome, L.A., and Papaioannou, V.E. (2001). DiGeorge syndrome phenotype in mice mutant for the T-box gene, Tbx1. Nature genetics *27*, 286-291.

Jonsson H, Peng SL. (2005). Forkhead transcription factors in immunology. Cell. Mol. Life Sci. 62:397–409

Kaestner KH, Knochel W, Martinez DE. (2000). Unified nomenclature for the winged helix/forkhead transcription factors. Genes Dev. 14:142–46

Kanzler, B., Foreman, R.K., Labosky, P.A., and Mallo, M. (2000). BMP signaling is essential for development of skeletogenic and neurogenic cranial neural crest. Development (Cambridge, England) *127*, 1095-1104.

Katsura, Y. (2002). Redefinition of lymphoid progenitors. Nature reviews *2*, 127-132.

Kawamoto, H., Ohmura, K., Fujimoto, S., and Katsura, Y. (1999). Emergence of T cell progenitors without B cell or myeloid differentiation potential at the earliest stage of hematopoiesis in the murine fetal liver. J Immunol *162*, 2725-2731.

Kawana, M., Lee, M.E., Quertermous, E.E., and Quertermous, T. (1995). Cooperative interaction of GATA-2 and AP1 regulates transcription of the endothelin-1 gene. Molecular and cellular biology *15*, 4225-4231.

Kaye, J., Hsu, M.L., Sauron, M.E., Jameson, S.C., Gascoigne, N.R., and Hedrick, S.M. (1989). Selective development of CD4+ T cells in transgenic mice expressing a class II MHC-restricted antigen receptor. Nature *341*, 746-749.

Kim, J., Jones, B.W., Zock, C., Chen, Z., Wang, H., Goodman, C.S., and Anderson, D.J. (1998). Isolation and characterization of mammalian homologs of the Drosophila gene glial cells missing. Proceedings of the National Academy of Sciences of the United States of America *95*, 12364-12369.

Kingston, R., Jenkinson, E.J., and Owen, J.J. (1984). Characterization of stromal cell populations in the developing thymus of normal and nude mice. European journal of immunology *14*, 1052-1056.

Kirby, M.L., and Bockman, D.E. (1984). Neural crest and normal development: a new perspective. The Anatomical record *209*, 1-6.

Klein, J.R. (1998). Thymus-independent development of gut T cells. Chemical immunology *71*, 88-102.

Klein, L., and Kyewski, B. (2000). "Promiscuous" expression of tissue antigens in the thymus: a key to T-cell tolerance and autoimmunity? Journal of molecular medicine (Berlin, Germany) *78*, 483-494.

Klug, D.B., Carter, C., Crouch, E., Roop, D., Conti, C.J., and Richie, E.R. (1998). Interdependence of cortical thymic epithelial cell differentiation and T-lineage commitment. Proceedings of the National Academy of Sciences of the United States of America *95*, 11822-11827.

Klug, D.B., Carter, C., Gimenez-Conti, I.B., and Richie, E.R. (2002). Cutting edge: thymocyte-independent and thymocyte-dependent phases of epithelial patterning in the fetal thymus. J Immunol *169*, 2842-2845.

Ko, L.J., and Engel, J.D. (1993). DNA-binding specificities of the GATA transcription factor family. Molecular and cellular biology *13*, 4011-4022.

Krumlauf, R. (1994). Hox genes in vertebrate development. Cell *78*, 191-201.

Kuratani, S., and Bockman, D.E. (1990a). Impaired development of the thymic primordium after neural crest ablation. The Anatomical record *228*, 185-190.

Kuratani, S., and Bockman, D.E. (1990b). The participation of neural crest derived mesenchymal cells in development of the epithelial primordium of the thymus. Archives of histology and cytology *53*, 267-273.

Kuratani, S., and Bockman, D.E. (1991). Capacity of neural crest cells from various axial levels to participate in thymic development. Cell and tissue research *263*, 99-105.

Kuratani, S.C. (1991). Alternate expression of the HNK-1 epitope in rhombomeres of the chick embryo. Developmental biology *144*, 215-219.

Kurihara, Y., Kurihara, H., Suzuki, H., Kodama, T., Maemura, K., Nagai, R., Oda, H., Kuwaki, T., Cao, W.H., Kamada, N.*, et al.* (1994). Elevated blood pressure and craniofacial abnormalities in mice deficient in endothelin-1. Nature *368*, 703-710.

Kurobe, H., Liu, C., Ueno, T., Saito, F., Ohigashi, I., Seach, N., Arakaki, R., Hayashi, Y., Kitagawa, T., Lipp, M.*, et al.* (2006). CCR7-dependent cortex-to-medulla migration of positively selected thymocytes is essential for establishing central tolerance. Immunity *24*, 165-177.

Kyewski B, Klein L. (2006). A central role for central tolerance. Annu. Rev. Immunol. 24:571–606

Laclef, C., Souil, E., Demignon, J., and Maire, P. (2003). Thymus, kidney and craniofacial abnormalities in Six 1 deficient mice. Mechanisms of development *120*, 669-679.

Laclef C, Souil E, Demignon J, Maire P. (2003). Thymus, kidney and craniofacial abnormalities in *Six1* deficient mice. Mech. Dev. 120:669–79

Lammer, E.J., Chen, D.T., Hoar, R.M., Agnish, N.D., Benke, P.J., Braun, J.T., Curry, C.J., Fernhoff, P.M., Grix, A.W., Jr., Lott, I.T.*, et al.* (1985). Retinoic acid embryopathy. The New England journal of medicine *313*, 837-841.

Laufer, T.M., DeKoning, J., Markowitz, J.S., Lo, D., and Glimcher, L.H. (1996). Unopposed positive selection and autoreactivity in mice expressing class II MHC only on thymic cortex. Nature *383*, 81-85.

Le Douarin, N.M., and Jotereau, F.V. (1975). Tracing of cells of the avian thymus through embryonic life in interspecific chimeras. The Journal of experimental medicine *142*, 17-40.

Lee, D., Prowse, D.M., and Brissette, J.L. (1999). Association between mouse nude gene expression and the initiation of epithelial terminal differentiation. Developmental biology *208*, 362-374.

Lee, M.E., Temizer, D.H., Clifford, J.A., and Quertermous, T. (1991). Cloning of the GATA-binding protein that regulates endothelin-1 gene expression in endothelial cells. J Biol Chem *266*, 16188-16192.

Lind, E.F., Prockop, S.E., Porritt, H.E., and Petrie, H.T. (2001). Mapping precursor movement through the postnatal thymus reveals specific microenvironments supporting

defined stages of early lymphoid development. The Journal of experimental medicine *194*, 127-134.

Lindsay, E.A., Vitelli, F., Su, H., Morishima, M., Huynh, T., Pramparo, T., Jurecic, V., Ogunrinu, G., Sutherland, H.F., Scambler, P.J.*, et al.* (2001). Tbx1 haploinsufficieny in the DiGeorge syndrome region causes aortic arch defects in mice. Nature *410*, 97-101.

Liston, A., Lesage, S., Gray, D.H., O'Reilly, L.A., Strasser, A., Fahrer, A.M., Boyd, R.L., Wilson, J., Baxter, A.G., Gallo, E.M.*, et al.* (2004). Generalized resistance to thymic deletion in the NOD mouse; a polygenic trait characterized by defective induction of Bim. Immunity *21*, 817-830.

Liston, A., Lesage, S., Wilson, J., Peltonen, L., and Goodnow, C.C. (2003). Aire regulates negative selection of organ-specific T cells. Nature immunology *4*, 350-354.

Lo, D., Ron, Y., and Sprent, J. (1986). Induction of MHC-restricted specificity and tolerance in the thymus. Immunologic research *5*, 221-232.

Lo, D., and Sprent, J. (1986a). Exogenous control of I-A expression in fetal thymus explants. J Immunol *137*, 1772-1775.

Lo, D., and Sprent, J. (1986b). Identity of cells that imprint H-2-restricted T-cell specificity in the thymus. Nature *319*, 672-675.

Malendowicz, L.K., Macchi, V., Brelinska, R., Trejer, M., Gottardo, G., and Nussdorfer, G.G. (1998). Endothelin-1 enhances thymocyte proliferation in monolaterally adrenalectomized rats with contralateral adrenocortical regeneration. Histology and histopathology *13*, 721-725.

Manley, N.R., and Capecchi, M.R. (1995). The role of Hoxa-3 in mouse thymus and thyroid development. Development (Cambridge, England) *121*, 1989-2003.

Manley, N.R., and Capecchi, M.R. (1998). Hox group 3 paralogs regulate the development and migration of the thymus, thyroid, and parathyroid glands. Developmental biology *195*, 1-15.

Manley, N.R., Selleri, L., Brendolan, A., Gordon, J., and Cleary, M.L. (2004). Abnormalities of caudal pharyngeal pouch development in Pbx1 knockout mice mimic loss of Hox3 paralogs. Developmental biology *276*, 301-312.

Mark, M., Ghyselinck, N.B., and Chambon, P. (2004). Retinoic acid signalling in the development of branchial arches. Current opinion in genetics & development *14*, 591-598.

Markowitz, J.S., Auchincloss, H., Jr., Grusby, M.J., and Glimcher, L.H. (1993). Class II-positive hematopoietic cells cannot mediate positive selection of $CD4^+$ T lymphocytes in class II-deficient mice. Proceedings of the National Academy of Sciences of the United States of America *90*, 2779-2783.

Marrack, P., Blackman, M., Burgert, H.G., McCormack, J.M., Cambier, J., Finkel, T.H., and Kappler, J. (1989). T-cell repertoire and thymus. Cold Spring Harbor symposia on quantitative biology *54 Pt 1*, 105-110.

Martinic MM, van den Broek MF, Rulicke T, Huber C, Odermatt B, et al. (2006). Functional $CD8^+$ but not $CD4^+$ T cell responses develop independent of thymic epithelial MHC. Proc. Natl. Acad. Sci. *USA* 103:14435–40

Merkenschlager, M., Graf, D., Lovatt, M., Bommhardt, U., Zamoyska, R., and Fisher, A.G. (1997). How many thymocytes audition for selection? The Journal of experimental medicine *186*, 1149-1158.

Merscher, S., Funke, B., Epstein, J.A., Heyer, J., Puech, A., Lu, M.M., Xavier, R.J., Demay, M.B., Russell, R.G., Factor, S.*, et al.* (2001). TBX1 is responsible for cardiovascular defects in velo-cardio-facial/DiGeorge syndrome. Cell *104*, 619-629.

Meyers, E.N., Lewandoski, M., and Martin, G.R. (1998). An Fgf8 mutant allelic series generated by Cre- and Flp-mediated recombination. Nature genetics *18*, 136-141.

Min D,Taylor PA, Panoskaltsis-Mortari A, Chung B, Danilenko DM, et al. (2002). Protection from thymic epithelial cell injury by keratinocyte growth factor: a new approach to improve thymic and peripheral T-cell reconstitution after bone marrow transplantation. Blood 99:4592–600

Minegishi, N., Ohta, J., Suwabe, N., Nakauchi, H., Ishihara, H., Hayashi, N., and Yamamoto, M. (1998). Alternative promoters regulate transcription of the mouse GATA-2 gene. J Biol Chem *273*, 3625-3634.

Miyasaka, M., Pabst, R., Dudler, L., Cooper, M., and Yamaguchi, K. (1990). Characterization of lymphatic and venous emigrants from the thymus. Thymus *16*, 29-43.

Miyawaki, S., Nakamura, Y., Suzuka, H., Koba, M., Yasumizu, R., Ikehara, S., and Shibata, Y. (1994). A new mutation, aly, that induces a generalized lack of lymph nodes accompanied by immunodeficiency in mice. European journal of immunology *24*, 429-434.

Moore-Scott, B.A., and Manley, N.R. (2005). Differential expression of Sonic hedgehog along the anterior-posterior axis regulates patterning of pharyngeal pouch endoderm and pharyngeal endoderm-derived organs. Developmental biology *278*, 323-335.

Morrison-Graham, K., Schatteman, G.C., Bork, T., Bowen-Pope, D.F., and Weston, J.A. (1992). A PDGF receptor mutation in the mouse (Patch) perturbs the development of a non-neuronal subset of neural crest-derived cells. Development (Cambridge, England) *115*, 133-142.

Muller SM, Terszowski G, Blum C, Haller C, Anquez V, et al. (2005). Gene targeting of VEGF-A in thymus epithelium disrupts thymus blood vessel architecture. Proc. Natl. Acad. Sci. *USA* 102:10587–92

Mulroy, T., McMahon, J.A., Burakoff, S.J., McMahon, A.P., and Sen, J. (2002). Wnt-1 and Wnt-4 regulate thymic cellularity. European journal of immunology *32*, 967-971.

Mulroy, T., Xu, Y., and Sen, J.M. (2003). beta-Catenin expression enhances generation of mature thymocytes. International immunology *15*, 1485-1494.

Murphy, K.M., Heimberger, A.B., and Loh, D.Y. (1990). Induction by antigen of intrathymic apoptosis of CD4+CD8+TCRlo thymocytes in vivo. Science (New York, NY *250*, 1720-1723.

Murphy, M., and Epstein, L.B. (1990). Decreased T cell receptor and CD3 expression by Down syndrome thymocytes: evidence for delayed maturation. Progress in clinical and biological research *360*, 117-130.

Naspetti, M., Aurrand-Lions, M., DeKoning, J., Malissen, M., Galland, F., Lo, D., and Naquet, P. (1997). Thymocytes and RelB-dependent medullary epithelial cells provide growth-promoting and organization signals, respectively, to thymic medullary stromal cells. European journal of immunology *27*, 1392-1397.

Nehls, M., Kyewski, B., Messerle, M., Waldschutz, R., Schuddekopf, K., Smith, A.J., and Boehm, T. (1996). Two genetically separable steps in the differentiation of thymic epithelium. Science (New York, NY *272*, 886-889.

Niederreither, K., Subbarayan, V., Dolle, P., and Chambon, P. (1999). Embryonic retinoic acid synthesis is essential for early mouse post-implantation development. Nature genetics *21*, 444-448.

Niederreither, K., Vermot, J., Le Roux, I., Schuhbaur, B., Chambon, P., and Dolle, P. (2003). The regional pattern of retinoic acid synthesis by RALDH2 is essential for the development of posterior pharyngeal arches and the enteric nervous system. Development (Cambridge, England) *130*, 2525-2534.

Nossal, G.J. (1994). Negative selection of lymphocytes. Cell *76*, 229-239.

Ohnemus, S., Kanzler, B., Jerome-Majewska, L.A., Papaioannou, V.E., Boehm, T., and Mallo, M. (2002). Aortic arch and pharyngeal phenotype in the absence of BMP-dependent neural crest in the mouse. Mechanisms of development *119*, 127-135.

Ohuchi, H., Kimura, S., Watamoto, M., and Itoh, N. (2000). Involvement of fibroblast growth factor (FGF)18-FGF8 signaling in specification of left-right asymmetry and brain and limb development of the chick embryo. Mechanisms of development *95*, 55-66.

Owen, J.J., McLoughlin, D.E., Suniara, R.K., and Jenkinson, E.J. (2000). The role of mesenchyme in thymus development. Current topics in microbiology and immunology *251*, 133-137.

Osada, M., Ito, E., Fermin, H.A., Vazquez-Cintron, E., Venkatesch, T., Friedel, R.H., Pezzano, M. (2006). The Wnt signaling antagonist Kremen1 isrequired for development of thymic architecture. Clinical Developmental Immunology 13, 299-319

Palmer, D.B., Viney, J.L., Ritter, M.A., Hayday, A.C., and Owen, M.J. (1993). Expression of the alpha beta T-cell receptor is necessary for the generation of the thymic medulla. Developmental immunology *3*, 175-179.

Palmer, E. (2003). Negative selection--clearing out the bad apples from the T-cell repertoire. Nature reviews *3*, 383-391.

Pan, X., Minegishi, N., Harigae, H., Yamagiwa, H., Minegishi, M., Akine, Y., and Yamamoto, M. (2000). Identification of human GATA-2 gene distal IS exon and its expression in hematopoietic stem cell fractions. Journal of biochemistry *127*, 105-112.

Pantelouris, E.M. (1968). Absence of thymus in a mouse mutant. Nature *217*, 370-371.

Paterson, D.J., and Williams, A.F. (1987). An intermediate cell in thymocyte differentiation that expresses CD8 but not CD4 antigen. The Journal of experimental medicine *166*, 1603-1608.

Patel SR, Gordon J, Mahbub F, Blackburn CC, Manley NR. (2006). Bmp4 and Noggin expression during early thymus and parathyroid organogenesis. Gene. Expr. Patterns 6:794–99

Peters, H., Neubuser, A., Kratochwil, K., and Balling, R. (1998). Pax9-deficient mice lack pharyngeal pouch derivatives and teeth and exhibit craniofacial and limb abnormalities. Genes & development *12*, 2735-2747.

Petrie HT, Zuniga-Pflucker JC. (2007). Zoned out: functional mapping of stromal signaling microenvironments in the thymus. Annu. Rev. Immunol. 25:649–79

Pignoni, F., Hu, B., Zavitz, K.H., Xiao, J., Garrity, P.A., and Zipursky, S.L. (1997). The eye-specification proteins So and Eya form a complex and regulate multiple steps in Drosophila eye development. Cell *91*, 881-891.

Pongracz, J., Hare, K., Harman, B., Anderson, G., and Jenkinson, E.J. (2003). Thymic epithelial cells provide WNT signals to developing thymocytes. European journal of immunology *33*, 1949-1956.

Pui, J.C., Allman, D., Xu, L., DeRocco, S., Karnell, F.G., Bakkour, S., Lee, J.Y., Kadesch, T., Hardy, R.R., Aster, J.C.*, et al.* (1999). Notch1 expression in early lymphopoiesis influences B versus T lineage determination. Immunity *11*, 299-308.

Radtke, F., Wilson, A., Stark, G., Bauer, M., van Meerwijk, J., MacDonald, H.R., and Aguet, M. (1999). Deficient T cell fate specification in mice with an induced inactivation of Notch1. Immunity *10*, 547-558.

Raff, M.C. (1992). Social controls on cell survival and cell death. Nature *356*, 397-400.

Rahemtulla, A., Fung-Leung, W.P., Schilham, M.W., Kundig, T.M., Sambhara, S.R., Narendran, A., Arabian, A., Wakeham, A., Paige, C.J., Zinkernagel, R.M.*, et al.* (1991).

Normal development and function of CD8+ cells but markedly decreased helper cell activity in mice lacking CD4. Nature *353*, 180-184.

Raviola E, Karnovsky MJ. (1972). Evidence for a blood-thymus barrier using electronopaque tracers. J. Exp. Med. 136:466–98

Revest, J.M., Spencer-Dene, B., Kerr, K., De Moerlooze, L., Rosewell, I., and Dickson, C. (2001a). Fibroblast growth factor receptor 2-IIIb acts upstream of Shh and Fgf4 and is required for limb bud maintenance but not for the induction of Fgf8, Fgf10, Msx1, or Bmp4. Developmental biology *231*, 47-62.

Revest, J.M., Suniara, R.K., Kerr, K., Owen, J.J., and Dickson, C. (2001b). Development of the thymus requires signaling through the fibroblast growth factor receptor R2-IIIb. J Immunol *167*, 1954-1961.

Ritter, M.A., and Boyd, R.L. (1993). Development in the thymus: it takes two to tango. Immunology today *14*, 462-469.

Roberts, C., Ivins, S.M., James, C.T., and Scambler, P.J. (2005). Retinoic acid down-regulates Tbx1 expression in vivo and in vitro. Dev Dyn *232*, 928-938.

Rodewald, H.R., Paul, S., Haller, C., Bluethmann, H., and Blum, C. (2001a). Thymus medulla consisting of epithelial islets each derived from a single progenitor. Nature *414*, 763-768.

Rodewald, H.R., Waskow, C., and Haller, C. (2001b). Essential requirement for c-kit and common gamma chain in thymocyte development cannot be overruled by enforced expression of Bcl-2. The Journal of experimental medicine *193*, 1431-1437.

Rodewald HR, Ogawa M, Haller C,Waskow C, DiSanto JP. (1997). Pro-thymocyte expansion by c-kit and the common cytokine receptor gamma chain is essential for repertoire formation. Immunity 6:265–72

Rodewald H-R, Fehling HJ. (1998). Molecular and cellular events in early thymocyte development. Adv. Immunol. 69:1–112

Ropke, C., Van Soest, P., Platenburg, P.P., and Van Ewijk, W. (1995). A common stem cell for murine cortical and medullary thymic epithelial cells? Developmental immunology *4*, 149-156.

Rossi S, Blazar BR, Farrell CL, Danilenko DM, Lacey DL, et al. (2002). Keratinocytegrowth factor preserves normal thymopoiesis and thymic microenvironment during experimental graft-vs-host disease. Blood 100:682–91

Rossi, S.W., Jenkinson, W.E., Anderson, G., and Jenkinson, E.J. (2006). Clonal analysis reveals a common progenitor for thymic cortical and medullary epithelium. Nature *441*, 988-991.

Rossi SW, Jeker LT, Ueno T, Kuse S, Keller MP, et al. (2007). Keratinocyte growth factor (KGF) enhances postnatal T-cell development via enhancements in proliferation and function of thymic epithelial cells. Blood 109:3803–11

Rossi SW, Kim MY, Leibbrandt A, Parnell SM, Jenkinson WE, et al. (2007) .RANK signals from CD4+3− inducer cells regulate development of Aire-expressing epithelial cells in the thymic medulla. *J. Exp. Med.* 204:1267–72

Rowen, L., Young, J., Birditt, B., Kaur, A., Madan, A., Philipps, D.L., Qin, S., Minx, P., Wilson, R.K., Hood, L.*, et al.* (2002). Analysis of the human neurexin genes: alternative splicing and the generation of protein diversity. Genomics *79*, 587-597.

Sainte-Marie, G. (1965). Plasmocytes in the Thymus of the Normal Rat. J Immunol *94*, 172-176.

Schluep, M., Willcox, N., Ritter, M.A., Newsom-Davis, J., Larche, M., and Brown, A.N. (1988). Myasthenia gravis thymus: clinical, histological and culture correlations. Journal of autoimmunity *1*, 445-467.

Schuddekopf K, Schorpp M, Boehm T. 1996. The whn transcription factor encoded by the nude locus contains an evolutionarily conserved and functionally indispensable activation domain. *Proc. Natl. Acad. Sci. USA* 93:9661–64

Sebzda, E., Mariathasan, S., Ohteki, T., Jones, R., Bachmann, M.F., and Ohashi, P.S. (1999). Selection of the T cell repertoire. Annual review of immunology *17*, 829-874.

Shah, D.K., Hager-Theodorides, A.L., Outram, S.V., Ross, S.E., Varas, A., and Crompton, T. (2004). Reduced thymocyte development in sonic hedgehog knockout embryos. J Immunol *172*, 2296-2306.

Shinkura, R., Kitada, K., Matsuda, F., Tashiro, K., Ikuta, K., Suzuki, M., Kogishi, K., Serikawa, T., and Honjo, T. (1999). Alymphoplasia is caused by a point mutation in the mouse gene encoding Nf-kappa b-inducing kinase. Nature genetics *22*, 74-77.

Shores, E.W., Van Ewijk, W., and Singer, A. (1991). Disorganization and restoration of thymic medullary epithelial cells in T cell receptor-negative scid mice: evidence that receptor-bearing lymphocytes influence maturation of the thymic microenvironment. European journal of immunology *21*, 1657-1661.

Smith, C.A., Williams, G.T., Kingston, R., Jenkinson, E.J., and Owen, J.J. (1989). Antibodies to CD3/T-cell receptor complex induce death by apoptosis in immature T cells in thymic cultures. Nature *337*, 181-184.

Sprent, J., and Kishimoto, H. (2001). The thymus and central tolerance. Transplantation *72*, S25-28.

Staal, F.J., Weerkamp, F., Baert, M.R., van den Burg, C.M., van Noort, M., de Haas, E.F., and van Dongen, J.J. (2004). Wnt target genes identified by DNA microarrays in immature CD34+ thymocytes regulate proliferation and cell adhesion. J Immunol *172*, 1099-1108.

Stalmans, I., Lambrechts, D., De Smet, F., Jansen, S., Wang, J., Maity, S., Kneer, P., von der Ohe, M., Swillen, A., Maes, C.*, et al.* (2003). VEGF: a modifier of the del22q11 (DiGeorge) syndrome? Nature medicine *9*, 173-182.

Su, D., Ellis, S., Napier, A., Lee, K., and Manley, N.R. (2001). Hoxa3 and pax1 regulate epithelial cell death and proliferation during thymus and parathyroid organogenesis. Developmental biology *236*, 316-329.

Su DM, Manley NR. (2000). Hoxa3 and Pax1 transcription factors regulate the ability of

fetal thymic epithelial cells to promote thymocyte development. J. Immunol. 164:5753–60

Su, D.M., Navarre, S., Oh, W.J., Condie, B.G., and Manley, N.R. (2003). A domain of Foxn1 required for crosstalk-dependent thymic epithelial cell differentiation. Nature immunology *4*, 1128-1135.

Suniara, R.K., Jenkinson, E.J., and Owen, J.J. (2000). An essential role for thymic mesenchyme in early T cell development. The Journal of experimental medicine *191*, 1051-1056.

Surh, C.D., and Sprent, J. (1994). T-cell apoptosis detected in situ during positive and negative selection in the thymus. Nature *372*, 100-103.

Throsby, M., Herbelin, A., Pleau, J.M., and Dardenne, M. (2000). CD11c+ eosinophils in the murine thymus: developmental regulation and recruitment upon MHC class I-restricted thymocyte deletion. J Immunol *165*, 1965-1975.

Tokoro, Y., Sugawara, T., Yaginuma, H., Nakauchi, H., Terhorst, C., Wang, B., and Takahama, Y. (1998). A mouse carrying genetic defect in the choice between T and B lymphocytes. J Immunol *161*, 4591-4598.

Toro, I., and Olah, I. (1967a). Penetration of thymocytes into the blood circulation. Journal of ultrastructure research *17*, 439-451.

Toro, I., and Olah, L. (1967b). Studies on the blood--thymus barrier. Acta biologica Academiae Scientiarum Hungaricae *18*, 135-150.

Traver, D., Akashi, K., Manz, M., Merad, M., Miyamoto, T., Engleman, E.G., and Weissman, I.L. (2000). Development of CD8alpha-positive dendritic cells from a common myeloid progenitor. Science (New York, NY *290*, 2152-2154.

Tsai, F.Y., Keller, G., Kuo, F.C., Weiss, M., Chen, J., Rosenblatt, M., Alt, F.W., and Orkin, S.H. (1994). An early hematopoietic defect in mice lacking the transcription factor GATA-2. Nature *371*, 221-226.

Tsai, P.T., Lee, R.A., and Wu, H. (2003). BMP4 acts upstream of FGF in modulating thymic stroma and regulating thymopoiesis. Blood *102*, 3947-3953.

Tsukamoto N, Itoi M, Nishikawa M, Amagai T. 2005. Lack of Delta like 1 and 4 expressions in nude thymus anlages. *Cell. Immunol.* 234:77–80

Universal Protein Resource (UniProt), Collaboration of European Bioinformatics Institute (EBI), Swiss Institute if Bioinformatics (SIB) and the Protein Information Resource (PIR). webpage: www.uniport.org

van Ewijk, W., Hollander, G., Terhorst, C., and Wang, B. (2000). Stepwise development of thymic microenvironments in vivo is regulated by thymocyte subsets. Development (Cambridge, England) *127*, 1583-1591.

van Ewijk, W., Shores, E.W., and Singer, A. (1994). Crosstalk in the mouse thymus. Immunology today *15*, 214-217.

van Ewijk, W., Wang, B., Hollander, G., Kawamoto, H., Spanopoulou, E., Itoi, M., Amagai, T., Jiang, Y.F., Germeraad, W.T., Chen, W.F.*, et al.* (1999). Thymic microenvironments, 3-D versus 2-D? Seminars in immunology *11*, 57-64.

Vermot, J., Niederreither, K., Garnier, J.M., Chambon, P., and Dolle, P. (2003). Decreased embryonic retinoic acid synthesis results in a DiGeorge syndrome phenotype in newborn mice. Proceedings of the National Academy of Sciences of the United States of America *100*, 1763-1768.

von Boehmer, H., and Fehling, H.J. (1997). Structure and function of the pre-T cell receptor. Annual review of immunology *15*, 433-452.

von Boehmer H. (2004). Selection of theT-cell repertoire: receptor-controlled checkpoints in T-cell development. Adv. Immunol. 84:201–38

Von Gaudecker, B., Kendall, M.D., and Ritter, M.A. (1997). Immuno-electron microscopy of the thymic epithelial microenvironment. Microscopy research and technique *38*, 237-249.

Wallin, J., Eibel, H., Neubuser, A., Wilting, J., Koseki, H., and Balling, R. (1996). Pax1 is expressed during development of the thymus epithelium and is required for normal T-cell maturation. Development (Cambridge, England) *122*, 23-30.

Wang, S.Y. (1994). A retinoic acid-inducible GATA-binding protein binds to the regulatory region of J6 serpin gene. J Biol Chem *269*, 607-613.

Weih, F., Carrasco, D., Durham, S.K., Barton, D.S., Rizzo, C.A., Ryseck, R.P., Lira, S.A., and Bravo, R. (1995). Multiorgan inflammation and hematopoietic abnormalities in mice with a targeted disruption of RelB, a member of the NF-kappa B/Rel family. Cell *80*, 331-340.

Wendling, O., Dennefeld, C., Chambon, P., and Mark, M. (2000). Retinoid signaling is essential for patterning the endoderm of the third and fourth pharyngeal arches. Development (Cambridge, England) *127*, 1553-1562.

Werdelin, O., Cordes, U., and Jensen, T. (1998). Aberrant expression of tissue-specific proteins in the thymus: a hypothesis for the development of central tolerance. Scandinavian journal of immunology *47*, 95-100.

Wilson, D.B., Dorfman, D.M., and Orkin, S.H. (1990). A nonerythroid GATA-binding protein is required for function of the human preproendothelin-1 promoter in endothelial cells. Molecular and cellular biology *10*, 4854-4862.

Wu, L., Li, C.L., and Shortman, K. (1996). Thymic dendritic cell precursors: relationship to the T lymphocyte lineage and phenotype of the dendritic cell progeny. The Journal of experimental medicine *184*, 903-911.

Wu, L., Scollay, R., Egerton, M., Pearse, M., Spangrude, G.J., and Shortman, K. (1991). CD4 expressed on earliest T-lineage precursor cells in the adult murine thymus. Nature *349*, 71-74.

Xu, P.X., Zheng, W., Laclef, C., Maire, P., Maas, R.L., Peters, H., and Xu, X. (2002). Eya1 is required for the morphogenesis of mammalian thymus, parathyroid and thyroid. Development (Cambridge, England) *129*, 3033-3044.

Xu, R.H., Ault, K.T., Kim, J., Park, M.J., Hwang, Y.S., Peng, Y., Sredni, D., and Kung, H. (1999). Opposite effects of FGF and BMP-4 on embryonic blood formation: roles of PV.1 and GATA-2. Developmental biology *208*, 352-361.

Yamamoto, M., Ko, L.J., Leonard, M.W., Beug, H., Orkin, S.H., and Engel, J.D. (1990). Activity and tissue-specific expression of the transcription factor NF-E1 multigene family. Genes & development *4*, 1650-1662.

Yamazaki, H., Sakata, E., Yamane, T., Yanagisawa, A., Abe, K., Yamamura, K., Hayashi, S., and Kunisada, T. (2005). Presence and distribution of neural crest-derived cells in the murine developing thymus and their potential for differentiation. International immunology *17*, 549-558.

Yu, Q., Erman, B., Park, J.H., Feigenbaum, L., and Singer, A. (2004). IL-7 receptor signals inhibit expression of transcription factors TCF-1, LEF-1, and RORgammat: impact on thymocyte development. The Journal of experimental medicine *200*, 797-803.

Zerrahn, J., Volkmann, A., Coles, M.C., Held, W., Lemonnier, F.A., and Raulet, D.H. (1999). Class I MHC molecules on hematopoietic cells can support intrathymic positive selection of T cell receptor transgenic T cells. Proceedings of the National Academy of Sciences of the United States of America *96*, 11470-11475.

Zou D, Silvius D, Davenport J, Grifone R, Maire P, Xu PX. (2006). Patterning of the third pharyngeal pouch into thymus/parathyroid by Six and Eya1. Dev. Biol. 293:499–512

Zuklys, S., Balciunaite, G., Agarwal, A., Fasler-Kan, E., Palmer, E., and Hollander, G.A. (2000). Normal thymic architecture and negative selection are associated with Aire expression, the gene defective in the autoimmune-polyendocrinopathy-candidiasis-ectodermal dystrophy (APECED). J Immunol *165*, 1976-1983.

Kyung-Jae, Na

Persönliche Daten

Privatadresse	Mittelstr 12 3012 Bern Schweiz
	Mobil: 0041 (0) 78 9097037 Email: nkyungjae@gmail.com
Geburtsdatum/-ort	12.09.1976 / Jindo-Kun, Süd-Korea
Familienstand	Ledig
Staatsangehörigkeit	Deutsch
Fremdsprachen	Deutsch (Muttersprache) Englisch (Verhandlungssicher) Koreanisch (Gut)
Verfügbarkeit	
Titel	Ph.D.

Arbeitserfahrung

08/2009 –

Clinical Trial Coordinator bei der Schweizerischen Arbeitsgemeinschaft für klinische Krebsforschung (SAKK), Bern, Schweiz

- Koordination und Management von klinischen Krebs Studien nach GCP/ICH Richtlinien in Europa und Schweiz (Phasen I-III)
- Planung von Krebsstudien (Phasen I-III)
- Durchführung von klinischen Krebsstudien nach GCP/ICH Richtlinien in Europa und Schweiz (Phasen I-III)
- Projektmanagement: Entwicklung von Brustkrebsstudien (CRF- und Protokollentwicklung und Initiierung der Studien), Finalisierung einer Lungenkrebsstudie (Data Bereinigung, Publikation), Durchführung einer Brustkrebsstudie und einer internationalen Leberkrebsstudie (Betreuung der Studie, elektronische Datenerfassung und Bereinigung)

06/2009 – 07/2009

Wissenschaftlicher Mitarbeiter im Rahmen des BNF-Projektes der Universität Bern bei:
Prof. Robert Rieben, Universität Bern, Department für klinische Forschung, Bern Schweiz

Fortbildungen

07/2010

eGCP Introduction Course at Vienna School of Medicine, Austria.

01/2010

Clinical Investigator I: Basic GCP and clinical research training course

10/2009

Projektmanagement, Konfliktmanagement, Präsentation Kurs bei Plural

04/2009

Grundkenntnisse der GMP bei CSL Behring

- Umsetzung der GMP Anforderung in einem Qualitätssystem
- Anforderung an die Dokumentation und Protokollierung
- Grundlagen der Validierung von Produktionsanlagen
- Auswirkung von GMP auf den Laborbetrieb

Universitäre Laufbahn

10/2003 –Oktober 2009 Promotion im Bereich Biochemie Ph.D.	Zentrum für Lehr und Forschung und Zentrum für Biomedizin, Pädiatrische Immunologie, Universität Basel, Basel, Schweiz. Supervisor: Prof. GA Holländer Projekt: „Identifying novel genes and its function in early thymus development"
10/1997 – 03/2003 Studium	Biochemie Studium an der Universität Bielefeld, Bielefeld, Deutschland
06/2002-02/2003 Diplomarbeit	New York University Medical School, the Skirball Institute of Biomedical Science, New York City, USA. Department of Pathology. Supervisor: Prof. DR Littman Projekt: „Expression of PKC-theta using the Lentiviral Vectorsystem"
06/2002 Diplomprüfung	Bioanorganische Chemie: 1.3 Biochemie: 1.0 Immunologie: 1.7 Gentechnologie: 1.7
04/2000 – 08/2000 Praktikum	Weizmann Institute of Science, Rehovot, Israel. Department of Immunology, Supervisor: Prof. I. Pecht Projekt: "MAFA, an inhibitory receptor on Mast cells"
01/2000	Vordiplom (Abschluss: 1.3, sehr gut)

Praktikum

9/2008 – 11/2008 Praktikum	Roland Berger Strategy Consultants GmbH Berlin, Deutschland Competence Center: Pharma & Healthcare Projekte: 2. Optimierung von Kapazitätenauslastung in einer Spezialklinik - Unterstützung bei der Ausarbeitung von Analyse zu Kapazitätenauslastung, Schichtplänen und Arbeitszeiten - Erstellung von Präsentations-

unterlagen

3. Fusion von Krankenkassen
   - Recherchen zu handelnden Personen in Krankenkassen
   - Erstellung von Landkarten mit Vertriebseinheiten
   - Recherchen von Pressemitteilungen und Datenbanken zur Erhebung von Kennzahlen auf dem GKV Markt
4. Vorbereitung zur Einführung eines neuen Medizinproduktes im Bereich Knorpel Tissue Engineering
   - Ermittlung von Zielgruppen
   - Analyse und Aufarbeitung von Erstattungswegen sowohl für den ambulaten als auch für den stationären Sektor

Schullaufbahn

1987 – 1996 Gymnasium	Gymnasium St. Leonhard, Aachen, Deutschland Abitur: 2.0
Sommer 1993	6 wöchiges Forschungsaufenthalt in KAIST (Korean Advanced Institute of Science and Technology), Taejon, South Korea
1986 – 1987 Grundschule	Grundschule Vaalserquatier, Aachen, Deutschland
1985 – 1986 Grundschule	Albert-Schweizer Grundschule, Aachen, Deutschland

Stipendien

2003 - 2008	Ph.D. Stipendium vom Swiss National Fond
2002 – 2003	Stipendium für Abschlussarbeiten der DAAD (Deutsche Akademische Auslandsdienst)
2002	Stipendium von Ostwestfälische-Lippische Universitätsgesellschaft
2000	Stipendium der „Deutsche Gesellschaft der Freunde des Weizmann-Instituts“

IT-Kenntnisse

Computerkenntnisse	Microsoft Office Word (sehr gut) Microsoft Office Exel (gut) Microsoft Office Power Point (sehr gut)

Publikationen

"Stabilized b-catenin in thymic epithelial cells blocks thymus development and function" Zuklys S, Gill J, Keller MP, Hauri-Hohl M, Zhanybekova S, Balciunaite G, **Na KJ**, Jeker LT, Hafen K, Tsukamoto N, Amagai T, Taketo MM, Krenger W, Holländer GA. – Journal of Immunology, 2009 March 1.